UNIVERSITY OF CALIFORNIA,

IRVINE

Unveiling the Underlying Mechanisms of Airineme-Mediated Cell-Cell Communication During Pigment Pattern Development in Zebrafish

DISSERTATION

submitted in partial satisfaction of the requirements
for the degree of

DOCTOR OF PHILOSOPHY

in Biological Sciences

With a concentration in Developmental and Cellular Biology

by

Raquel Lynn Bowman

Dissertation Committee:
Associate Professor Dr. Dae Seok Eom, Chair
Professor Dr. Christine Suetterlin
Associate Professor Dr. Michael Parsons
Assistant Professor Dr. Katherine Thompson-Peer
Assistant Professor Dr. Pablo Lara-Gonzalez

2026

DEDICATION

To my parents, sister, stepfather, partner, and dear friends, whose love and support over the past four years carried me through this journey. Thank you for always believing in me and for helping me believe in myself.

TABLE OF CONTENTS

Page

LIST OF FIGURES

Page

LIST OF TABLES

ACKNOWLEDGMENTS

I would like to acknowledge my PI and mentor Dr. Dae Seok Eom. I started in your lab as an undergraduate Bio199 student. As an undergraduate researcher I was given opportunities that may not have been afforded to me had I been in a different lab, and for that I'm very grateful. As I approached the end of my undergraduate studies, time stopped. We were in a global pandemic and suddenly every plan I had for myself was stalled. Then, you offered me a position as a lab technician. At first, I was hesitant to take the position. I was scared of how it might change my future and if it was a role I could succeed in. Many fish feedings and experiments later, I found myself learning a lot but also enjoying it. Later on I applied to graduate school, but unfortunately wasn't admitted. I still remember that day. I felt embarrassed and my future felt uncertain. You changed my life the day you took me in as a direct-admit. You took a chance on me, and it's a decision I reflect on often. Not many graduate students can say they've known and trained with their mentor for as long as I have. I've experienced many ups and downs while in graduate school, but I wouldn't change any of it. You've shaped me into the scientist that I am today. I remember when I first started in the lab in 2019, I looked up to you and wanted to be just like you. An accomplished scientist. Someone who can design experiments and knows what the next step is. From 2019 to 2026, that hasn't changed. You still inspire me. Thank you for being my mentor and taking a chance on me.

I'd like to acknowledge my committee member Dr. Michael Parsons. When I first joined the Eom lab, I'd often see you walking down the hallway and felt intimidated. Even so, it became a personal mission of mine and Yi's to know you. We started throwing smiles and hellos your way until one day, you started waving back. I'm so glad we did, because if not, I would've never gotten to hear your stories about Johns Hopkins, England, what kind of tea is the best tea, and what your latest drawings have been. If I hadn't met you, I might never have gotten involved in UCI BioEYES, a program which has become near and dear to my heart. Outside of getting to know you and BioEYES, you have also been an incredible committee member and mentor. I feel incredibly lucky that these past years I've been able to come to you whenever I have a question about science. You always take the time to answer my questions both patiently and thoroughly. Thank you for all the laughs and answers to my questions.

I'd like to acknowledge my committee member Dr. Christine Suetterlin. Selecting committee members can be a daunting task. The first thing most students do is ask the PIs they have an established rapport with. I did that. I asked Dr. Parsons to be a committee member, and then realized, I didn't know many other PIs. Other students had recommendations here and there. Who has been helpful. Who has challenged them. Ultimately, my PI and I decided you would be a great pick based on your scientific expertise. You've challenged me scientifically, held me accountable, and expected better of me. I grew from those experiences and I am grateful I had them. If someone asked me what kind of committee member you were, I'd say your critiques were always fair, that you were encouraging, that you went above and beyond for students, and that you're someone I deeply admire. I look up to you as a woman in science, and more often than not, catch myself saying "Christine is so cool". Thank you for saying yes when I asked you to be my committee member.

I'd like to acknowledge my committee member Dr. Katie Thompson-Peer. When I was looking for committee members, your name came up more than a few times. Fellow graduate students always expressed that you were kind, uplifting, and supportive. I'd like to add to that list. Not once did I ever feel nervous meeting with you or having you at a committee meeting. No matter what circumstance I've met you in, you've always come into the room or welcomed me into the room with a smile and a warmness that extends all around you. In committee meetings, you've offered countless suggestions on how to improve the quality of my work. You've challenged me and asked questions about my work that I would've never thought about otherwise. You've helped me break down larger tasks into smaller bite-sized pieces, making them more accessible. You've lent an ear on days where I needed someone to listen. You remind me that science is about asking good questions and uplifting future scientists – offering others a smile, welcoming them into the space, and helping them grow. Thank you for welcoming me into that space.

I'd like to acknowledge my committee member Dr. Pablo Lara-Gonzalez. Naturally as graduate students we all talk to one another about our projects, our lives, and also our PIs. Over the past few years, it's always been clear how much your lab adores you. Your expertise in cell biology was part of why I chose you as a committee member, but so was this reputation. Your lab always mentioned how kind, compassionate, and considerate you were. Any time I've come by your lab, you've always welcomed me with a smile and a hello. The kind that makes you feel like you're not an intruder to the lab, but a welcome visitor. When I've brought up concerns or had questions along the way of my Ph.D. journey, you never hesitated to make time for me, and helped me brainstorm possible solutions. For me, having you as a committee member felt like I had someone in my corner. Thank you for being in my corner and helping me make it to the end.

I'd like to acknowledge my former labmate and dear friend Dr. Yi Wang. When I first started in the Eom Lab back in 2019, I was a Bio199 student and you were a volunteer. Then I became a technician, and you a masters student. When the pandemic hit, there were just three of us. You, me, and Zach. I used to drive home for lunch everyday, and you used to eat alone in your car. One day I asked if you wanted to have lunch together, and from that point on, the lab never felt like a lonely place again. Getting a Ph.D. is never easy, but having a friend who understands and goes through the trials and tribulations with you makes it easier. In the last six years, we made it through the pandemic, survived six-day fish feedings, laughed together, celebrated together, cried together, and encouraged each other to keep going. We've had countless memories together in the Eom Lab. Inside jokes that no one else will ever get. Stories others can't believe. And most importantly, a friendship that has withstood the tests of time. Thank you for being the best labmate and one of my dearest friends.

I'd like to acknowledge all the members of the Eom Lab, both past and present. Being away from home has always been hard for me. I didn't get to visit home often during my Ph.D., but I still count myself as one of the luckiest people in Dev Cell, because I have a lab that feels like family when family is far away. From our first set of undergrads, when it was Daniel, Andrew, Yi, and I. Having game nights and making snowmen in the -80C. To the days of Kia, Eddie, Lo,

and Andy. Getting lunch, going to the gym, and making coffee runs. Then to Oliver, Jack, Naomi, Sangjoon, Thomas, and Jiyea. Trips to Brandywine, watching the world cup, and going to the beach. And lastly (but by no means least), Natalia, Alvin, Isha, and Mattea. Even more coffee runs and days full of laughter. Each and every one of you has helped me along my journey. Teaching me patience, kindness, sharing laughs with me, and encouraging me on days where things feel impossible.

I'd like to acknowledge the other labs on the fourth floor of Nat Sci II. It's been a pleasure of mine to get to know the people who share the same floor as me in Nat Sci II. Going on coffee runs with Eddie and Alex from the Parsons Lab, lunches between Yi, myself, and Ren from the Plikus Lab, playing soccer and borrowing reagents from Yikai and Richard from the Blumberg Lab, having tea time and sharing laughs with Arul, Cameron, and Alfredo from the Schilling Lab, Coffee runs with Chelsea from the Baker Lab, talking about Chicago, soccer and ultimate frisbee with Ira and Clark from the Cho Lab. You've all helped me along my scientific journey by providing advice and your expertise. I feel so lucky to have known and made friends with all of you. One of the biggest things I'm going to miss from my PhD, is all of you. Thank you for being the best lab neighbors a PhD student could have.

I'd like to acknowledge Dr. Peter Donovan. I can say with confidence and I think most would agree, you're one of a kind. The first time I met you was in your stem cell biology course for graduate students, and from that class I learned three important things about you: 1) questions always come in three parts, 2) young padawans should always be brave enough to ask questions, and 3) the 'secret garden' in the school of medicine is actually an assortment of cacti in a parking lot. With how busy you are, it's a wonder how you're able to be as dedicated to students as you are. You've lent an ear to me many times over the years, offering me sage advice, cheering me on, and always reminding me that I'm smarter than I think I am. Thank you for being an unofficial mentor to me and taking an interest in my personal development and my life.

I'd like to acknowledge Dr. Rob Steele. I was introduced to you by Dr. Ira Blitz back when Dr. Parsons and I were trying to add new curriculum to the BioEYES outreach program. We had ordered hydra from the internet and instead just received tubes of water sans hydra in the mail. Ira gave me your contact information because he knew you'd have hydra on hand. I went into that interaction not expecting much (other than hydra of course), but ended up with so much more. I've never met someone so passionate about science that they continue to pursue research after retirement. Any time I've had a question about hydra, needed hydra, or needed a speaker, you've always said yes. I don't think I could ever get tired of hearing your anecdotes about collecting hydras out in different parts of the world and the funny circumstances that come along with it. I'm very grateful to have met you during my PhD journey and I hope one day to be half as passionate about research as you are.

I'd like to acknowledge my friends. To Kathleen, you have been with me through some of the biggest ups and downs in my life. You are one of my dearest friends. You know what I'm thinking before I even say it. I'm so incredibly grateful to have a friend like you and that you've

been a part of my journey. I'll never stop being grateful that Dr. Parsons paired us to do BioEYES together. To Patrick and Grace, thank you for being my friends and for being my role models. Patrick, you are one of the friendliest people I know and incredibly generous with your time. You've helped me countless times with imaging and image analysis, never asking for anything in return. Grace, you are an encyclopedia of knowledge. It always amazes me how you're able to come up with questions on the fly, and still express profundity. To my close friends Pari and Kim, you've both seen me at my best and my worst throughout this process. You both know me better than almost anyone. Thank you for sticking with me for this whole ride and being a support system for me. To Yikai and David, thank you for not only being my friends but also my co-reps for the graduate student representatives. I was a little in over my head about being a student representative when we started this whole thing. I just knew I wanted to connect more with the department and make friends with everyone. You both gave life to every idea that I had and added even more ideas on top of those. Being a student representative with you both has been such a great joy of mine. I get to plan fun things with the department and even better, I get to plan them with my friends.

I'd like to acknowledge Mayra Rubio. You are a woman after my own heart. You are a fashionista whose outfits are always to die for, and are one of the most creative people I've ever met. Having you as an advisor for the graduate representatives was one of the best and most fun experiences I've had in graduate school. I feel so at home talking with you and always look forward to planning things with you.

I'd like to acknowledge Dr. Star Lee. I had no idea teaching was something I might want to do someday until I met you. Although Dev Cell GAANN isn't running anymore, I've learned so much from that program and from you. You've taught me how to be more empathetic as an instructor and how to communicate with students more effectively. I've made so many meaningful connections with students because of the things you've taught me. Thank you for being a teacher to me and teaching me these important lessons.

I'd like to acknowledge my partner Noel Salvador. I'm not sure how to even begin to describe how you've been there for me over the past four years. Meeting you changed the trajectory of my life. Four years ago, I was a very different person. I could say you've encouraged me, believed in me, comforted me on the hard days, and that would all be true. But you've done much more than that. You've inspired me. You work harder than anyone I've ever met. When situations are impossible or unfair, you handle them with patience and with grace. When I'm struggling to make a decision or have hardships, you give me perspective. And most importantly, you give me the space to be myself without needing to be anything else, loving me anyways. Thank you for being you and for being by my side during this whole journey.

I'd like to acknowledge my family. To my dad, you have been one of the biggest supporters my entire life. When things are going wrong and I feel like I have nowhere else to go, you've always been the person I go to first. You've never once doubted that I would become a Ph.D. You've always believed I could do anything I set my mind to. To my mom, no one could ever love me as fiercely as you do. You would do anything to support, love, and protect me, and

you have. I know how proud you are of me, but I didn't do it alone, you've helped me every step of the way. To Steve, the best bonus day I could ever hope to ask for. I'm so glad you're a part of my family. Thank you for always being there, supporting me, and being a part of my life. And last but not least, to my sister Kristina. Some people are lucky to just get along with their siblings. I'm far more lucky than that. You're not just my sister, you're my best friend. You've been part of this whole Ph.D. with me, all the highs and lows, and in betweens. Thank you to my family, you mean more to me than words could ever express.

The text of Chapter 1 of this dissertation is an adaptation of the material as it appears in Bowman, R.L., Wang, D., Eom, DS. (2023). A macrophage subpopulation promotes airineme-mediated intercellular communication in a matrix metalloproteinase-9 manner. Cell Reports 42. https://doi.org/10.1016/j.celrep.2023.112818, used with permission from Cell Reports Publications. The coauthors listed in this publication are Raquel L. Bowman, Daoqin Wang, and Dae Seok Eom.

The text of Chapter 2 of this dissertation is an adaptation of the material as it appears in Bowman, R.L., Kim, J., Parsons, M.J., Eom, DS. (2025). CD44 facilitates adhesive interactions in airineme-mediated intercellular signaling. Frontiers in Cell and Developmental Biology, 13. https://doi.org/10.3389/fcell.2025.1522710, used with permission from Frontiers Publications. The coauthors listed in this publication are Raquel L. Bowman, Jiyea Kim, Michael J. Parsons, and Dae Seok Eom.

Financial support was provided by NIGMS-National Institute of General Medicine Sciences (R35GM142791) and GAANN-Graduate Assistance in Areas of National Need program.

VITA

RAQUEL LYNN BOWMAN

YEAR	DEGREE	INSTITUTION
2022-2026	Ph.D. in Biological Sciences	University of California, Irvine
2022-2025	M.S. in Biological Sciences	University of California, Irvine
2016-2020	B.S. in Biological Sciences	University of California, Irvine

FIELD OF STUDY

Developmental and Cell Biology, cell-cell communication, macrophages, specialized signaling filopodia - airinemes

PUBLICATIONS

1. **Bowman, R. L.**, Wang, D. & Eom, D. S. A macrophage subpopulation promotes airineme-mediated intercellular communication in a matrix metalloproteinase-9 dependent manner. *Cell Reports* **42**, 112818 (2023).

2. **Bowman, R. L.**, Kim, J., Parsons, M. J. & Eom, D. S. CD44 facilitates adhesive interactions in airineme-mediated intercellular signaling. *Front. Cell Dev. Biol.* **13**, 1522710 (2025).

3. Parsons, M.J., **Bowman, R. L.**, Parada, K. N. L., Bojorquez, D., Lewis, C., Del Padre, B., Wiles, T. J., Lee, S. W. UCI BioEYES: A graduate-student-led model for sustainable, inclusive science outreach. *Zebrafish.* 15458547261476961 (2026).

AWARDS AND RECOGNITION

Edward A. Steinhaus Award	Jun. 2024
Latine Excellence and Achievement Award (LEAD)	Apr. 2026
Graduate Assistance in Areas of National Need (GAANN)	Sept 2023 – Mar 2026

TEACHING

Developmental and Cell Biology Lab	Fall 2023; Fall 2024; Fall 2025

MENTORSHIP EXPERIENCE

Research Discovery Program (RDP)	Winter – Spring 2024; Winter – Spring 2026

PRESENTATIONS

Saber West (Irvine, CA)	Jan 2026
Southern California Zebrafish Meeting (Los Angeles, CA)	Nov 2024
Society for Developmental Biology (SDB) (Atlanta,GA)	Jul 2024
Society for Developmental Biology (SDB) (Chicago, IL)	Jul 2023
Southern California Zebrafish Meeting (Irvine, CA)	Dec 2023
6th Annual UCI Skin Symposium (Irvine, CA)	Jan 2023
Math Fish Meeting (Irvine, CA)	Apr 2022

OUTREACH

SoCal BioEYES (Co-Leader)	Oct 2023 – Sept 2026

ABSTRACT OF THE DISSERTATION

Unveiling the Underlying Mechanisms of Airineme-Mediated Cell-Cell Communication During Pigment Pattern Development in Zebrafish

by
Raquel L. Bowman
Doctor of Philosophy in Developmental and Cellular Biology
University of California, Irvine, 2026
[Associate Professor] Dae Seok Eom, Chair

Cell-cell communication (CCC) is essential for coordinating important developmental processes, including tissue patterning. Although cells can communicate through well-characterized mechanisms such as endocrine, synaptic, juxtacrine, and paracrine signaling, these are not the only signaling modalities that exist in nature. Cells can also communicate via specialized filopodia, allowing for direct targeting. There are several subclasses of signaling filopodia, including airinemes, which are the focus of this dissertation. Airinemes are a unique class of specialized filopodia that mediate signaling during zebrafish pigment pattern development through the coordinated activities of xanthoblasts, macrophages, and melanophores. Airinemes originate as surface blebs (airineme blebs) on xanthoblasts that are recognized and extracted by migrating macrophages, which transport airineme vesicles and deposit them onto target melanophores. Despite previous work establishing the importance of airinemes in pigment pattern formation, several aspects of airineme-mediated CCC remained unresolved, including the identity of the macrophage population responsible for airineme transport, the molecular mechanisms governing macrophage-airineme interactions, and basic characterization of airineme blebs.

This dissertation addresses these questions through three complementary studies. First, I identified at least two morphologically and behaviorally distinct macrophage populations in the zebrafish skin and demonstrated that amoeboid macrophages, which overlap with the previously described ectoderm-derived macrophage population known as metaphocytes,

preferentially localize to the hypodermis where airineme-projecting xanthoblasts reside. I further demonstrated that metaphocyte migration into the hypodermis requires MMP9. Second, I identified the cell-surface glycoprotein CD44 as a mediator of interactions between metaphocytes and airineme bleb-bearing xanthoblasts. Cell-specific disruption of the CD44 extracellular domain reduced airineme frequency, demonstrating that CD44-dependent interactions contribute to airineme-mediated signaling. Finally, I established size- and morphology-based criteria for identifying putative airineme blebs and used these criteria to characterize their developmental distribution and potential maturation. Putative airineme blebs increased in abundance prior to peak airineme production, and a subset exhibited CD44a as well as phosphatidylserine (PS), a previously established recognition signal for macrophage-mediated airineme extraction.

Together, these findings support a model in which airineme-mediated CCC is assembled through a series of regulated cellular and molecular interactions involving airineme bleb formation, macrophage recognition and transport, and delivery of signaling cargo to target cells. This work expands our understanding of how immune cells can acquire specialized roles in developmental CCC and provides a framework for investigating the formation and maturation of airineme blebs and other membrane-associated signaling structures.

INTRODUCTION

From embryonic development to immune responses, multicellular organisms depend on the accurate transmission and interpretation of signals between cells (Su et al., 2024). When communication between cells is disrupted or improperly regulated, it can lead to numerous pathological conditions including improper differentiation, uncontrolled growth, and disease (Su et al., 2024; Armingol et al., 2021). Thus, understanding the mechanisms governing signaling transmission between cells have been a longstanding goal in developmental biology.

A fundamental feature of cell-cell communication (CCC) is the interaction between extracellular ligands and their cognate receptors. Binding of ligands such as hormones, growth factors, or neurotransmitters to receptors on recipient cells, triggers intracellular signaling cascades that alter cell behavior through changes in gene expression and other downstream responses (Armingol et al., 2021). Although ligand-receptor interactions are a common feature of CCC, the specific mechanisms by which ligands reach their cognate receptors differs considerably. Because signaling molecules differ in their biochemical properties and because communicating cells are separated by different distances and tissue environments, cells have evolved multiple strategies to ensure accurate ligand delivery. Traditionally, four classical modes of CCC have been recognized: endocrine, juxtacrine, synaptic and paracrine signaling (Figure 1). More recently, advances in imaging and molecular technology have resulted in the identification of additional mechanisms for CCC which are mediated by ‘specialized filopodia’, including intercellular bridges, cytonemes, tunneling nanotubes, and airinemes (Figure 3). Each of these mechanisms is described below, with particular emphasis on the airineme-mediated communication pathway which is the focus of this dissertation.

CLASSIC CELL-CELL COMMUNICATION MECHANISMS

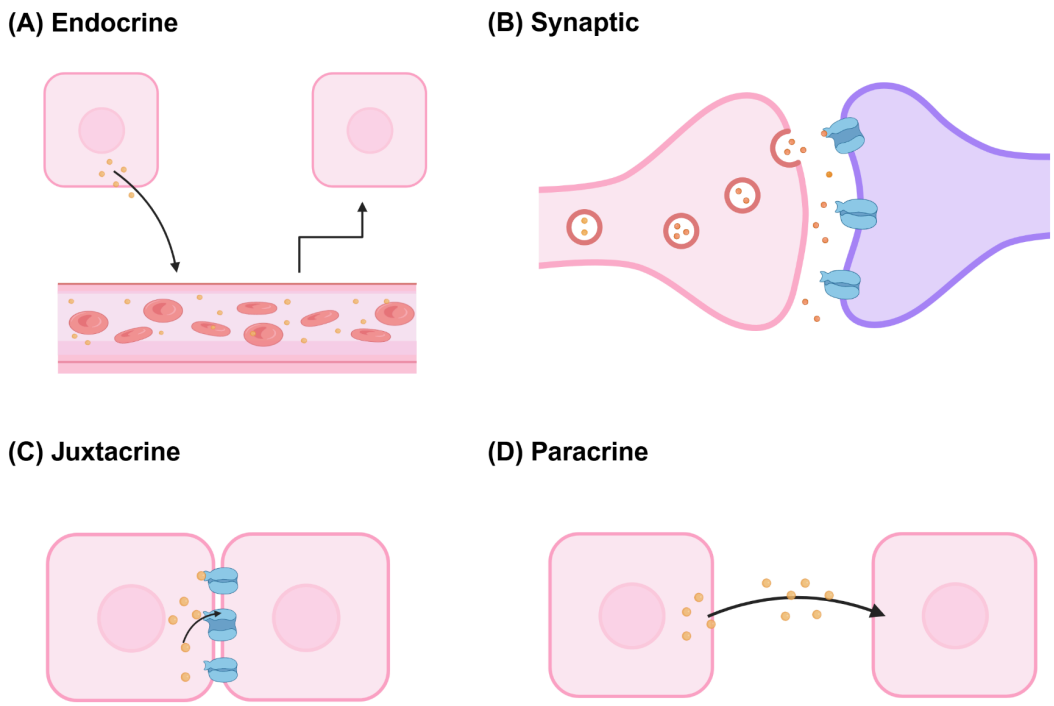

Figure 1. Classic mechanisms of CCC.

(A) Endocrine Signaling. Signal-sending cells release hormones into the bloodstream, allowing them to reach and bind to receptors on target cells. (B) Synaptic signaling. Signal-sending neurons release neurotransmitters, which diffuse across the synaptic cleft and bind to receptors on target cells (C) Juxtacrine signaling. Signal-sending and receiving cells are directly touching one another, allowing for direct binding of signaling molecules to membrane-bound receptors without diffusion. (D) Paracrine Signaling. Signal-sending cells release signaling molecules into ECM where they freely diffuse and make contact with receptors on nearby target cells.

Endocrine Signaling

In endocrine signaling (Figure 1A), signaling molecules known as hormones reach distant target cells through the bloodstream, achieving communication at a distance through non-directed diffusion (Lone et al., 2024; Su et al., 2024). Endocrine cells release hormones in response to physiological cues such as changes in blood glucose concentration, ion levels, or other homeostatic cues. For example, β cells in the pancreas secrete insulin in response to

elevations in blood glucose (Su et al., 2024). Following release, hormones travel through the bloodstream and bind to specific receptors on distant target cells which can be located either on the cell surface or within the cell (Su et al., 2024). The specificity of this interaction is governed by selective expression of receptors on target cells (Su et al., 2024). Signal termination occurs either extracellularly or intracellularly by proteases or via the ubiquitin-proteasome pathway (Lone et al., 2024).

A well-studied example of endocrine signaling is the insulin pathway. In response to elevated blood glucose, β cells in the pancreas take up glucose through glucose transporters (Lone et al., 2024; Haeusler et al., 2017). Once inside the cell, glucose undergoes cellular metabolism, triggering membrane depolarization and subsequent opening of voltage-gated calcium channels (Ca^{2+}) and release of insulin via exocytosis (Tokarez et al., 2018). After release, insulin travels from the pancreas to the liver where approximately 50-80% of insulin is degraded (Tokarez et al., 2018). The remaining hormone exits the liver through the hepatic vein to the heart and enters arterial circulation to reach peripheral tissues (Tokarez et al., 2018). Upon binding its receptor, insulin activates downstream signaling cascades, including the PI3K/AKT pathway, which regulates glucose uptake and other cellular responses (Haeusler et al., 2017). Following activation, this signaling pathway can be terminated in several ways including ligand-induced internalization and lysosomal degradation, recycling back to the cell surface, or serine/threonine phosphorylation (Haeusler et al., 2017).

Synaptic Signaling

Synaptic signaling (Figure 1B) is a specialized form of short-range CCC that enables rapid and highly directional communication between neurons and specific target cells. In this CCC mechanism, presynaptic neurons synthesize signaling molecules known as neurotransmitters, which are packaged and stored in synaptic vesicles prior to release (Su et al., 2024). Upon arrival of an action potential, neurotransmitters are released into the synaptic

cleft, the narrow extracellular space separating the pre- and postsynaptic cells. Following release, neurotransmitters diffuse across the synaptic cleft and bind to specific receptors on the postsynaptic cell (Su et al., 2024). Following receptor activation, signaling can be terminated in one of several ways including reuptake, where neurotransmitters are recycled back to the presynaptic neuron through endocytosis, or are alternatively endocytosed by nearby glial cells, degradation by enzymes, or diffusion, where neurotransmitters diffuse away from the synaptic cleft (Rusakov et al., 2011).

The neuromuscular junction is a well-characterized example of synaptic signaling. In motor neurons, the arrival of an action potential at the presynaptic terminal opens voltage-gated Ca^{2+} channels. The resulting increase in intracellular Ca^{2+} triggers the fusion of presynaptic vesicles containing acetylcholine (ACh) with the presynaptic membrane, releasing ACh into the synaptic cleft (Bouzat and Mukhtasimova, 2018; Petrov et al., 2018). ACh diffuses across the synaptic cleft and binds to nicotinic receptors on the postsynaptic cell membrane. Ligand binding triggers membrane depolarization and opens voltage-gated sodium channels, generating an action potential and initiating muscle contraction (Bouzat and Mukhtasimova, 2018; Petrov et al., 2018). Signaling is terminated primarily through hydrolysis of ACh by acetylcholinesterase, with additional clearance occurring through diffusion of ACh out of the synaptic cleft (Bouzat and Mukhtasimova, 2018). Although synaptic signaling enables rapid and precise communication between presynaptic neurons and specialized target cells, it is a highly specialized form of CCC that does not apply broadly to other cell types. Moreover, synaptic signaling relies on synapses that restrict communication to short distances, making this mechanism unsuitable for long-range signaling.

Juxtacrine Signaling

Similar to synaptic signaling, juxtacrine signaling (Figure 1C) is a mechanism for short-range CCC that requires direct cell-cell contact. Commonly, juxtacrine signaling is

mediated by nondiffusible, membrane-anchored ligands which bind and activate membrane receptors (Bosenberg and Massague, 1993; Singh and Harris, 2005). Following activation of the cognate receptor, signal termination is mediated by recycling of receptor and ligand components or lysosomal degradation (Siebel and Lendahl, 2017).

Of particular relevance to this thesis is Delta-Notch signaling, which is a well-characterized juxtacrine pathway. Signal-sending cells express Delta ligands, which bind to the ectodomains of Notch receptors on signal-receiving cells (Dawson et al., 2025). Binding of the Delta ligand to Notch receptor triggers proteolytic cleavage of the receptor by a disintegrin and metalloproteinase (ADAM10) (Dawson et al., 2025). The resulting receptor fragment is cleaved once more by γ-secretase complex, producing Notch intracellular domain (NICD) which translocates into the nucleus and activates downstream target genes (Dawson et al., 2025; Vanorny and Mayo, 2017). Following activation, the signal is terminated when either the receptor and ligand components are recycled back to the cell surface or targeted for lysosomal degradation (Siebel and Lendahl, 2017). Although juxtacrine signaling enables precise communication between adjacent cells, signal transmission is limited by the requirement that communicating cells must maintain physical contact with each other.

Paracrine Signaling

Paracrine signaling (Figure 1D) is another mechanism for short-range CCC, but unlike synaptic signaling, is not restricted to neurons. In this CCC mechanism, signal-sending cells secrete signaling molecules which diffuse across extracellular space and bind to receptors on nearby target cells (Deguchi et al., 2025; Su et al., 2024). Proteins, peptides, lipids, and gases can all act as mediators of paracrine signaling, with each having its own distinct mechanism of secretion. Some of these mechanisms include shedding via proteases, exocytosis of intracellular vesicles, passive diffusion, secretion through channel opening, and release via

exosomes (Deguchi et al., 2025). Following secretion, signaling molecules diffuse across extracellular space and bind to their cognate receptors.

Unlike the previously described CCC mechanisms, paracrine signal transmission requires signaling molecules to diffuse across extracellular space via passive diffusion. Classically, passive diffusion was thought to homogenize molecular concentrations over time (Turing, 1952). In contrast with this idea, the mathematical modeling of Alan Turing suggested that passive diffusion of signaling molecules could be a mechanism for generating contrast between regions, leading to changes in spatial patterning (Turing, 1952). Building on Turing's work, Lewis Wolpert further postulated that tissues behave in a regulatory manner. He famously analogized this idea to the French flag. If any portion of the flag were removed, all three colors of the flag and their boundaries would still remain intact (Wolpert, 1969). In biological context, even if a portion of tissue was removed, normal patterning would still occur. Wolpert reasoned that cells could achieve the distinct cell fates every time if signaling molecules established concentration gradients which resulted in different thresholds that cells could read, interpret, and respond to (Wolpert, 1969). Subsequent developmental studies provided experimental evidence supporting this theoretical framework.

Perhaps one of the most well-characterized examples of paracrine signaling is the development of the chick limb bud. In normal chicken wings, three digits are formed, which are known as 2, 3, and 4 (Figure 2A) (Tickle, 2005). Strikingly, early grafting experiments demonstrated that grafting of the posterior region of the limb bud to the anterior region resulted in an extra set of digits being formed (Tickle and Towers, 2017; Riddle et al., 1993). Moreover, the extra digits were duplicated, mirror-like images of the original three digits, suggesting that in the posterior region of the limb there exists a zone of polarizing activity (ZPA) (Figure 2B) (Riddle et al., 1993). It remained unclear, however, by which mechanism digit specification occurred.

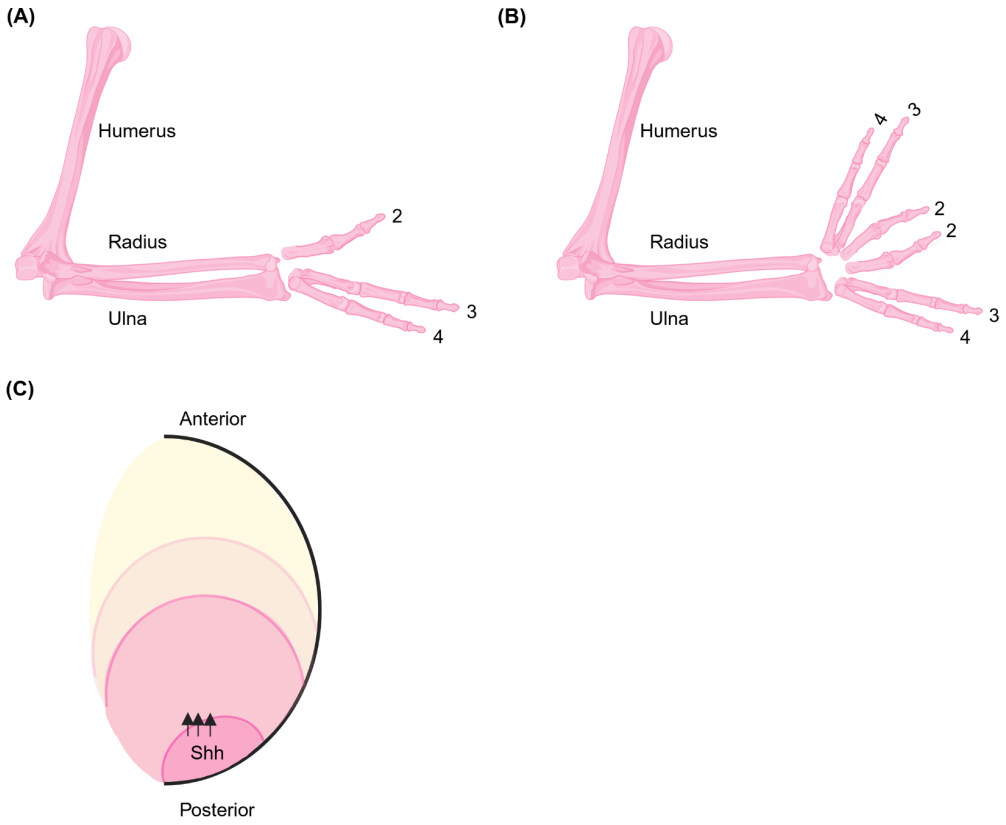

Figure 2. Digit patterning in chick embryos.

(A) Normal chicken wings develop three digits known as 2, 3, and 4 (B) When posterior regions of the limb bud are grafted to the anterior region, digits 2, 3, and 4 are all duplicated in a mirror-like fashion to the original three digits (C Subsequent studies showed that Shh is expressed at higher concentrations at the posterior region and lower concentrations at the anterior region of the limb bud. The differences in Shh concentration specify digit patterning in the developing limb bud.

Consistent with the theoretical framework proposed by Turing and Wolpert, researchers hypothesized that the ZPA may involve a concentration-dependent response. In support of this, researchers found that when fewer ZPA cells were grafted, less ectopic digits were formed. Moreover, the ectopic digits that did form did not resemble the more posterior digits (Harfe et al., 2004). The specific signaling molecule produced by the ZPA was found to be sonic hedgehog

(Shh), an orthologue of Drosophila hedgehog (Hh). When Shh is ectopically expressed in the anterior region of the limb bud, an extra set of digits is formed, similar to early grafting experiments (Riddle et al., 1993). In contrast, when Shh is ectopically expressed at the posterior limb bud, no effect on digit formation is observed (Riddle et al., 1993). This suggested that limb bud cell fate was mediated by cell response to varying concentrations of Shh signaling (Figure 2C).

In addition to Shh concentration, researchers showed that limb bud cell fate is also dependent on Shh exposure duration. When chick limb buds were implanted with beads soaked in a high concentration of Shh and the bead was removed after a period of 10 hr, normal limbs were formed (Harfe et al., 2004). In a follow-up experiment, researchers implanted Shh-treated or buffer soaked beads into limb buds, removed them after a period of 10 hr, then replaced the bead with a second Shh-soaked bead and left it for a period of 16 hr before removal. In the case where limb buds were treated with a buffer-soaked bead which was subsequently replaced with a Shh-soaked bead, an ectopic digit 2 was formed. When limb buds were treated with a Shh-soaked bead which was replaced with a secondary Shh-soaked bead, three or four ectopic digits were formed (Harfe et al., 2004). Additionally, studies using cyclopamine, a small molecule inhibitor of Shh, have shown temporal specification of Shh signaling in the chick limb bud. When cyclopamine is added 4 hr after the onset of Shh signaling, only anterior digit 1 is formed. Only when cyclopamine is added 8 hr after the onset of Shh signaling does a full set of digits form, further supporting the idea that both Shh concentration and duration of exposure control limb bud cell fate (Tickle and Towers, 2017; Harfe et al., 2004).

In addition to Shh signaling, the work of Turing and Wolpert has also been validated in Drosophila embryos. Researchers have shown that the maternal gene bicoid (bcd), which is known to be required for anterior segmented patterning of the head and thorax, also acts in a concentration-dependent manner (Driever and Nusslein-Volhard, 1988). Furthermore, they showed that when bicoid copy number was altered, the subsequent changes in Bicoid protein

gradient affect the boundaries of downstream target genes such as hunchback (hb) (Driever and Nusslein-Volhard, 1988). When Bicoid protein gradient is increased, the concentration threshold for activating hb is achieved more posteriorly. Conversely, when Bicoid protein gradient is decreased, concentration threshold for activating hb is reached more anteriorly (Driever and Nusslein-Volhard, 1988). This work suggests that like Shh, Bicoid protein forms a concentration gradient that cells are able to interpret and respond to, further strengthening the models proposed by Turing and Wolpert.

SPECIALIZED FILOPODIA SIGNALING MECHANISMS

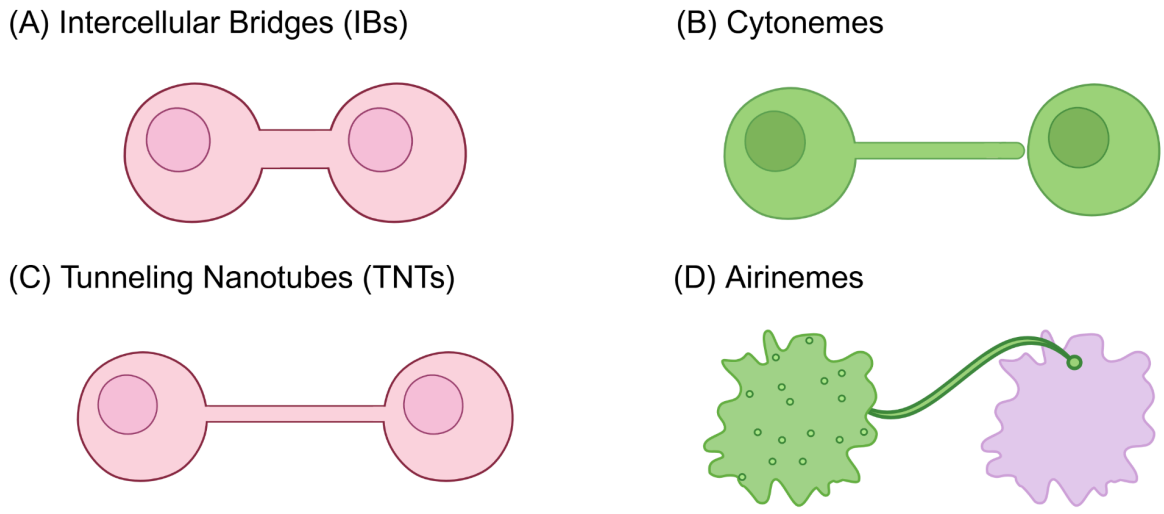

Figure 3. Filopodial-mediated CCC.

(A) Intercellular Bridges. Provide cytoplasmic continuity between cells making the transfer of metabolites, gene products, and organelles possible. (B) Cytonemes. Signal-sending cells extend long, straight filopodia-like structures that make direct contact with target cells. Signaling molecules can be retained within the filament or at its tip. (C) Tunneling Nanotubes (TNTs). Can be close-ended or open-ended. Close-ended TNTs can play a role in electric coupling. Open-ended TNTs provide cytoplasmic continuity between cells and allow the transfer of proteins, vesicles, organelles, etc. (D) Airinemes. Undifferentiated xanthoblasts in the stripe

region of zebrafish extend airinemes which deliver Delta ligands to nearby target melanophores in the interstripe.

While juxtacrine, paracrine, endocrine, and synaptic signaling are well-studied mechanisms for CCC, each mechanism has limitations. Endocrine signaling enables cells to communicate with distant targets via the bloodstream, but communication is relatively slow and lacks spatial precision. Synaptic signaling is a specialized CCC mechanism which enables quick and precise communication, but is used only by neurons to communicate with specialized targets. Juxtacrine signaling is precise, but requires physical contact between cells, limiting signaling range. Paracrine signaling enables cells to communicate with nearby target cells, without requiring direct physical contact between signal-sending and signal-receiving cells. It does, however, require that signaling ligands cross extracellular space via passive diffusion. Although diffusion-based gradients successfully explain many developmental patterning events, several signaling molecules possess biochemical properties that make unrestricted passive diffusion unlikely. For example, Hh proteins undergo several post-translational modifications, including the covalent attachment of a cholesterol moiety to its C-terminus to gain full activity. The addition of a cholesterol moiety anchors Hh to the plasma membrane, thereby restricting free extracellular diffusion, and limiting its range of action (Ramirez-Weber and Kornberg, 1999; Peters et al., 2004). Another example is Transforming growth factor-beta (TGF-β) which is secreted from cells in a tightly bound complex consisting of latency-associated peptide and a latent TGF-β-binding protein, leaving TGF-β in the ECM, until triggered for release. Consequently, local signaling activity depends not only on diffusion but also on regulated activation by proteins such as integrins and proteases (Robertson and Rifkin, 2016). Given these limitations for passive diffusion, it raises the question of whether there are additional mechanisms for CCC that exist in nature.

In addition to diffusion-based mechanisms, researchers have found that signaling molecules can also cross extracellular space via thin, actin/tubulin-rich membranous protrusions called ‘specialized filopodia’. They are produced and extended from signal-sending cells and signal-receiving cells, carrying signaling molecules and/or receptors either within the filament or at its tip, and make direct contact with distant target cells (Figure 3). Four examples of specialized filopodia structures can be found in nature including intercellular bridges, cytonemes, tunneling nanotubes, and airinemes, all of which will be described below in greater detail (Eom, 2020; Kornberg and Roy, 2014b; Fawcett et al., 1955).

Intercellular Bridges

Intercellular bridges (IBs) (Figure 3A) were first observed in the eggs of land slugs (*Limax)*. They were described by researchers as “bridge-like” structures that appeared to connect the cells of dividing eggs (Mark, 1881). Technological advancements, including the development of electron microscopy, enabled researchers to visualize these structures with higher resolution and further characterize them. Electron microscopy revealed that they were formed by incomplete cell division, resulting in the retention of cytoplasmic continuity between dividing cells (Fawcett et al., 1955). Composed of both actin and tubulin, intercellular bridges are cytoplasmic channels that allow direct cytoplasmic continuity, permitting the exchange of signaling molecules, ions, and metabolites (Greenbaum et al., 2011). IBs have been identified in a variety of tissues, including large multinucleate structures called syncytia, and in the developing spermatids of numerous species, including cats, guinea pigs, and hydra, where they play a role in synchronizing differentiation. They also play a role in facilitating the exchange of gene products, metabolites, and even organelles between connected cells (Greenbaum et al., 2011). IBs are ultimately eliminated when the membrane is severed by members of the Endosomal Sorting Complex Required for Transport (ESCRT) in a process called abscission.

Cytonemes

Signaling filopodia were first observed in the primary (PMCs) and secondary mesenchymal cells (SMCs) of gastrulating sea urchins (Miller et al., 1995). Researchers found that PMCs and SMCs actively extend filopodia during migration. In PMCs, for example, filopodia were observed extending and making contact with ectoderm as cells migrated along the wall of the blastocoel (Miller et al., 1995). The filopodia were observed to be long, thin, and enriched in filamentous actin (F-actin). Researchers hypothesized that these filopodia may be necessary for migration. Further investigation and advances in videomicroscopy, however, revealed that migrating PMCs extended few, if any, filopodia (Miller et al., 1995). Instead it was observed that during interactions between PMCs and the ectoderm, filopodia were abundant, leading researchers to speculate that these structures may play a role in CCC. Consistent with this, researchers showed that thin filopodia were extended more frequently in response to ectoderms treated with nickel chloride (NiCl2), a known inhibitor of dorsoventral patterning, consistent with the hypothesis that filopodia respond to developmental patterning cues (Miller et al., 1995).

Subsequent studies of thin filopodia confirmed that these structures were not unique to sea urchins. They were also identified in the wing imaginal discs of Drosophila. Researchers named these structures “cytonemes” (Figure 3B) due to their thin, thread-like appearance and cytoplasmic origins (Ramirez-Weber and Kornberg, 1999). Consistent with studies conducted in sea urchins, researchers noticed that cytonemes were more frequently produced when anterior and posterior wing pouch fragments were cultured next to fragments from the central region of the wing pouch, suggesting that these structures may extend in response to chemoattractants. Subsequent studies have revealed that cytonemes respond specifically to signaling proteins such as *Hh*, Decapentaplegic (*Dpp*), Wingless (*Wg*), *Branchless* (*Bnl*), Notch and Epidermal growth factor (EGFR) (Roy et al., 2011; Liu et al., 2026). Cytoneme filaments range in length from 5 μm to several hundred μm, allowing for precise communication over long distances (Liu et al., 2026). Signaling molecules are trafficked within cytoneme filaments or at their tips,

allowing for direct ligand-receptor contact between signal-sending and signal-receiving cells (Roy et al., 2011). For example, in the air sac primordium of flies, researchers showed that signal-sending cells extend cytonemes containing *Bnl* ligand, which make direct contact with cytonemes on recipient cells containing its cognate receptor, Breathless (Btl) (Du et al., 2018). Evidence that cytonemes mediate direct ligand-receptor interactions across long distances, challenged the long-standing view that signaling molecules reach distant target cells exclusively through passive diffusion.

To date these structures have been identified across diverse species and tissue types, including mouse limb bud cells, the developing neural tube, and the keratinocytes of developing zebrafish (*Danio rerio*), suggesting that cytoneme-mediated signaling is evolutionarily conserved (Ramirez-Weber and Kornberg, 1999; Wang et al., 2025; Hall et al., 2024). Current studies suggest cytoneme retraction, receptor-mediated endocytosis, and decoupling and disassembly may play a role in cytoneme signal termination, although the underlying mechanisms remain incompletely understood (Hall et al., 2024).

Tunneling Nanotubes (TNTs)

Tunneling Nanotubes (TNTs) (Figure 3C) were first identified in the cultured pheochromocytoma PC12 cells of rats (Rustom et al., 2004). PC12 cells were observed extending filopodia-like protrusions that appeared directed towards neighboring cells. Interestingly, researchers noticed that when an extension made contact with a neighboring cell, it connected both cells, resulting in cytoplasmic continuity (Rustom et al., 2004). Researchers named these structures tunneling nanotubes. Unlike IBs, TNTs do not arise from incomplete cytokinesis. Two principal mechanisms of TNT formation have been described: (1) filopodia-like extension and fusion with neighboring cells and (2) cell dislodgement, where migrating cells move apart from one another but remain connected through membrane tethers (Rustom et al.,

2004; Korenkova et al., 2025; Liu et al., 2026). TNTs can extend several hundred micrometers, enabling long-distance communication between cells (Liu et al., 2026).

TNTs are heterogeneous in both composition and morphology. Some are composed solely of F-actin, while others contain both F-actin and microtubules (Liu et al., 2026). Additionally, TNTs may form as either open-ended or closed-ended structures, each associated with distinct cellular functions. Open-ended TNTs, for instance, allow for the transfer of various cargoes including proteins, RNAs, and organelles such as mitochondria (Rustom et al., 2004; Belian and Zurzolo, 2026; Henderson et al., 2023). For example, structured illumination microscopy (SIM) time-lapse imaging of mature murine A20 B cells and mature human tonsil primary B cells demonstrated bidirectional intercellular transfer of vesicular structures through open-ended TNTs. Closed-ended TNTs have a different function, they facilitate electrical coupling between cells via Ca^{2+} diffusion through gap junctions (Belian and Zurzolo, 2026). TNTs have been identified across various organisms and tissue types, including mice, zebrafish, and numerous cultured cell lines (Belian and Zurzolo, 2026; Brou and Zurzolo, 2025; Korenkova et al., 2025). The termination of TNTs, however, remains poorly understood and represents an area of active investigation.

Airinemes

Airinemes (Figure 3D), which are the focus of this dissertation, were first observed in undifferentiated pigment cells of metamorphic-stage zebrafish (Danio rerio) (Eom et al., 2015). Before further discussion of airinemes, it is necessary to first elucidate how zebrafish pigment patterning is formed. Zebrafish exhibit characteristic dark and light stripes along the trunk of the body and fins (Figure 4A). Contributing to the formation of these stripes are three pigment cell types, black melanophores, yellow-orange xanthophores, and iridescent iridophores (Watanabe and Kondo, 2015; Frohnhofer et al., 2013; Parichy et al., 2009). In adult fish, the dark stripes are melanophores with superficial iridophores (S-iridophores) situated on top of them (Frohnhofer et

al., 2013; Watanabe and Kondo, 2015; Parichy et al., 2000). In the interstripe regions are clusters of S-iridophores with yellow xanthophores above them. The specific arrangement of each of these cells is dependent upon the interactions between them.

During development, zebrafish undergo two distinct patterning events, the first of which begins during embryonic development and persists through early larval development, and the second during larval-to-adult transformation (Figure 4B) (Patterson and Parichy, 2013). In the first patterning event, pigment cells derive directly from neural crest progenitors. Xanthophore pigment cells widely distribute themselves over the body flank while melanophores generate primitive stripes at the horizontal myoseptum (Patterson and Parichy, 2013; Parichy et al., 2000). During larval-to-adult transformation, early larval patterning is replaced, with pigment cells deriving from post-embryonic latent precursors (Patterson and Parichy, 2013). Melanophores begin to differentiate and contribute to the dark stripes, while xanthophores and iridophores make up the interstripes (Patterson and Parichy, 2013; Parichy et al., 2000).

Studies involving fish lacking one or more pigment cell types have highlighted the importance of each pigment cell in coordinating patterning (Figure 4D). For example, in nacre (nac) mutants, which lack both larval and adult melanophores, a prominent interstripe is formed but the boundaries of xanthophores and iridophores are irregular (Frohnhofer et al., 2013). Additionally in shady (shd) mutants, which lack iridophores, instead of forming stripes, melanophores cluster together forming spotted patterns (Frohnhofer et al., 2013). In panther/pfeffer (pfe) mutants where xanthophores are lost, melanophores do not organize into stripes and persist as individual spots. Moreover, the loss of xanthophores results in ectopic melanophores in the interstripe (Frohnhofer et al., 2013). The necessity of inter-pigment cell communication has been further validated by transplantation experiments. For example, in shd mutants, stripe patterning is lost, but when cells from nac;pfe double mutants are transplanted into shd mutants, stripe patterning is restored (Frohnhofer et al., 2013). Thus, how the three

pigment cell types interact with one another to regulate pigment patterning has been a long-standing question in the field of developmental biology.

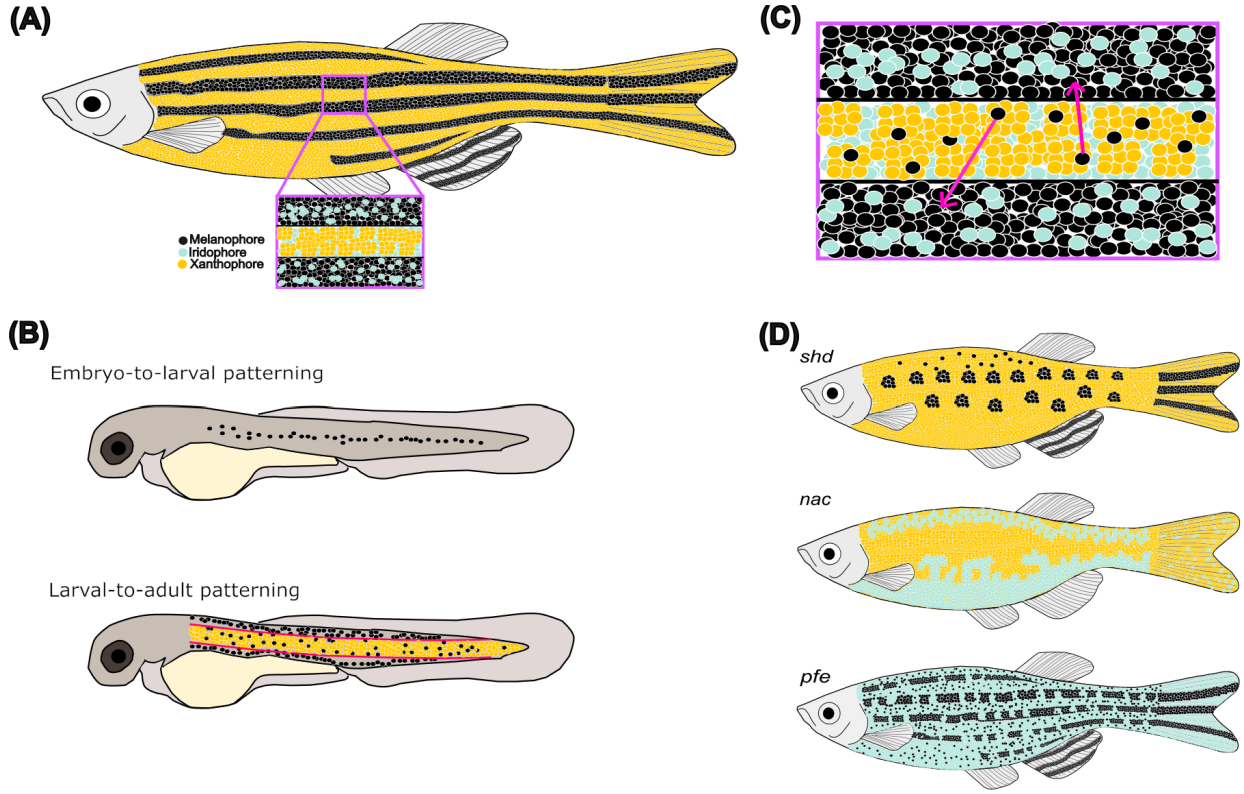

Figure 4. Zebrafish stripe patterning.

(A) Wild-type zebrafish pigment pattern. Melanophores and iridophores make up the stripes while xanthophores and iridophores make up the interstripes. (B) Top – the first pigment pattern event in zebrafish where melanophores populate the horizontal myoseptum. Bottom – the second pigment pattern event in zebrafish where melanophores and xanthophores begin to organize into stripes. Magenta lines indicate the boundaries between the developing stripes. Not pictured: iridophores. (C) Zoomed in image of the zebrafish trunk, showing the movement of interstripe melanophores to the prospective stripe regions. (D) Three zebrafish pigment pattern mutants. Shd mutants lack iridophores and have widespread distribution of xanthophores and spotted patterns of melanophores. Nac mutants lack melanophores and have widespread

distribution of xanthophores and iridophores. Pfe mutants lack xanthophores and have ectopic melanophores as well as broken up stripes. Expression of iridophores is widespread.

Of significance to this thesis are the specific interactions that occur between melanophores and xanthophores. It has been shown that as pigment cells organize into stripes, melanophores are situated in both the interstripe and prospective stripe regions. A portion of these cells die within the interstripe, while the persisting cells migrate into the prospective stripe regions (Parichy et al., 2000). In wild-type fish, melanophores located more dorsally within the interstripe tend to migrate ventrally, to the developing ventral stripe. Meanwhile, melanophores located more ventrally tend to migrate dorsally, contributing to the developing dorsal stripe (Figure 4C) (Parichy et al., 2000). Despite these observations, the cellular mechanisms by which pigment cells communicate to coordinate melanophore positioning during stripe formation remain incompletely understood.

Addressing this knowledge gap, researchers found that undifferentiated xanthophores (xanthoblasts) residing in the prospective stripe region extend long, cellular protrusions during the metamorphic stages when stripe patterning forms. Researchers named these structures “airinemes”, after Iris, the messenger of the gods, and Sir George Biddell Airy, who described the diffraction limits of optical resolution. In contrast with cytonemes, airinemes contain both F-actin and microtubules and exhibit several other distinctive structural and functional characteristics (Table 1) (Eom et al., 2015). Additionally, unlike IBs, cytonemes, and TNTs, airinemes have a meandering morphology, with large vesicles at their tips, which contain Delta-C ligands (Eom et al., 2015).

Table 1. Comparing cytonemes and airineme protrusions based on composition and functionality.

Feature	Cytonemes	Airinemes
Length	5 to several hundred	up to 250 um
Composition	Actin	Actin and Tubulin
Morphology	Straight/No vesicles	Curvy/Vesicle at the tips of filaments
Macrophage Involvement?	No	Yes
Signaling Pathways Involved	Wnt, Notch, Hh, BMP, FGF	Notch
Found in which species?	Drosophila, zebrafish, sea urchins, mice	Zebrafish

Airineme production is temporally restricted to the developmental timepoints where early stripe patterning occurs, which is approximately when fish reach a standardized standard length (SSL) of 7 to 8 (Parichy et al., 2009). Airinemes make contact with and stabilize on embryonic and newly differentiated melanophores residing in the interstripe, promoting their migration into the prospective stripe region (Figure 5). Researchers hypothesized that these structures may play a role in pigment pattern consolidation. Consistent with this, researchers observed that the disruption of airinemes via overexpression of actin regulator cdc42DN resulted in the expression of ectopic melanophores in the interstripe, suggesting that these structures may be necessary for melanophore clearance (Eom et al., 2015).

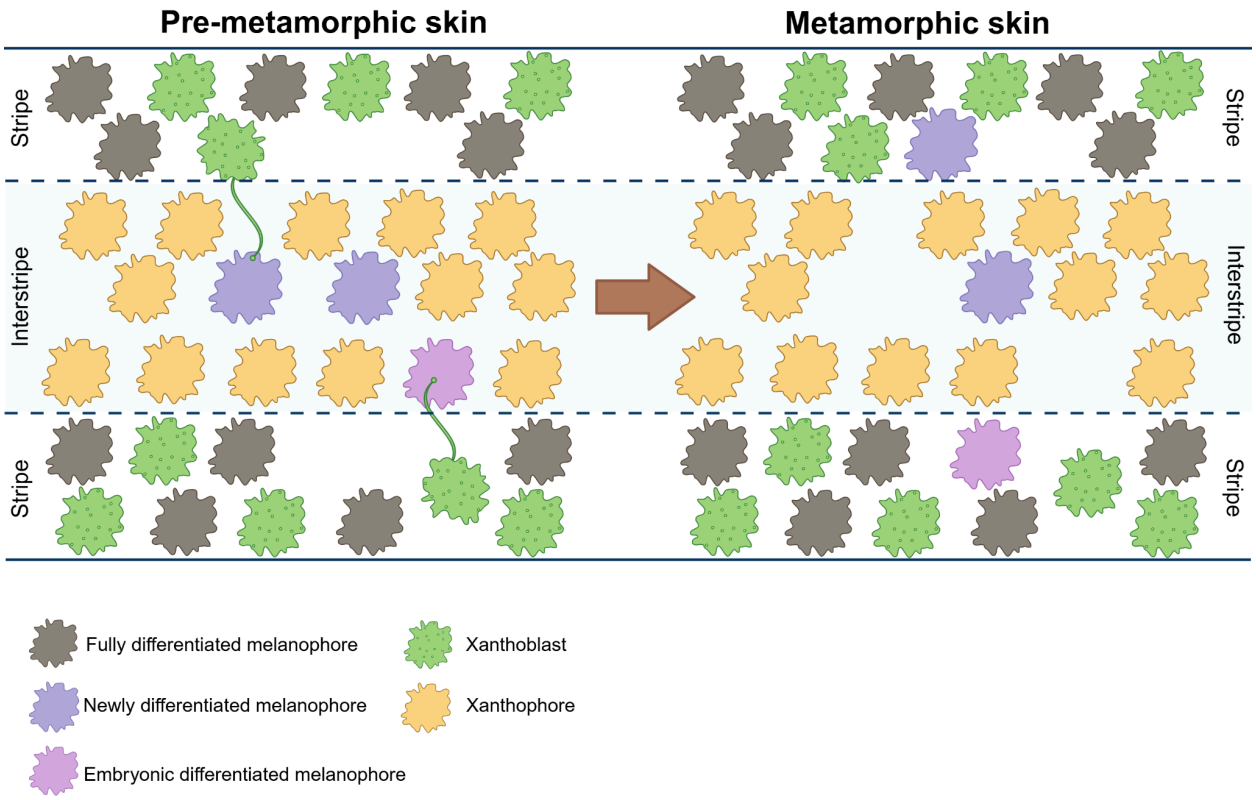

Figure 5. Airineme-mediated melanophore clearance during metamorphosis.

In pre-metamorphic skin, embryonic and newly differentiated melanophores (magenta, purple) are intermingled with mature xanthophores (yellow) in the interstripe region. As the fish develops and enters metamorphosis, immature xanthophores [xanthoblasts] (green) extend airinemes which make contact with embryonic and newly differentiated melanophores, triggering their movement into the stripe regions.

Subsequent studies on airinemes revealed that these structures have a striking dependence on tissue-resident macrophages for signal delivery. Researchers observed that macrophages recognize and make contact with airinemes at their origin points on the surface of xanthoblasts (airineme blebs), and partially engulf them (Eom and Parichy, 2017). The recognition of these structures by macrophages is mediated by exposure of phosphatidylserine (PS), a signal typically associated with apoptotic cell clearance and phagocytosis (Figure 6).

Moreover, macrophages were observed pulling airinemes through extracellular space and depositing them onto target melanophores, leading researchers to hypothesize that macrophages may be necessary for airineme-mediated signaling. Consistent with this, macrophage ablation significantly reduced airineme frequency, leading to melanophore persistence in the interstripe. These findings were particularly novel, as macrophages had been largely associated with immune functions such as phagocytosis, yet were now being implicated in CCC.

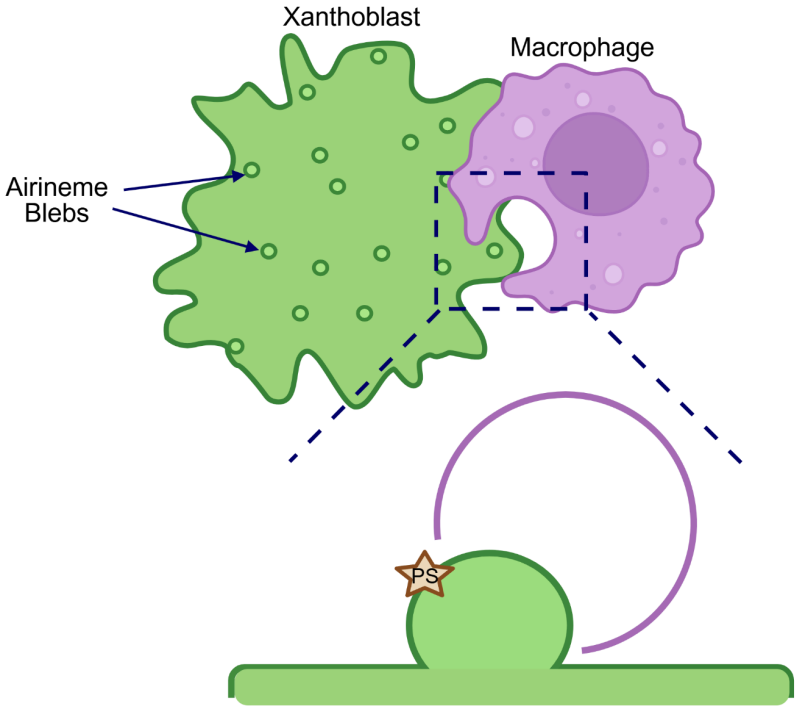

Figure 6. Macrophage recognition of PS-positive airineme blebs.

Migrating macrophages recognize the expression of phosphatidylserine (PS) on airineme blebs. The PS signal, which is normally used by cells to initiate phagocytosis, causes the macrophages to partially engulf airineme blebs and pull them through extracellular space.

To date, airinemes have only been described in zebrafish. Further investigation into the molecular mechanisms underlying airineme-mediated CCC has revealed that Delta-C ligands contained within airineme vesicles bind to Notch receptors on target cells (Eom et al., 2015).

Following signaling, the stabilized airineme vesicle is phagocytosed by a secondary macrophage on the target melanophore, terminating the airineme-mediated interaction (Eom and Parichy, 2017). Despite these findings, several questions regarding airineme biogenesis and function have gone unanswered including (1) which subpopulations of macrophages are involved in airineme-mediated CCC, (2) the specific adhesive interactions that occur between macrophages and airinemes, and (3) which airineme blebs become mature airinemes. Each of these unknowns is addressed in the following chapters.

In Chapter 1 of my thesis, I will characterize two different subpopulations of macrophages in zebrafish skin. I will show that these two subpopulations are distinct from each other both morphologically and behaviorally. Building upon these findings, I will provide evidence showing that among these two subpopulations, one is preferentially involved in airineme-mediated CCC. Lastly, I will provide a mechanistic explanation for how the airineme-associated macrophage subpopulation can migrate through skin tissue to interact with airineme-projecting cells.

In Chapter 2 of my thesis, I will examine in greater detail the specific interactions between macrophages and airineme-producing cells. Building on previous work done in the lab, I will demonstrate how the cell-surface glycoprotein CD44 is necessary for establishing trans adhesive interactions between macrophages and airineme precursors. Moreover, I will show that the loss of these interactions leads to a decrease in airineme frequency, resulting in pigment pattern defects.

In Chapter 3 of my thesis, I establish criteria for the identification of airineme blebs, characterize their spatial and temporal distribution during development, investigate how airineme bleb localization impacts macrophage preference, and determine whether known molecular markers can be used to identify airineme blebs.

CHAPTER 1: A MACROPHAGE SUBPOPULATION PROMOTES AIRINEME-MEDIATED INTERCELLULAR COMMUNICATION IN A MATRIX METALLOPROTEINASE-9 DEPENDENT MANNER

This chapter contains work published as Bowman, R.L., Wang, D., Eom, DS. A macrophage subpopulation promotes airineme-mediated intercellular communication in a matrix metalloproteinase-9 dependent manner. Cell Reports **42**, 112818 (2023). https://doi.org/10.1016/j.celrep.2023.112818

The author contributions to this work are as follows: Conceptualization, R.L.B., D.W., and D.S.E.; Investigation: R.L.B., D.W., and D.S.E.; Writing – original draft, D.S.E.; Writing – review and editing, R.L.B. and D.S.E.; Funding acquisition: D.S.E.; Supervision: D.S.E.

ABSTRACT

Tissue-resident macrophages are heterogeneous and perform location-dependent functions. Skin resident macrophages play intriguing roles in long-distance intercellular signaling by mediating cellular protrusions called airinemes in zebrafish. These macrophages relay signaling molecules containing airineme vesicles between pigment cells, and their absence disrupts airineme-mediated signaling and pigment pattern formation. It is unknown if the same macrophages control both these signaling and typical immune functions or if a separate subpopulation functions in intercellular communication. With high-resolution imaging and genetic ablation approaches, we identify a macrophage subpopulation responsible for airineme-mediated signaling. These seem to be distinct from conventional skin-resident macrophages by their ameboid morphology and faster or expansive migratory behaviors. They

resemble ectoderm-derived macrophages termed metaphocytes. Metaphocyte ablation markedly decreases airineme extension and signaling. In addition, these ameboid/metaphocytes require matrix metalloproteinase-9 for their migration and airineme-mediated signaling. These results reveal a macrophage subpopulation with specialized functions in airineme-mediated signaling, which may play roles in other aspects of intercellular communication.

INTRODUCTION

Intercellular signaling in multicellular organisms is essential for development and homeostasis. Uncontrolled regulation of such signaling causes various human diseases, and altered intercellular communication is a hallmark of aging (López-Otín et al., 2013). Intercellular communication mechanisms include endocrine, paracrine, juxtacrine, and neuronal signaling, with diffusion-based local signaling thought to be a dominant dissemination mechanism in paracrine signaling (Lander et al., 2002; Müller and Schier, 2011; Wolpert, 1973; Wolpert, 2009). In recent years, growing evidence has suggested that cells can communicate with each other via long, thin cellular protrusions extended by signal sending or receiving cells (Eom et al., 2015; Ljubojevic et al., 2021; Roy et al., 2014; Stanganello and Scholpp, 2016). These can be classified based on their cytoskeletal composition, mode of signal delivery, morphology, and more. The growing list of such protrusions that have been identified include cytonemes, tunneling nanotubes, airinemes, intercellular bridges, and migrasomes (Caviglia and Ober, 2018; Daly et al., 2022; González-Méndez et al., 2019; Jiang et al., 2019). They are found in a variety of cell types and species, such as fruit fly, sea urchin, zebrafish, and cultured mammalian cells, and their signaling roles have been functionally validated (Eom, 2020). These signal-carrying protrusions are orders of magnitude longer than typical filopodia and can extend or retract in a highly dynamic fashion. They directly contact target cells and deliver the major

morphogens in many paracrine contexts. In addition, membrane ligand and receptor-mediated intercellular communication, such as Delta-Notch signaling, can also be mediated over long distances via such signaling cellular protrusions (Eom et al., 2015; Cohen et al., 2010; De Joussineau et al., 2003; Huang and Kornberg, 2015).

Previously, we identified a class of signaling cellular protrusion called airinemes critical for interactions between zebrafish pigment cells. They are unique in having large vesicle-like structures at their tips (Eom et al., 2015). They are highly curved, and mathematical models suggest that such complex shapes are optimized to search for target cells (Park et al., 2022). Airinemes preferentially extend from undifferentiated yellow pigment cells, xanthoblasts, and their vesicles contain Delta C ligand, which they deliver to melanophores. Notch activation in target melanophores induces them to migrate from prospective interstripe to stripes, establishing stripe pigment formation. When airineme extensions are inhibited, target melanophores are retained in the interstripe, which leads to failure of proper stripe consolidation. Intriguingly, we have also found that skin-resident macrophages play an essential role in airineme-mediated signaling. Skin-resident macrophages recognize the bulged membrane blebs from the surface of airineme-producing xanthoblasts. These blebs, precursors of airineme vesicles, are grabbed and extracted by macrophages, and, as they migrate, filaments trail behind. Macrophages drag the vesicles along as they migrate through the tissue, deposit them onto the surface of target melanophores, and continue to wander. Thus, the highly curved airineme trajectories observed reflect complex migratory paths of skin-resident macrophages. Deposited vesicles on target melanophores then remain for 1 h or longer, even after filament retraction, an interval presumed to be sufficient for activation of Notch signaling. Afterward, other macrophages phagocytose the deposited airineme vesicles. Thus, macrophages seem to initiate and terminate airineme-mediated long-range Notch-Delta signaling. When the skin-resident macrophages were depleted, airineme extension was

markedly decreased, suggesting that macrophages are essential for airineme extension (Eom et al., 2015; Eom, 2020; Eom and Parichy, 2017).

Macrophages are well described immune cells that phagocytose foreign pathogens and apoptotic bodies, critical for self-defense and maintaining homeostasis (Guilliams et al., 2020; Herbomel and Levraud, 2005; Herbomel et al., 1999; Varol et al., 2015). Tissue-resident macrophages (TRMs) are highly heterogeneous immune populations found in different local niches with unique tissue-specific functions. Unlike conventional macrophages derived from hematopoietic stem cells, TRMs originate in various tissues as shown by fate mapping studies in mice (Ginhoux and Guilliams, 2016; Perdiguero et al., 2015; Schulz et al., 2012). In zebrafish, ectoderm-derived skin resident macrophages are called metaphocytes. Endoderm-derived metaphocytes are also found in the gills and intestine of zebrafish. While metaphocytes express phagocytic genes, they seem not professional phagocytes. Instead, they are specialized for capturing external soluble antigens and transferring them to other immune cells (Lin et al., 2020; Lin et al., 2019).

Prior studies have suggested that, occasionally, the specialized functions of TRMs are not directly involved in immunity (Blériot et al., 2020). During development, they play essential roles in tissue remodeling (Eom and Parichy, 2017; Bohaud et al., 2021). Microglia, macrophages in the postnatal brain in mice, for example, are critical for synaptic pruning (Paolicelli et al., 2011). Other roles for TRMs include blood vessel pruning and regression and fin regeneration in zebrafish (Korn and Augustin, 2015; Petrie et al., 2014). TRMs in skin are essential in airineme-mediated intercellular signaling during postembryonic tissue remodeling (Eom, 2020; Eom and Parichy, 2017).

Both typical and atypical functions of macrophages depend on their ability to migrate. Macrophages can infiltrate most tissues and migrate between cells *in vivo* by degrading extracellular matrix with extracellular proteinases such as matrix metalloproteinases (MMPs), cathepsins, and urokinase-type plasminogen activator (Vérollet et al., 2011). A few studies have

shown that MMP9 activity is critical in macrophage migration in mice and zebrafish (Gong et al., 2008; Travnickova et al., 2021).

Here we use high-resolution live imaging and genetic cell ablation to show that a skin-resident macrophage subpopulation resembling metaphocytes is essential in airineme-mediated intercellular communication between pigment cells in zebrafish. Consistent with this hypothesis, metaphocyte-specific ablation abrogates airineme extension and subsequent signaling. Last, we show that the ability of these macrophage subpopulations to mediate airineme signaling depends on MMP9 activity. Our study shows macrophage heterogeneity and the diversity of cellular functions performed by TRMs in cellular protrusion-mediated intercellular signaling.

RESULTS

Two distinct macrophage subpopulations in zebrafish skin

Skin-resident macrophages play essential roles in airineme-mediated long-range intercellular communication (Eom, 2020; Eom and Parichy, 2017). Here we asked if the same macrophage population performs both its typical innate immune functions and the airineme-mediated signaling roles or if there are other subpopulations of macrophages specialized for airineme signaling. To look for distinct macrophage subpopulations in the zebrafish skin, we first examined mpeg1+ cells, a widely recognized marker specific to macrophages in zebrafish (Ellet et al., 2011). We used a transgenic reporter line, Tg(mpeg1:tdTomato), to visualize these cells at the metamorphic stages where macrophage/airineme-mediated signaling most frequently occurs (Eom et al., 2015; Ellet et al., 2011). High-resolution, confocal time-lapsed imaging revealed two morphologically distinct mpeg1+ macrophages. The first type includes cells that are relatively large, dendritic, and

express a higher level of mpeg1, while the second type is relatively smaller, ameboid in shape, and expresses less mpeg1 (Figures 7A and 7B). These two subpopulations also seemed to traverse different depths of the skin, which led us to ask how deep each population traveled, given that airineme-producing xanthoblasts are restricted to the hypodermis. For this, we measured the distance between each macrophage subpopulation and xanthoblasts. While both subpopulations were spread throughout the skin, there were significantly more ameboid cells located basally in the hypodermis than dendritic macrophages found mostly in the epidermis (Figures 7A and 7C). Based on their morphology and relative locations, ameboid and dendritic macrophages seem to be two distinct subpopulations, which led us to ask if these two subpopulations also behave differently. Studying their migration patterns revealed that ameboid macrophages migrate significantly faster than dendritic macrophages (Figure 7D). Strikingly, the migration speed of the ameboid macrophages matched with the speed of airineme extension, indicating that ameboid macrophages were more likely to interact with airineme vesicles than dendritic macrophages at these metamorphic stages (Eom et al., 2015).

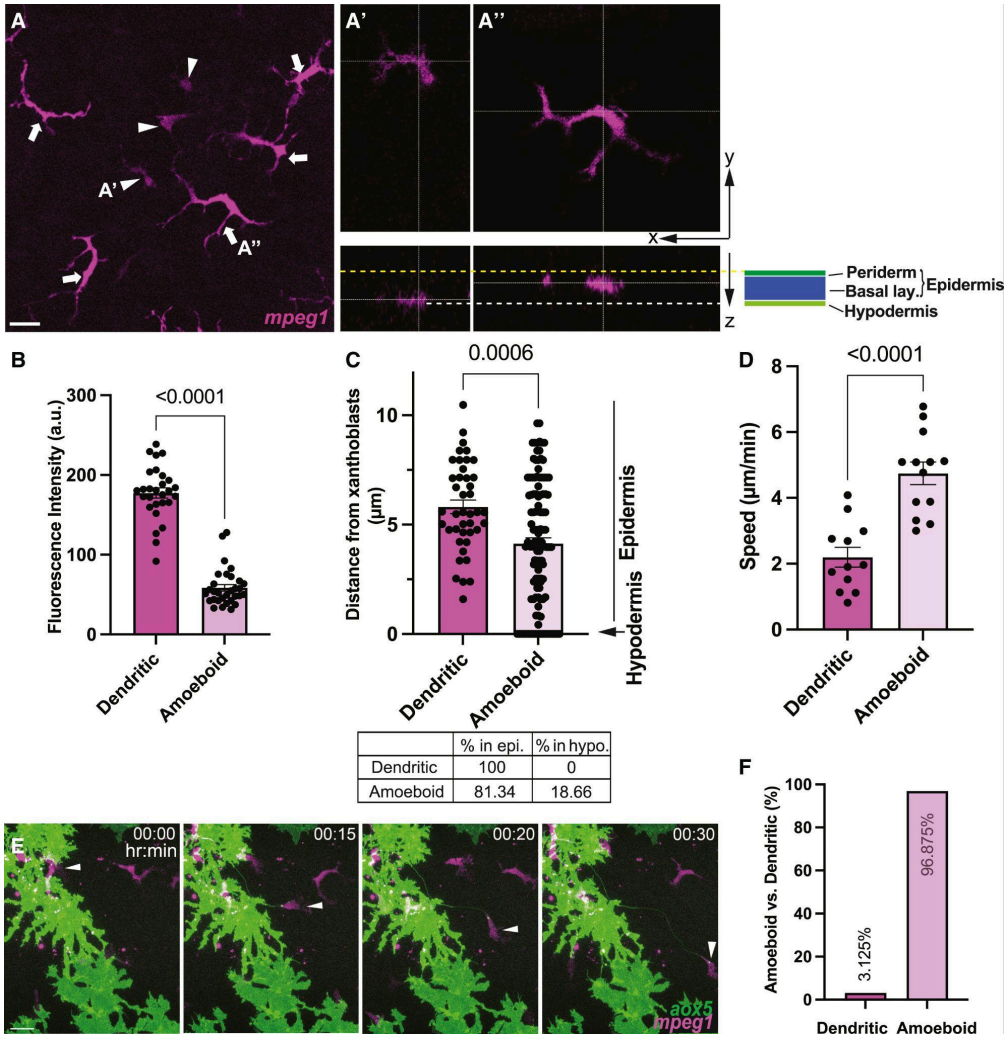

Figure 7. Two distinct macrophage subpopulations in zebrafish skin.

(A) mpeg1+ ameboid (arrowheads) and dendritic (arrows) macrophages shown in maximum projection image. (A') Ameboid macrophages at hypodermis. (A") Dendritic macrophages at epidermis. Yellow dotted line denotes apical margin of epidermis. White dotted line denotes hypodermal layer. Epidermis comprises both periderm and basal layer (see Figure 8). (B) Significantly lower mpeg1 expression in ameboid population compared to the dendritic population; n = 28 dendritic, n = 31 ameboid cells. (C) Ameboid macrophages are localized more basally than dendritic and reach hypodermis (arrow); n = 63 dendritic, n = 122 ameboid cells. (D) Migration speed of dendritic and ameboid macrophages; n = 12 dendritic, n = 13

ameboid cells. (E) Airinemes are pulled by ameboid macrophages (arrowheads). Still images from time-lapse movie. (F) Percentages of airineme-pulling macrophage subpopulations. Statistical significances were assessed by Student t test. Scale bars, 20 μm. Bars display mean, and error bars display SEM.

Ameboid mpeg1+ macrophages interact with airineme vesicles

Indeed, *ex vivo* high-resolution live confocal imaging revealed that ameboid macrophages almost exclusively interacted with airineme vesicles and pulled them as compared with dendritic macrophages (Figures 7E and 7F, arrowhead). Overall, our observations suggest that, among the two distinct macrophage subpopulations in zebrafish skin, the ameboid macrophage subpopulation preferentially interacts with airinemes.

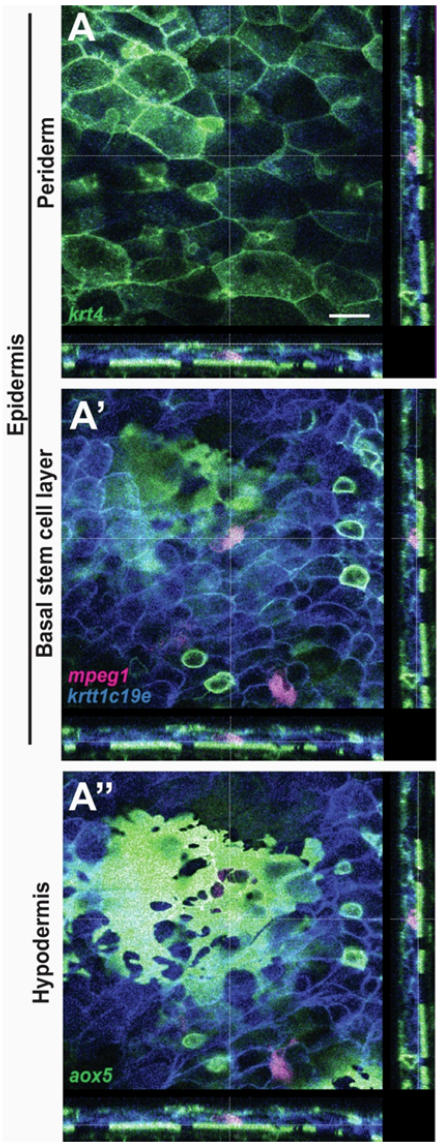

Figure 8. Metamorphic zebrafish skin layers, Related to Figure 7.

(A) Visualization of the peridermal layer using Tg(krt4:palmEGFP). (A') Basal stem cell layer and intermediate layer between the periderm, indicated by Tg(krtt1c19e:lyn-tdtomato), peudo-colored in blue. (A") Hypodermis labeled with the injected xanthophore-lineage marker aox5:palmEGFP. Amoeboid mpeg1+ macrophages (magenta) observed on top of xanthoblasts in the hypodermal layer. Scale bar: 20μm.

As mentioned, airinemes extend most frequently during metamorphic stages (SSL 7.5)

(Eom et al., 2015). Thus, we asked if the ameboid subset of macrophages proportionally expands at these stages. However, both overall skin-resident macrophage (mpeg1+) numbers and the ameboid subpopulation increased in similar proportions, with the ameboid population maintained at 24%–29% of total macrophages during SSL5.5–8.5 (Figure 9A).

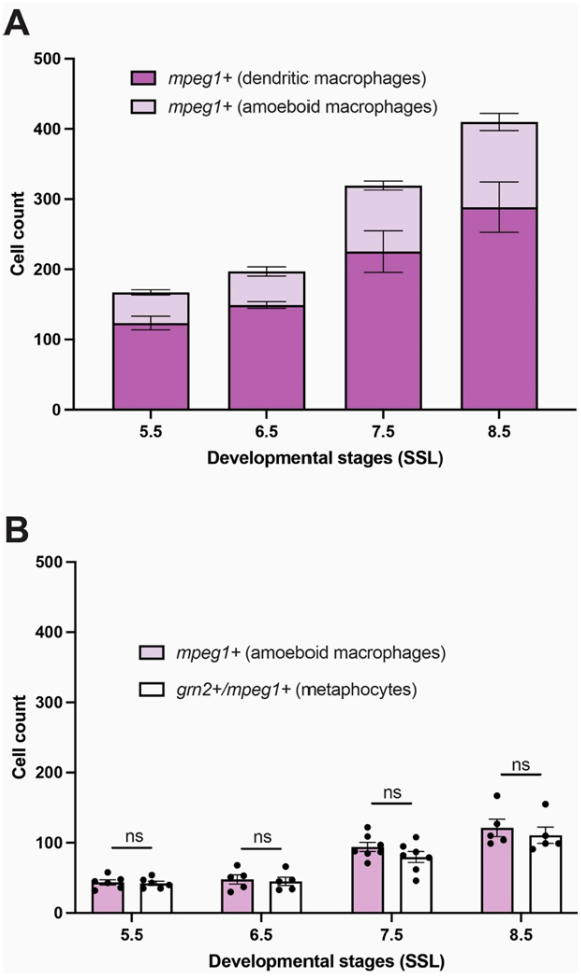

Figure 9. Skin-resident macrophage populations in various developmental stages in zebrafish, Related to Figure 7 and 8.

(A) Developmental stage-dependent cell counts in both dendritic and amoeboid macrophage subpopulation. The proportion of amoeboid macrophages gradually increases as fish develops (~24% at SSL5.5 to ~29% at SSL8.5), but no dramatic expansion at SSL 7.5 (n=8 trunks at SSL5.5, 5 at SSL 6.5, 7 at SSL 7.5, 6 at SSL8.5). (B) Numbers of amoeboid macrophages

(mpeg1+) and metaphocytes (mpeg1+/grn2+) are not differ in various developmental stages in Tg(mpeg1:tdtomato), Tg(mpeg1:tdtomato; grn2:EGFP); n=5 trunks at SSL 5.5, n=5 at SSL 6.5, n=7 at SSL 7.5, n=5 at SSL 8.5.

Airineme-pulling ameboid macrophages overlap with metaphocytes

Traditionally, macrophages have been classified largely into two subpopulations based on their polarization (Guilliams et al., 2020; Davies et al., 2013; Rostam et al., 2017). Classically activated M1 macrophages are round, while alternatively activated M2 macrophages are more elongated (Varol et al., 2015; Vereyken et al., 2011). To determine if airineme-associated ameboid macrophages are M1 like, we examined the M1 marker, tumor necrosis factor alpha (Vereyken et al., 2011; Roh-Johnson et al., 2017). However, neither ameboid nor dendritic macrophages expressed this marker (Figure 10A). This result is consistent with our previous finding that airineme extension is independent of macrophage activation (Eom et al., 2015).

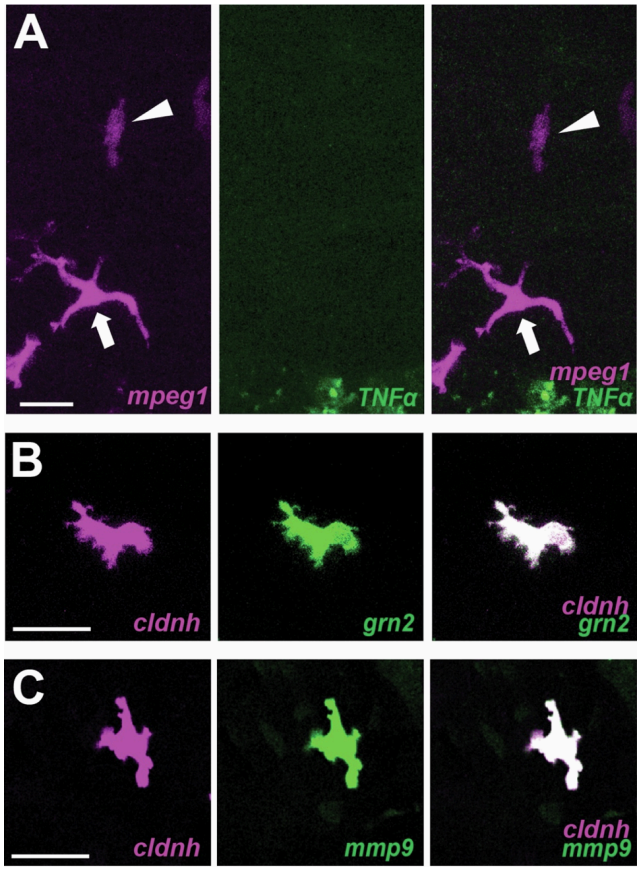

Figure 10. Amoeboid macrophage subpopulation, Related to Figure 9 and 4.

(A) Neither amoeboid (arrowhead) and dendritic (arrow) macrophages are TNFα positive. Tg(mpeg1:tdtomato; TNFα:EGFP) were imaged. (B) Amoeboid macrophage subpopulation express both metaphocyte markers (grn2 and cldnh). (C) Amoeboid macrophages express metaphocyte marker, cldnh and mmp9. cldnh:mCherry construct was injected into Tg(grn2:EGFP) or Tg(mmp9:EGFP). Scale bars: 20μm.

Ectoderm- or endoderm-derived macrophages termed metaphocytes have been recently identified in zebrafish (Lin et al., 2020; Lin et al., 2019; Kuil et al., 2020). Metaphocytes are transcriptionally similar to conventional TRMs in the epidermis and comparable with conventional macrophages, which originate during hematopoiesis (Lin et al., 2019; Davies et al., 2013). Interestingly, it has been suggested that metaphocytes function by delivering antigens

rather than responding to immune-related events. Moreover, their morphology resembles that of the airineme-pulling ameboid macrophage subpopulation (Figures 7A–A′) (Lin et al., 2020; Lin et al., 2019; Kuil et al., 2020). Thus, we hypothesized that metaphocytes promote airineme-mediated intercellular signaling. We first tested whether ameboid macrophages express metaphocyte markers. Metaphocyte-specific reporter lines in which EGFP expression is driven by the promoter of either claudin-h (cldnh) or granulin2 (grn2) were crossed with the macrophage reporter, *Tg(mpeg1:tdTomato)* (Lin et al., 2020; Lin et al., 2019). Tg(cldnh:EGFP; mpeg1:tdTomato) and Tg(grn2:EGFP; mpeg1:tdTomato) both label ameboid mpeg1+ macrophages, while dendritic populations do not express either metaphocyte marker (Figure 11A [arrowheads] and Figure 10B). In addition, the number of ameboid macrophages and metaphocytes (grn2+/mpeg1+) at each developmental stage were similar, suggesting that the airineme interacting ameboid macrophage subpopulation largely overlaps with metaphocytes in zebrafish skin (Figure 9B).

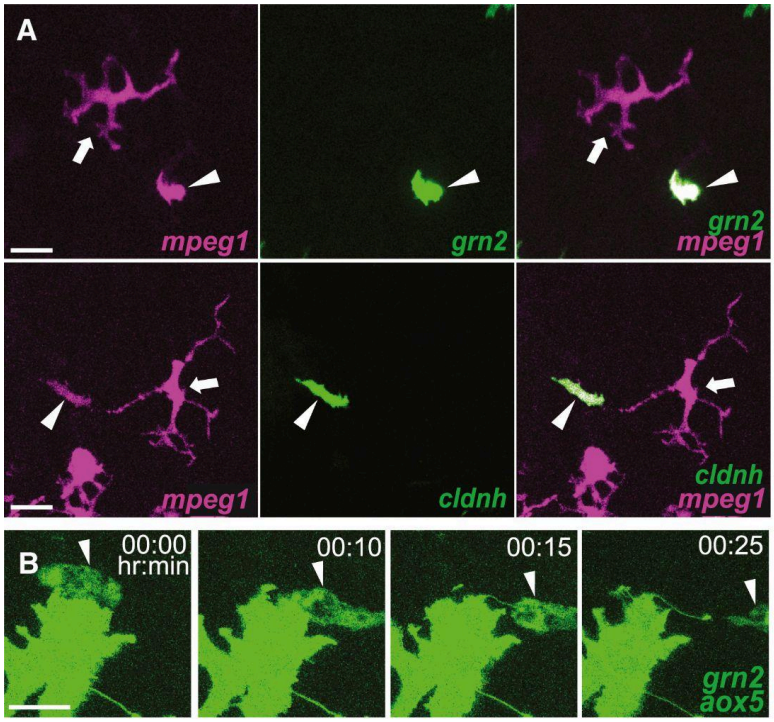

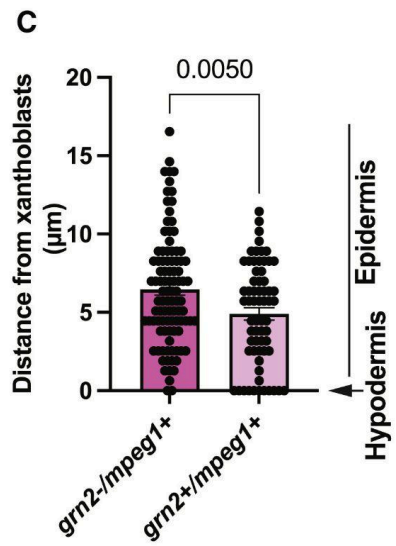

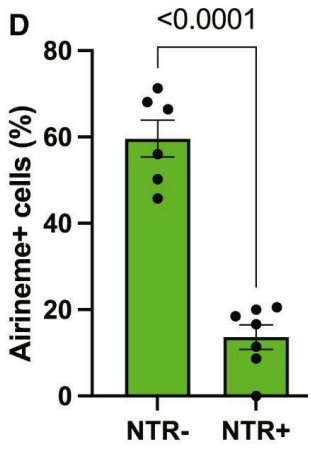

	% in epi.	% in hypo.
Dendritic (*grn2-/mpeg1+*)	97.9	2.04
Amoeboid (*grn2+/mpeg1+*)	83.07	16.9

Figure 11. Airineme pulling ameboid macrophages overlap with ectoderm-derived metaphocytes. (A) Coexpression of metaphocyte markers, grn2 and cldnh, in ameboid macrophage subpopulation (mpeg1+, arrowheads). Note that dendritic (mpeg1+, arrows)

macrophages do not express metaphocyte markers. (B) Still images from a time-lapse movie showing airinemes being pulled by grn2+ metaphocytes. (C) Similar to the ameboid macrophage population, metaphocytes are more frequently located in the hypodermis. (D) Airineme extension was quantified by counting the number of cells that extended airinemes at least once out of all imaged cells. Xanthoblasts of metaphocyte depleted fish (NTR+) were less likely than controls (NTR–) to extend airinemes; n = 6 (controls), n = 7 (depleted) time-lapse positions, three trunks each. The few airinemes extended in the depleted were associated with residual metaphocytes. Statistical significances were assessed by Student t test. Scale bars, 20 μm (A), 10 μm (B). Bars display mean, and error bars display SEM.

We confirmed that metaphocytes associate with airinemes with *ex vivo* live imaging (Figure 11B). Furthermore, their distribution among the skin layers is consistent with that of the ameboid population shown in Figure 7C (see also Figure 11C). Thus, if metaphocytes are an airineme-pulling macrophage subpopulation, we expect a significant inhibition of airineme extension in the absence of metaphocytes. To test this idea, we specifically ablated metaphocytes by using a transgenic line, Tg(grn2:EGFP-v2a-nfsB) that expresses the enzyme nitroreductase (NTR; *nfsB*) in metaphocytes. NTR converts the innocuous prodrug metronidazole into a toxic metabolite that kills cells (Curado et al., 2008; Pisharath and Parsons, 2009). In conditions where metaphocytes were effectively depleted while xanthoblasts and the dendritic macrophage subpopulation remained unaltered (see Methods), we observed a significant reduction in airineme extension (Figures 11D, 12). These findings suggest that the ameboid macrophage subpopulation overlaps with metaphocytes, and they are responsible for airineme-mediated signaling.

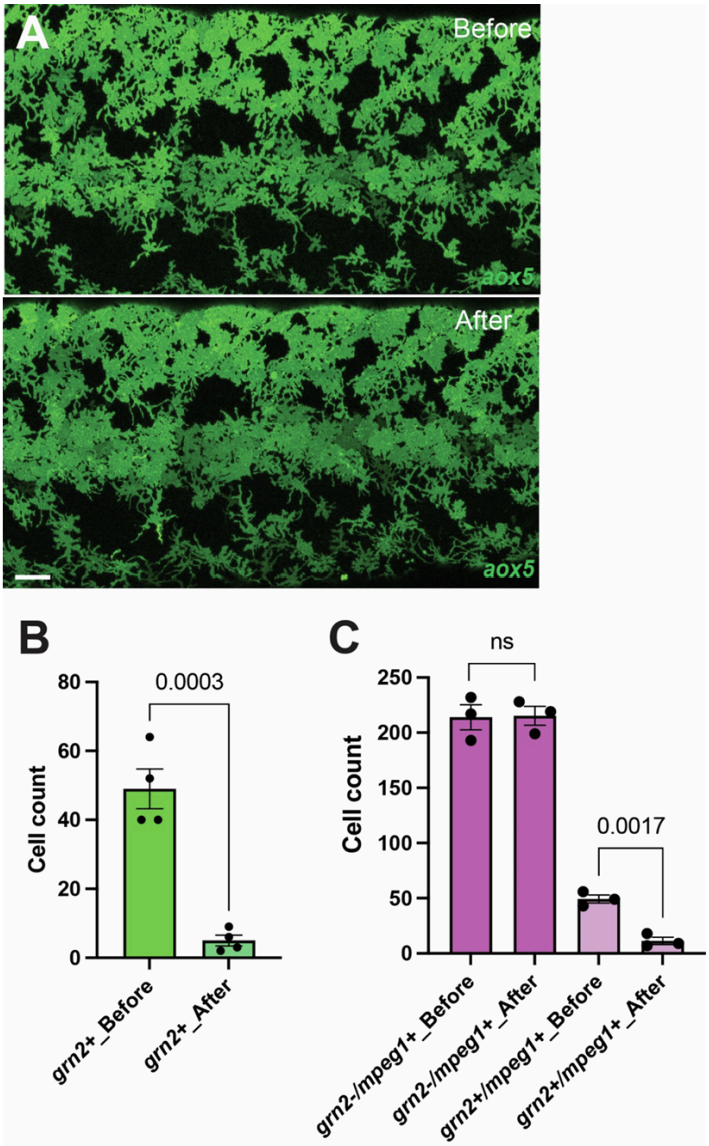

Figure 12. Metaphocyte-specific ablation, Related to Figure 9.

(A) Xanthophore-lineage cells remained unaffected by metaphocyte depletion. (B) Effective ablation of metaphocytes was observed in Tg(grn2:nfsB) fish treated with mtz (n=4, 4 trunks). (C) Metaphocyte depletion was specific, with no significant effect on the dendritic population (n=3 trunks each). Scale bar: 20μm (A).

Metaphocyte-mediated airineme extension is responsible for pigment pattern development

Airineme-mediated signaling is critical for pigment pattern formation. During metamorphosis, signal molecule-bearing airineme vesicles are relayed to target melanophores by macrophages. The target cells receive signals from airineme vesicles and are directed to migrate out of the interstripe and coalesce into the stripes (Eom et al., 2015; Eom, 2020; Eom and Parichy, 2017). Thus, we asked if metaphocytes are responsible for pigment pattern formation. Repeated metaphocyte ablation during pigment pattern development exhibited melanophore retention in interstripe, while the controls had few to no melanophores at SSL 12 (see Methods) (Parichy et al., 2009). The total numbers of melanophores were not altered in either the controls or the experimental, suggesting airineme target melanophore migration into stripes was hindered in the absence of metaphocytes (Figure 13A and 13B). The disorganized pigment patterns observed resembled the phenotypes found when airinemes were inhibited, or all mpeg1+ macrophages in the skin were depleted (Eom et al., 2015; Eom and Parichy, 2017). Our data suggest that metaphocytes are responsible for pigment pattern formation via airineme-mediated signaling.

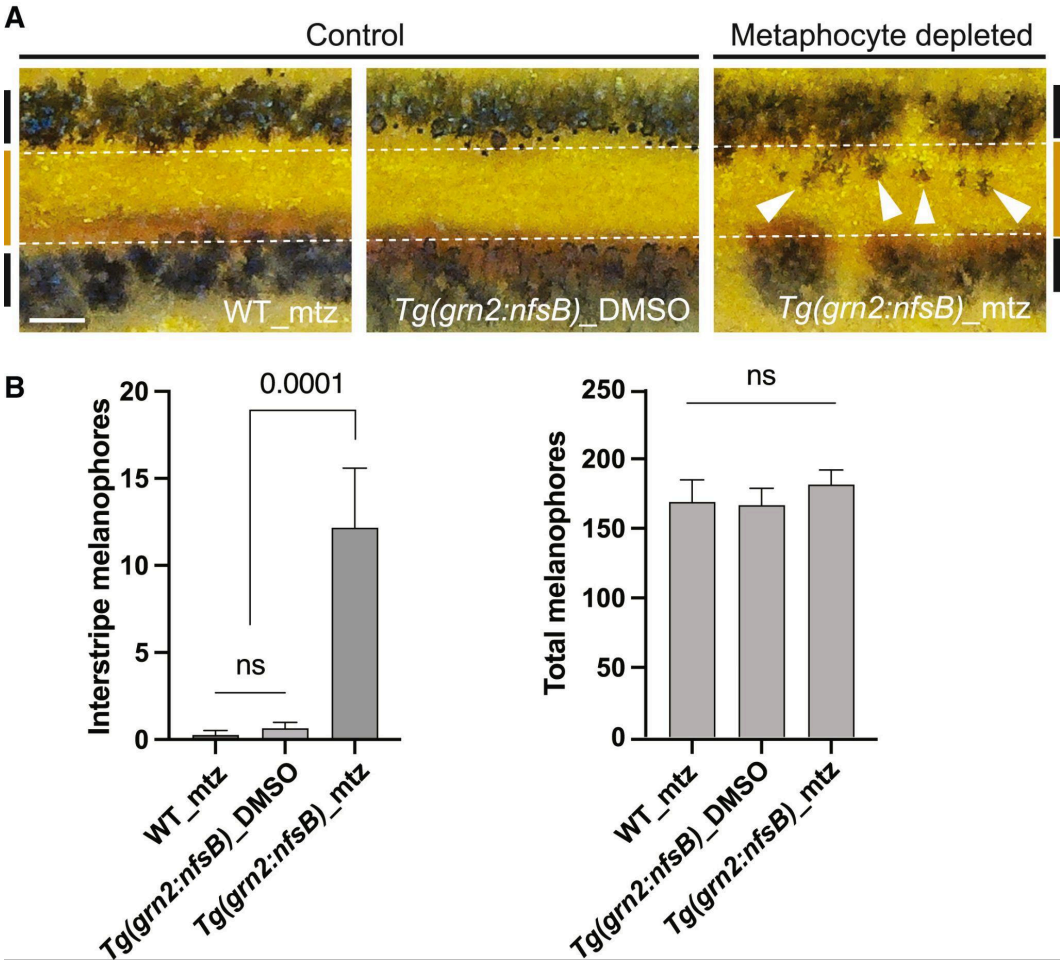

Figure 13. Metaphocyte-mediated airineme extension is responsible for melanophore pattern formation.

(A) In two controls, melanophores reside in the stripe region (denoted by black bars at far left and right, and white dotted lines) and the border of the interstripe (orange bar). Metaphocyte depletion results in melanophores retention in the interstripe (arrowheads). (B) Numbers of melanophores in the interstripe. Metaphocyte-depleted fish (Tg(grn2:nfsB)_mtz) had significantly more melanophores in the interstripe than the controls (WT_mtz and Tg(grn2:nfsB)_DMSO) and displayed a disorganized pigment pattern, although total melanophore numbers did not differ; data are means ± SEM. At stage 12, standardized standard length (SSL); n = 4, WT_mtz, n = 15, Tg(grn2:nfsB)_DMSO, n = 11, Tg(gnr2:nfsB)_mtz trunks. Statistical significances were assessed by Student t test. Scale bar, 200μm (A). mtz,

metronidazole.

Metaphocyte migration and airineme extension are MMP9 dependent

We asked what underlying molecular mechanism differentiates ameboid/metaphocytes from the dendritic macrophage subpopulation. MMPs are a critical component of macrophage migration. Among many MMPs, MMP9 has been suggested to be required for macrophage migration and phagocytosis (Gong et al., 2008; Travnickova et al., 2021). Therefore, we hypothesized that differential MMP9 requirement governs migratory behavior between ameboid/metaphocytes and dendritic macrophages in zebrafish skin. To test if *mmp9* is differentially expressed in these two macrophage subpopulations, we generated Tg(mmp9:EGFP; mpeg1:tdTomato), which labels both macrophage subpopulations and *mmp9*-positive cells (Ando et al., 2017). We observed that ameboid/metaphocytes exhibited strong *mmp9* expression, but the dendritic population showed no detectable reporter expression (Figures 14A and 10C). Consistently, only ameboid/metaphocyte migration speed was significantly decreased in the presence of MMP9 inhibitor. However, dendritic cell migration was unchanged, suggesting that MMP9 is indispensable for ameboid/metaphocyte migration (Figures 14B and 14C and 15). Consistent with airinemes interacting specifically with ameboid/metaphocytes, we observed similar decreases in airineme extension speed in the presence of an MMP9 inhibitor (Figure 14D). Surprisingly, we discovered that airineme extension frequency was significantly compromised upon treatment with this MMP9 inhibitor (Figure 14E). We reasoned this might be caused by the drug preventing metaphocyte infiltration into the hypodermis. Indeed, we observed that the localization of ameboid/metaphocytes along the apical-basal axis was shifted apically in the presence of MMP9 inhibitor compared with controls. Thus, limited access of ameboid/metaphocytes to the hypodermal layer could cause the significant decreases in airineme extension frequency seen in MMP9 inhibitor-treated

animals (Figure 14F). Last, we observed that the airineme extension was significantly reduced when we ablated *mmp9*+ cells with Tg(mmp9:nfsB-EGFP) (Figures 14G, 15) (Ando et al., 2017). Furthermore, we observed similar melanophore retention in the interstripe of *mmp9*+ cell-depleted fish, resembling the effect seen in metaphocyte depletion (Figure 16). However, we did not detect any significant changes in the proportion of both macrophage populations or morphological alterations, as assessed by quantifying the number and the length of protrusions in both populations (Figures 17A, 17B, and 17C).

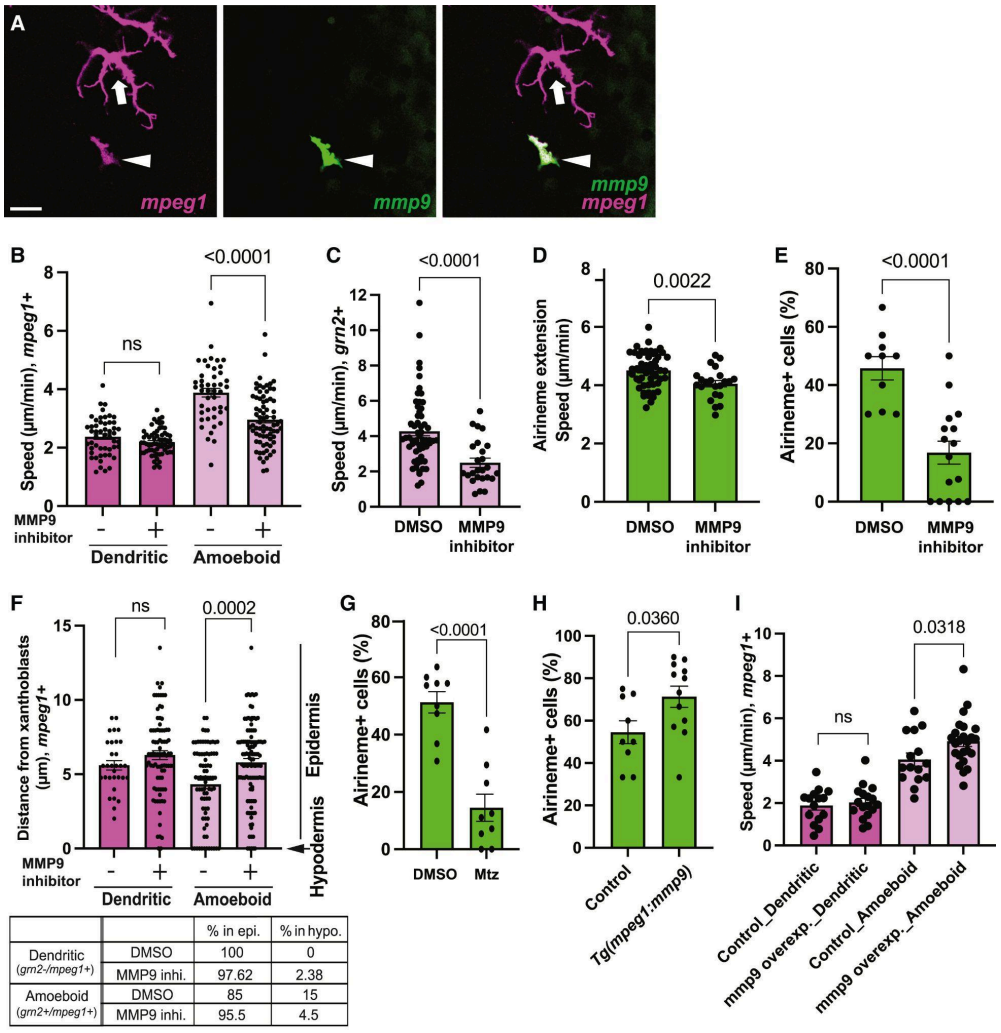

		% in epi.	% in hypo.
Dendritic (*grn2-/mpeg1+*)	DMSO	100	0
	MMP9 inhi.	97.62	2.38
Amoeboid (*grn2+/mpeg1+*)	DMSO	85	15
	MMP9 inhi.	95.5	4.5

Figure 14. MMP9 manipulations affect metaphocyte migration speed and airineme extension frequency.

(A) Differential expression of MMP9 in ameboid (arrowhead) and dendritic macrophage

*subpopulation (arrow). (B) Treatment with an MMP9 inhibitor significantly reduced the migration speed of the ameboid macrophage subpopulation, while dendritic macrophages were unaffected (n = 51, 64, 45, and 68 cells), four trunks each. *The n numbers represent the experimental groups from left to right order for all the following figure legends. (C) Consistently, the migration speed of grn2+ metaphocytes was significantly decreased in MMP9 inhibitor-treated fish (n = 28 and 31 cells; 4 trunks each). (D) Airineme extension speed reduction in the presence of MMP9 inhibitor (n = 53 and 23; 3 trunks each). (E) Xanthoblasts in MMP9 inhibitor treated fish had fewer airinemes than controls (n = 10 and 16 time-lapse positions; 4 and 5 trunks). (F) Localization of ameboid macrophages were shifted more apically upon MMP9 inhibitor treatment but no effects on dendritic macrophage subpopulation (n = 31, 45, 80, and 75 cells; 3, 3, 4, and 5 trunks). (G) Xanthoblasts in mmp9+ cell-depleted fish had fewer airinemes than controls (n = 9 and 9 time-lapse positions; 3 trunk each). (H) Xanthoblasts in mmp9 overexpressed fish extend more airinemes than controls (n = 9 and 12 time-lapse positions; 4 trunk each). (I) The migration speed of the ameboid macrophage subpopulation was increased, while dendritic macrophages remained unaffected (n = 15, 17, 15, and 24 cells; 3 trunk each). Scale bar, 20 μm (A). Statistical significances were assessed by Student t test. Bars display mean, and error bars display SEM.*

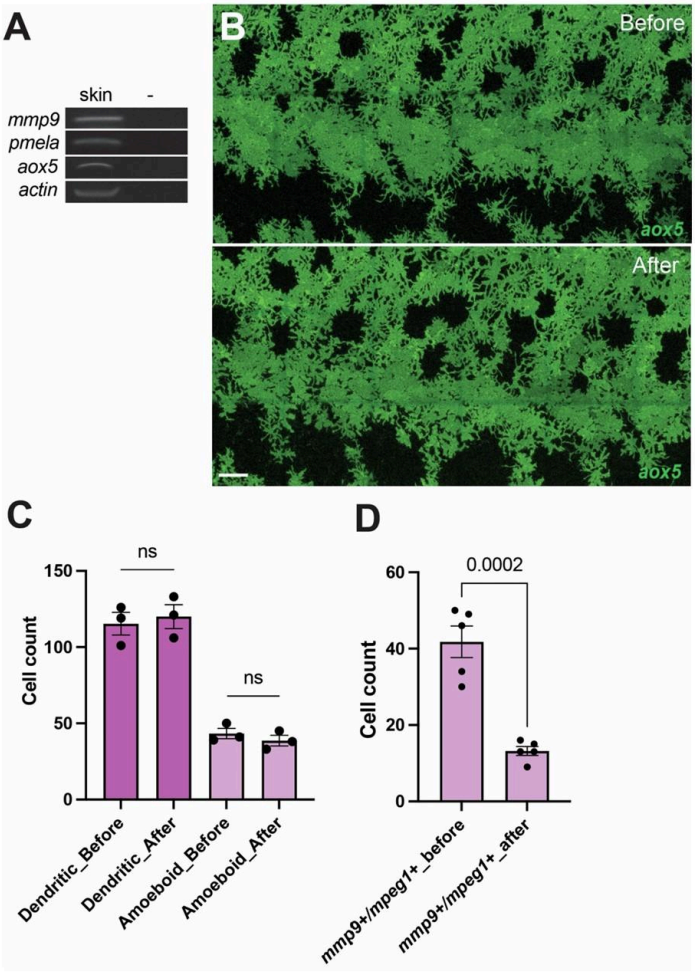

Figure 15. MMP9 inhibitor treatment does not affect the number of xanthophore-lineage cells and mpeg1+ macrophages, Related to Figure 4.

(A) RT-PCR revealed endogenous mmp9 expression in metamorphic zebrafish skin. aox5 marks xanthophore lineages, pmela for melanophores, and actin control. (B) Xanthophore-lineage cells are unaffected by MMP9 inhibitor treatment. (C) Neither dendritic nor amoeboid macrophage numbers were changed upon MMP9 inhibitor treatment (n=3 trunk each). (D) Effective ablation of mmp9+ cells was observed in Tg(mmp9:nfsB) fish treated with mtz (n=5 trunk each). Scale bar: 20μm (B).

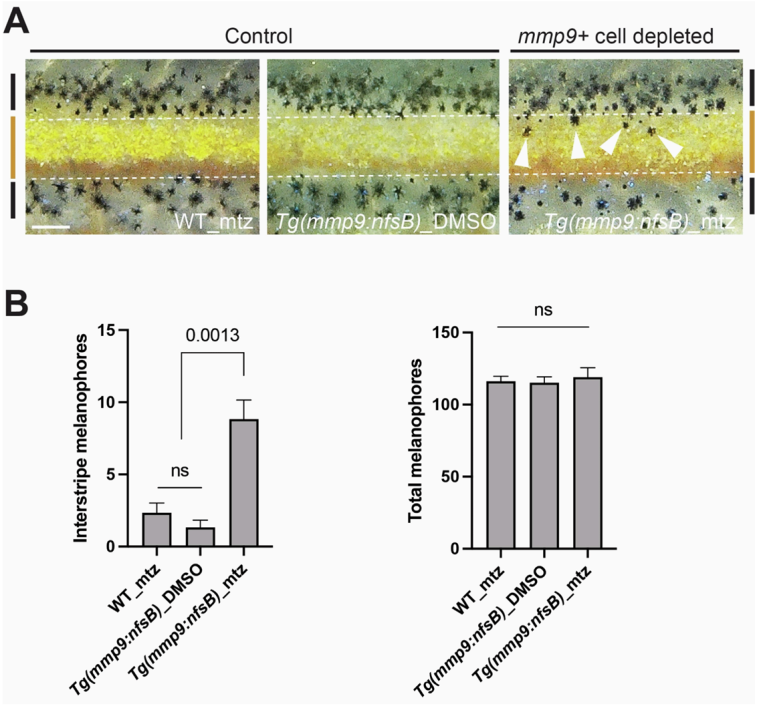

Figure 16. Melanophore retention in the interstripe of mmp9+ cell depleted fish, Related to Figure 4.

(A) In two controls, melanophores reside in the stripe region (denoted by black bars at far left and right, and white dotted lines) and border the interstripe (orange bar). In contrast, mmp9+ cell depletion results in melanophores retention in the interstripe (arrowheads). (B) Numbers of melanophores in the interstripe. mmp9+ cell depleted fish (Tg(mmp9:nfsB)_mtz) had significantly more melanophores in the interstripe than controls (WT_mtz and Tg(mmp9:nfsB)_DMSO). However, there were no significant differences in total melanophore numbers; data are means ± SEM. At stage 12 standardized standard length (SSL) (n=6, WT_mtz, n=6, Tg(mmp9:nfsB)_DMSO, n=6, Tg(mmp9:nfsB)_mtz trunks). Statistical significances were assessed by Student's t-test. Scale bar: 200μm (A).

To further confirm the role of *mmp9* in metaphocytes, we overexpressed *mmp9* in both macrophage subpopulations, *Tg(mpeg1:mmp9-v2a-nVenus)*. We observed an increase in

airineme extension in the *mmp9* overexpressed fish (Figure 14H). Expectedly, the migration speed of the ameboid population was significantly increased, and the dendritic cells remained unaffected in this transgenic line (Figure 14I). However, both ameboid and dendritic macrophage populations did not show significant changes in their localization within the skin layers and proportion of both macrophage populations (Figures 17D and 17E). We speculate that the increased migration speed of metaphocytes enhances their chances of contacting airineme blebs on the surface of xanthoblasts, resulting in a higher incidence of airineme extension.

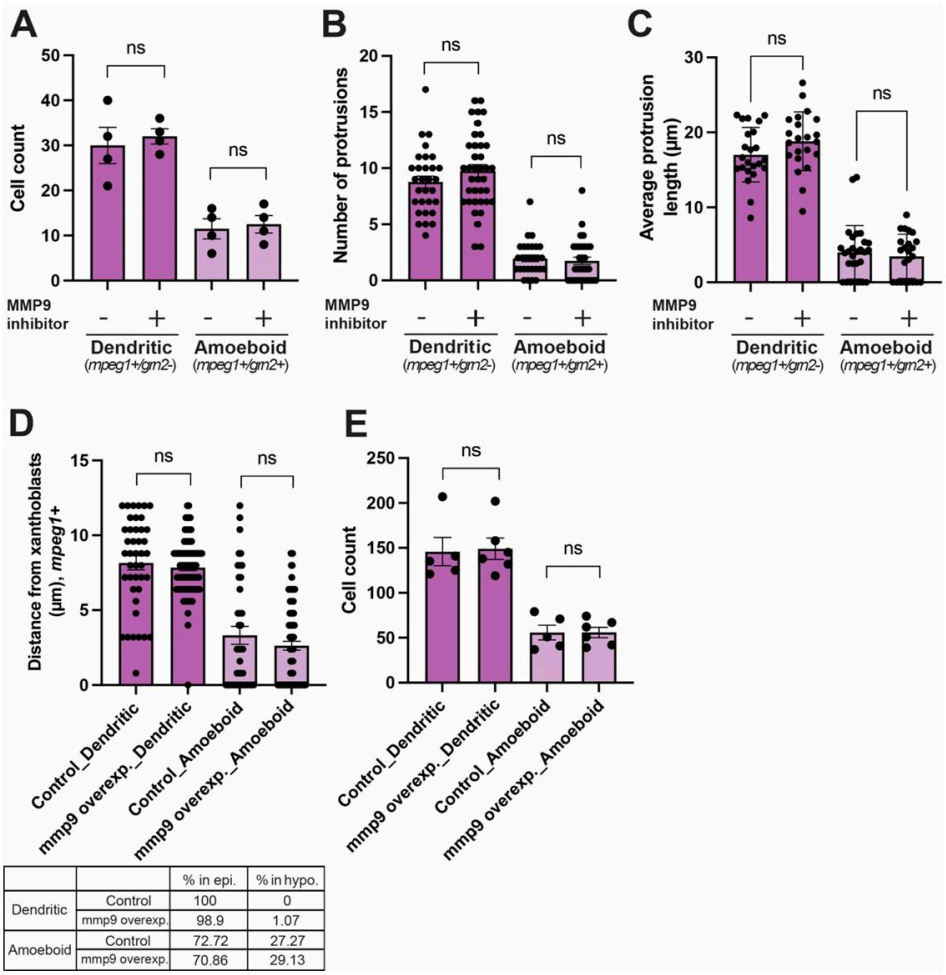

		% in epi.	% in hypo.
Dendritic	Control	100	0
	mmp9 overexp.	98.9	1.07
Amoeboid	Control	72.72	27.27
	mmp9 overexp.	70.86	29.13

Figure 17. Melanophore retention in the interstripe of mmp9+ cell depleted fish.

(A) In two controls, melanophores reside in the stripe region (denoted by black bars at far left

and right, and white dotted lines) and border the interstripe (orange bar). In contrast, mmp9+ cell depletion results in melanophores retention in the interstripe (arrowheads). (B) Numbers of melanophores in the interstripe. mmp9+ cell depleted fish (Tg(mmp9:nfsB)_mtz) had significantly more melanophores in the interstripe than controls (WT_mtz and Tg(mmp9:nfsB)_DMSO). However, there were no significant differences in total melanophore numbers; data are means ± SEM. At stage 12 standardized standard length (SSL) (n=6, WT_mtz, n=6, Tg(mmp9:nfsB)_DMSO, n=6, Tg(mmp9:nfsB)_mtz trunks). Statistical significances were assessed by Student's t-test. Scale bar: 200μm (A).

Together, these findings suggest that ameboid/metaphocyte-mediated airineme signaling depends on MMP9 activity.

DISCUSSION

Several features of airinemes distinguish them from other signaling cellular protrusions, such as cytonemes and tunneling nanotubes. One of the most striking differences is that airinemes require macrophages as delivery vehicles for relaying airineme vesicles to the target melanophores intermingled with non-target cells (Daly et al., 2022; Eom, 2020). Airinemes may need these cells to help them extend through the densely packed tissue environment, especially airinemes with large vesicles at their tips (Hirata et al., 2003).

Our study suggests that ameboid macrophages/metaphocytes in metamorphic zebrafish skin specifically perform such a delivery role in airineme signaling. We have shown that the behaviors of this macrophage subpopulation correlate with airineme-mediated signaling since they migrate faster and can infiltrate deeper into hypodermis than the dendritic subpopulation. Our study also suggests that MMP9-dependent migration of metaphocytes is critical for

airineme-mediated intercellular communication. However, dendritic macrophages do not seem to express MMP9, and their migration was not affected by both MMP9 inhibitor treatment and *mmp9* overexpression. Additionally, it has been observed that *mmp9* does not play a role in the fate determination between metaphocytes and dendritic macrophages (Figures 17A and 17E). There are 26 MMP-orthologs in zebrafish and 24 different MMP genes in humans. Thus, it will be interesting to study whether combinatorial MMP expression control or fine-tune macrophages' migratory behaviors in different subpopulations or disease contexts. This idea is supported by studies showing that MMP-mediated macrophage infiltration is associated with various human pathophysiologies (Lagente et al., 2009; Nighot et al., 2021; Pedersen et al., 2015).

Our results are consistent with previous reports showing that ameboid/metaphocytes are specialized for antigen delivery, but less reactive to immunogenic processes (Lin et al., 2019). Metaphocytes in metamorphic zebrafish skin are also specialized for airineme vesicle delivery. However, from our previous studies, we observed that metaphocytes engulf and eliminate the airineme vesicles when they are docked on non-target cells, suggesting they are still phagocytes. However, airineme vesicles are not phagocytosed while airinemes extend and when they contact target cells (Eom et al., 2015; Eom and Parichy, 2017). Thus, it seems that the target recognition mechanism is tightly linked to determining metaphocytes to phagocytose the airineme vesicles. We speculate that these ameboid/metaphocytes control target recognition in airineme-mediated intercellular communication. One possibility is that metaphocytes scan the surfaces of cells along their migration paths and deposit airineme vesicles onto specific target melanophores. Thus, cell membrane receptor/ligand interactions between metaphocytes and target cells might provide a cue for target cell specificity, and this might prevent airineme vesicle phagocytosis. Alternatively, it is possible that interactions between airineme vesicles and target cell membranes underlie this target specificity and metaphocytes simply act as delivery vehicles.

However, the molecular mechanisms behind metaphocytes' target-specific behaviors remain to be elucidated.

We identified two distinct macrophage subpopulations in metamorphic zebrafish skin, consistent with previous descriptions of metaphocytes in adult zebrafish (Lin et al., 2020; Lin et al., 2019). However, the localization of metaphocytes in adults is near the peridermal epidermis and conventional dendritic macrophages stay relatively more basally, while we find that our ameboid, metaphocyte-like cells lie more basally than dendritic macrophages (Figures 7C and 11C). This discrepancy may simply reflect stage-dependent differences in these cell types. In our study, we have shown that airinemes are most frequently observed during metamorphosis, where robust tissue remodeling, including pigment pattern formation, occurs, but their extension frequency diminishes as fish develop (Eom et al., 2015). Thus, it is conceivable that metaphocytes repurpose their function to relay antigens in adult zebrafish skin.

It is important to note that, in rare cases, we observed ameboid macrophages that did not express metaphocyte markers. We also observed that *grn2*+ metaphocytes displayed a varying degree of reporter expression in the transgenic lines. This may reflect their maturation status or suggest the existence of additional macrophage subpopulations. However, these non-metaphocyte ameboid macrophages make up a much smaller portion than most ameboid/*grn2*+ metaphocytes in metamorphic zebrafish skin.

Taken together, our study revealed that airineme-vesicles interact specifically with an ameboid macrophage subpopulation, most likely ectoderm-derived macrophages called metaphocytes. Moreover, metaphocytes are responsible for airineme-mediated signaling via MMP9 activity-dependent fashion. Our study suggests that macrophage involvement in airineme-mediated signaling is not an experimental side effect but highly regulatory and that airinemes achieve intercellular signaling by using TRM heterogeneity and versatility. Our study also demonstrates the complex and cooperative nature of the cellular protrusion-based intercellular signaling between pigment cells in zebrafish skin. Requirements for macrophages

in other cellular protrusion-mediated signaling modalities are unknown, which is an interesting avenue for future studies.

MATERIALS AND METHODS

RESOURCE AVAILABILITY

Lead contact

Further information and requests for resources and reagents should be directed to and will be fulfilled by the lead contact, Dae Seok Eom (dseom@uci.edu).

Materials availability

This study generated two zebrafish transgenic lines, *Tg(mpeg1:mmp9-v2a-nVenus)irrt15Tg* and *Tg(krt4:palmEGFP)irrt1Tg*, and a construct *cldnh:mCherry*. They are available from the lead contact without restriction.

Data and code availability

- All original data reported in this paper will be shared by the lead contact upon request.
- No original code has been generated in this study.
- Any additional information required to reanalyze the data reported in this paper is available from the lead contact upon request

EXPERIMENTAL MODEL AND SUBJECT DETAILS

Zebrafish

Fish were maintained at 28.5 C, 16:8 L:D. Zebrafish were wild-type AB^{wp} or its derivative WT (ABb), as well as, *Tg(cldnh:EGFP)*, *Tg(grn2:EGFP;mpeg1.1:LoxP-DSRedx-LoxP-EGFP), Tg(grn2:EGFP-v2a-nfsB)*^{hkz}, provided by Z. Wen, *Tg(tyrp1b: palmmcherry)*$^{wp.rt}$ *Tg(mpeg1:Brainbow)*^{w201}, which expresses tdTomato in the absence of Cre-mediated

recombination; *Tg(mmp9:EGFP)*^{tyt206}*, Tg(mmp9:EGFP-v2a-nfsB)*^{tyt207}, provided by A. Kawakami. *Tg(krtt1c19e:lyn-tdtomato)*^{sq} was provided by T. Carney. Experiments were performed prior to the development of secondary sexual characteristics, so the number of females and males used in the study could not be determined, however, all stocks used generated approximately balanced sex ratios, so the experiments likely sampled similar numbers of females and males. All animal work in this study was conducted with the approval of the University of California Irvine Institutional Animal Care and Use Committee (Protocol #AUP-22–023) in accordance with institutional and federal guidelines for the ethical use of animals.

METHOD DETAILS

Transgenesis and transgenic line production

Tg(krt4:PALMegfp)

We acquired Gateway 5 entry vector p5E:krt4 construct from T. Carney. This construct was assembled with its middle entry vector, pME:PALMegfp and p3E:polyA into pDest backbone. *Tg(mpeg1:mmp9-v2a-nVenus)*: To examine the impact of *mmp9* overexpression in both dendritic and ameboid macrophage subpopulations, we generated *mpeg1:mmp9-v2a-nVenus* construct using Gateway assembly into Tol2 backbone and injected into WT(ABb). The *mmp9* cDNA (ZDB-GENE-040426–2132) was isolated out of cDNA from WT(ABb). The resulting constructs included a Tol2 sequence which allowed for utilization of the Tol2 transposon system to randomly incorporate the plasmid of interest into WT(ABb) fish.

cldnh:mcherry construct

The same *cldnh:EGFP* construct was subcloned to generate *cldnh:mCherry* to label *cldnh* positive cells other than green fluorescent protein using Gibson assembly.

Drug treatments

Metaphocyte long-term ablation

Fish were treated with drugs during dark cycles and then washed and changed into system water without drugs at light cycles. *Tg(grn2:EGFP-v2a-nfsB)* fish were split into two groups: DMSO control and metronidazole (Mtz)-treated experimental, and WT(ABb) were used as an additional control group to assess off target effects of Mtz. Fish in Mtz groups were given 7mM of Mtz dissolved in DMSO. Fish from each group began treatment starting from SSL 7.0 and continued to receive treatment until reaching SSL 12.0. During treatment fish were fed 3 times per day using 1–2 drops of brine shrimp. Upon reaching SSL 12.0, fish were euthanized using tricaine and embedded into a 1% agarose gel in a sterile Petri dish. Colored images were taken using a Koolertron LCD digital microscope.

Overnight treatments

Metaphocytes were ablated overnight for time lapse imaging using fish injected with *aox5:palmEGFP* into *Tg(grn2:EGFP-v2a-nfsB)*. Fish were treated with either 10 mM Mtz or DMSO as a control. MMP9+ cells were ablated for time lapse imaging using fish injected with *aox5:palmEGFP* into *Tg(mmp9:EGFP-v2a-nfsB)*. Fish were treated with either 5 mM Mtz or DMSO as a control. MMP9 inhibition for overnight time lapse was using fish injected with *aox5:palmEGFP* into *Tg(mpeg1:tdtomato)* or WT. Fish were treated with either 0.1 mM MMP9 inhibitor II or DMSO as a control.

Time-lapse and still imaging

Ex vivo imaging of pigment cells and macrophages was done using a Leica TCS SP8 confocal microscope equipped with a resonant scanner and two HyD detectors. Time-lapse images taken at 5-min intervals over a span of 10 h. Overnight time-lapse imaging was performed when larvae reached SSL 7.5 except where indicated. NTR ablation experiments were performed by administering either 10 mM Mtz into *Tg(grn2:EGFP-v2a-nfsB)* or 5 mM, *Tg(mmp9:EGFP-v2a-nfsB)* overnight for airineme extension frequency measures.

Cell counts and distributions

Pigment pattern

Fish were imaged upon reaching SSL 12.0. Images were taken of the entire trunk and were later cropped to include only the area underneath the dorsal fin. Total melanophore counts and melanophores in the interstripe region were quantified using the cell counter plugin from ImageJ. Total number of melanophores and melanophores in the interstripe region were averaged.

Developmental stage cell population counts

Dendritic and ameboid cell populations were quantified using the cell counter plugin from ImageJ. Dendritic cells were determined by several characteristics including *mpeg1*+ (ameboid & dendritic macrophages) reporter expression level, cell morphology, migration speed, branching. Total numbers for each group were averaged across individuals. *gnr2*+ cells (metaphocytes) were also quantified using the cell counter plugin of ImageJ and averaged across individuals.

Axial localization of skin-resident macrophages

Localization of ameboid and dendritic populations was determined using z stack information provided by images taken on Leica TCS SP8 confocal microscope. Distance from the hypodermis was measured and determined by co-injected *aox5:palmEGFP*+ cells. Thus, smaller numbers indicate closer to the hypodermis and larger numbers closer to the epidermis.

Reverse transcription polymerase chain reaction (RT-PCR) analysis of gene expression in zebrafish skin

Fish at SSL 7.5 were skinned (n = 10) and treated with 500uL of 0.05% Trypsin in phosphate buffer saline (PBS) for 3 min at 28°C to dissociate the cells. Cell dissociation was subsequently stopped by adding 500uL of 1X Defined Trypsin Inhibitor (DTI). Tissues were further lysed at room temperature through the addition of 1 mL TRIzol reagent. After, the sample was treated

using 0.2 mL chloroform and the top layer was extracted to obtain total RNA. Samples were cleaned using cold isopropanol and ethanol washes. cDNA was synthesized using a SuperScript III cDNA synthesis kit (ThermoFisher). Amplifications were 35 cycles *(actin, mmp9, aox5, pmela)* at 98°C, 30s; 98°C, 10s; 72°C, 10s; 72°C, 20s; 72°C, 2m; 4°C, hold. *Aox5 (*5′-CAGAGTGACGTCTGGTCTTACG-3′; 5′-GGACATCTGATAGCCACACTTG-3′), *pmela* (5′-CTCGGAGTTCTGTTTTTCGTTT-3′, 5′-AAGGTACTGCGCTTATTCCTGA-3′), *actin* (5′-CTTGCTC CTTCCACCATGAA-3’; 5′-CTGCTTGCTGATCCACATCT-3′), *mmp9* (5′-CATTAAAGATGCCCTGATGTATCCC-3’; 5′-AGTGGTGGTCCGTGGTTGAG-3′).

QUANTIFICATION AND STATISTICAL ANALYSIS

Statistical analyses were performed using GraphPad Prism software version 9.0 for Mac (GraphPad Software, San Diego, CA, USA). Continuous data were displayed as mean ± SEM, using an unpaired two-tailed Student’s t-test.

CHAPTER 2: CD44 FACILITATES ADHESIVE INTERACTIONS IN AIRINEME-MEDIATED INTERCELLULAR SIGNALING

This chapter contains work published as Bowman, R.L., Kim, J., Parsons, M.J., Eom, DS. CD44 facilitates adhesive interactions in airineme-mediated intercellular signaling. Front. Cell Dev. Biol. **13**, 1522710 (2025). https://doi.org/10.3389/fcell.2025.1522710.

The author contributions to this work are as follows: Conceptualization, R.L.B and D.S.E.; Methodology, J.K., M.J.P, D.S.E.; Formal Analysis, R.L.B., J.K., M.J.P, D.S.E.; Investigation, R.L.B., J.K., D.S.E.; Resources, M.J.P. and D.S.E; Validation, R.L.B., J.K., M.J.P., D.S.E.; Writing – Original Draft, R.L.B. and D.S.E; Writing – Review and Editing, R.L.B., J.K., M.J.P., D.S.E.; Supervision, D.S.E.; Project Administration, D.S.E.; Funding Acquisition, D.S.E.

ABSTRACT

Specialized cellular protrusions facilitate local intercellular communication in various species, including mammals. Among these, airinemes play a crucial role in pigment pattern formation in zebrafish by mediating long-distance Notch signaling between pigment cells. Remarkably, airinemes exhibit large vesicle-like structures at their tips, which are pulled by macrophages and delivered to target cells. The interaction between macrophages and Delta-ligand-carrying airineme vesicles is essential for initiating airineme-mediated signaling, yet the molecular details of this interaction remain elusive. Through high-resolution live imaging, genetic *in vivo* manipulations, and *in vitro* adhesion assays, we found that adhesive interactions via the extracellular domain of CD44, a class I transmembrane glycoprotein, between

macrophages and airineme vesicles are critical for airineme signaling. Mutants lacking the extracellular domain of CD44 lose their adhesiveness, resulting in a significant reduction in airineme extension and pigment pattern defects. Our findings provide valuable insights into the role of adhesive interactions between signal-sending cells and macrophages in long-range intercellular signaling.

INTRODUCTION

Proper signal delivery between cells is essential for development and homeostasis in multicellular organisms. Even single-celled organisms communicate with each other for their survival in specific environments (Combarnous and Nguyen, 2020). Consequently, understanding the mechanisms of intercellular signaling has been a central topic in biology and medicine for decades. Although several cell-to-cell communication modalities have been identified, recent advancements in microscopy and techniques have enabled us to uncover previously unappreciated mechanisms across various species and contexts. Specialized cellular protrusions, also known as signaling filopodia, are one of them. These are long, thin cellular extensions similar to neuronal axons or dendrites but are present in non-neuronal cells, spanning from sea urchins to mice *in vivo* (Daly et al., 2022; Hall et al., 2024; Kornberg and Roy, 2014a). This suggests that signaling filopodia may represent a general mechanism of intercellular communication in living organisms.

Distinguished by their cytoskeletal composition, morphology, and signaling mode, these can be categorized into several types with different terms, including cytonemes, airinemes, tunneling nanotubes, and others (Daly et al., 2022; Eom, 2020; Zhang and Scholpp, 2019). All of them are extended by either signal-sending or signal-receiving cells, or both, establishing physical contact with their specific target cells. Signaling molecules, including major

morphogens, are moved along the protrusions, or are packaged into vesicles and delivered (Kornberg and Roy, 2014b; Roy et al., 2011; Yamashita et al., 2018).

Airinemes were initially identified in pigment cells in developing zebrafish (Eom et al., 2015). Airinemes are frequently extended by unpigmented yellow pigment cells called xanthoblasts, particularly during metamorphic stages when pigment pattern development takes place (Figures 16A,B). Unlike fully differentiated xanthophores, xanthoblasts display bleb-like bulged membrane structures at their surface, serving as the origin of airineme-vesicles at the tips of the airinemes (Figure 17A, yellow arrowheads). The initial step of airineme-mediated signaling involves the interaction of a specific skin-resident macrophage subpopulation, termed metaphocytes, with these blebs (Bowman et al., 2023; Eom and Parichy, 2017). This subset of macrophages plays an essential role in airineme-mediated intercellular communication, a unique feature not reported in other signaling cellular protrusions that typically involve signal-sending and -receiving cells for their signaling events. Live imaging experiments have shown that macrophages engulf the blebs, pulling them as they migrate, with filaments extending behind the migrating macrophages (Bowman et al., 2023; Eom and Parichy, 2017) (Figure 17A, white arrowhead). Subsequently, macrophages release the blebs (now referred to as airineme vesicles) onto the surface of target melanophores (Eom, 2020).

The target cells for airinemes are embryonic melanophores and newly differentiating melanophores, rather than fully differentiated melanophores. These target melanophores are situated in the developing interstripe of the metamorphic zebrafish and receive Notch signals through airineme vesicles containing the DeltaC ligand. It has been suggested that the Notch signal activated by airinemes subsequently triggers Kita signaling, which is essential for melanophore migration and survival (Eom et al., 2015; Parichy et al., 1999). Consequently, target melanophores within the interstripe gradually migrate out of the interstripe and coalesce into the stripes (Patterson and Parichy, 2019). Inhibiting airineme extension or depleting macrophages leads to melanophore retention in the interstripe, emphasizing the critical role of

airinemes and macrophages in orchestrating pigment patterning during zebrafish development (Bowman et al., 2023; Eom et al., 2015; Eom and Parichy, 2017).

In the initial step of airineme/macrophage-mediated signaling, it is probable that mechanisms exist for macrophages to recognize and adhere to airineme blebs. A previous study showed that airineme blebs express a high level of phosphatidylserine, a phospholipid used as an ‘eat-me’ signal for macrophages to initiate phagocytosis (Davies et al., 2013; Eom and Parichy, 2017; Ginhoux and Guilliams, 2016). However, the necessity and molecular nature of adhesive interactions between these structures remain unknown.

CD44 is a class I transmembrane adhesion protein with broad expression across various cell types, including lymphocytes, immune cells, fibroblasts, neuronal cells, and more (Ponta et al., 2003). Notably, its overexpression in several cancer stem cells suggests a significant role in cancer development and progression (Chen et al., 2018; Weng et al., 2022). Different CD44 isoforms exhibit distinct functions in interacting with ligands and other binding molecules, emphasizing their role in diverse tumor progression in humans (Gunthert et al., 1995; Wang et al., 2009).

Like Notch receptors, CD44 can undergo cleavage by membrane type 1 matrix metalloprotease and subsequent cleavage by γ-secretase. This sequential cleavage releases the intracellular domain (ICD) of CD44 into the cytosol, allowing its translocation into the nucleus. The CD44-ICD functions as a transcription factor that induces genes associated with cell survival, migration, metastasis, and others (Miletti-Gonzalez et al., 2012; Skandalis, 2023). Meanwhile, the extracellular domain (ECD) of CD44 facilitates adhesion with other cells expressing CD44 or interacts with several ligands in the extracellular matrix (ECM). One such ligand is hyaluronic acid (HA), and CD44-HA interaction is known to regulate cytoskeleton dynamics and tumor progression in some contexts. Furthermore, CD44-ECD-mediated homophilic cell-to-cell adhesion is well-documented in tumors and can facilitate tumor cell aggregation and metastasis (Kawaguchi et al., 2020; Liu et al., 2019). The multifaceted roles of

CD44 highlight its significance in both physiological and pathological cellular processes, making it a crucial focus in cancer research and therapeutic development.

In this study, we demonstrate that CD44, through its extracellular domain, plays a crucial role in the adhesive interaction between the blebs of airineme-producing xanthoblasts and airineme-pulling macrophages. This interaction is critical for airineme-mediated intercellular communication and the formation of pigment patterns in zebrafish.

RESULTS

Gene knock-out of cd44a using CRISPR/Cas9 results in a substantial decrease in airineme extension

To identify candidate genes involved in adhesive interaction between macrophages and airineme vesicles, we conducted gene expression profiling between xanthophores and airineme-producing xanthoblasts. Among several adhesion proteins analyzed, cd44a exhibited the most significant gene expression difference between these two cell types (log2 fold change of 10.13). To investigate the role of cd44a in airineme-mediated signaling, we designed a single-guide RNA (sgRNA) against cd44a and injected it into one-cell-stage embryos with Cas9 protein, along with an *aox5:palmEGFP* construct to label the cell membrane and airinemes of xanthophore-lineages. Control groups included embryos that received cd44a sgRNA injection without Cas9 protein and embryos injected only with Cas9 protein into wild-type embryos. The fish were raised until metamorphic stages (SSL 7.5), when airineme extension is most frequent (Eom et al., 2015; Parichy et al., 2009). We counted the number of cells extending airinemes out of the total cells imaged at 5-min intervals over a period of 10 h during overnight time-lapse

imaging (Eom et al., 2015). This method was also used for subsequent quantifications to measure airineme extension frequency. Our results showed that embryos injected with cd44a sgRNA/Cas9 had a significant reduction in airineme extension compared to the two controls, suggesting that cd44a may be required for proper airineme signaling (Figure 18).

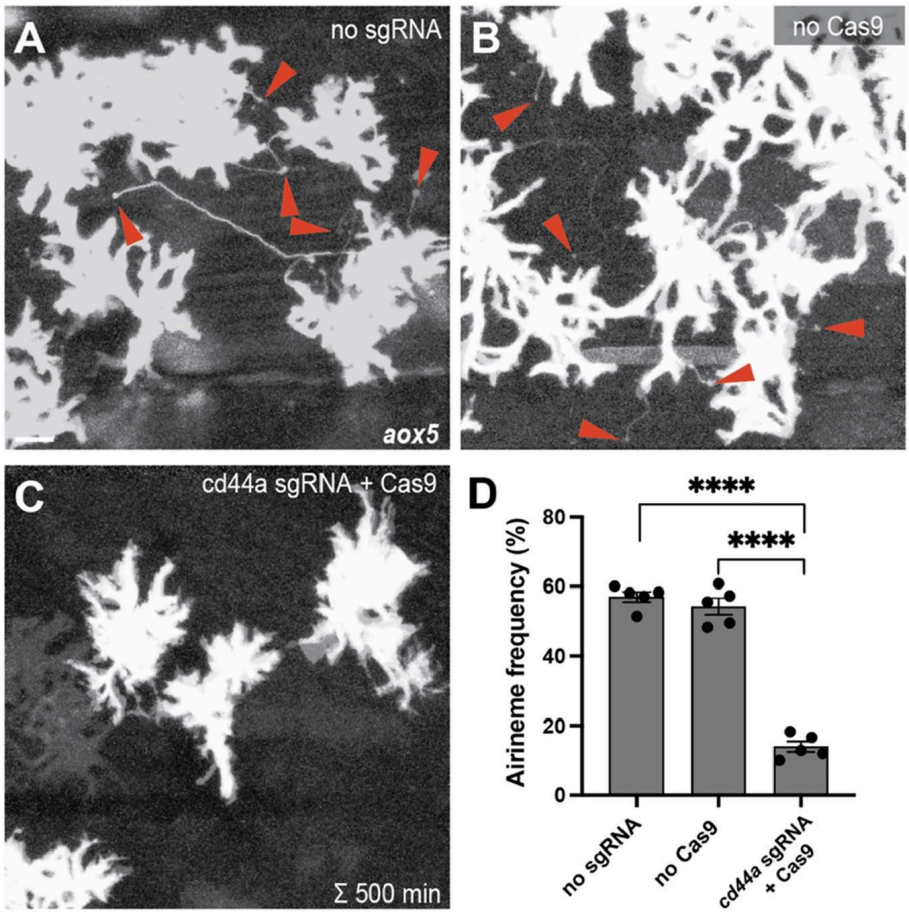

Figure 18. Gene knock-out of cd44a results in a significant reduction in airineme extension. (A,B) Merged time-lapse frames over 500 min display airinemes. Red arrowheads mark airineme vesicles. (C,D) The extension of airinemes was significantly decreased in embryos injected with cd44a sgRNA/Cas9, ($F_{2,\ 12}$) = 172.8, P < 0.0001, 5 larvae each). Statistically significant results were evaluated using one-way ANOVA, followed by Tukey's HSD post hoc test. Scale bars represent 20 µm. Error bars denote mean ± SEM. Images were overexposed to visualize thin airineme filaments.

CD44 expression in macrophages and xanthophore-lineages

The role of CD44 in cell-cell or cell-ECM interactions is well-established in various contexts (Chen et al., 2018; Ponta et al., 2003; Senbanjo and Chellaiah, 2017). Given this, we predicted that CD44 is expressed in either airineme-producing xanthoblasts or macrophages, or potentially both. To investigate the localization of CD44 protein under native regulatory elements, we recombineered an 82 kb BAC (Bacterial Artificial Chromosome) containing the zebrafish cd44a coding sequence and regulatory elements to generate an mCherry fusion transgenic line, *TgBAC(cd44a:cd44a-mCherry)*. To assess CD44 protein expression in xanthoblasts, we injected an *aox5:palmEGFP* construct into *TgBAC(cd44a:cd44a-mCherry)*. The CD44-mCherry signal was detected in various cell types, including xanthophore lineages (Figure 19A). Interestingly, we were able to detect enriched CD44 expression in the airineme vesicles (Figure 19A, white arrowhead) and airineme blebs (Figure 19A, yellow arrowheads; Figure 19), which are the precursors of airineme vesicles. To examine CD44 expression in macrophages, we injected a *mpeg1:palmEGFP* construct, which labels cell membranes of all macrophages. We confirmed that macrophages, specifically metaphocytes, also express CD44 (Figure 19B, arrowheads) (Vachon et al., 2006). Metaphocytes were easily distinguishable by their amoeboid morphology compared to the dendritic population in the zebrafish skin (Bowman et al., 2023; Kuil et al., 2020; Lin et al., 2020; Lin et al., 2019). CD44-mCherry expression was not confined to specific subcellular structures except for airineme blebs but was distributed throughout the cells in xanthophore lineages. Since CD44 is a membrane protein, we expected to see it mainly at the cell surface. However, in macrophages, CD44 was strongly expressed in the center of the cell and was also found throughout the entire cell. Thus, our findings confirm that CD44 protein is expressed in both xanthoblasts and macrophages (Figures 19A,B). We also collected EGFP-labelled xanthophore lineages from *Tg(aox5:palmEGFP)* and

macrophages from *Tg(mpeg1:palmEGFP)* using fluorescence-activated cell sorting (FACS). We confirmed cd44 mRNA expression in both cell types using RT-PCR. For negative controls in this experiment, we tested multiple tissues and organs in zebrafish. We found that heart tissue consistently lacked cd44 expression and thus used it as a negative control (Figure 19C). To confirm that the CD44-mCherry expression observed in TgBAC(cd44:cd44-mCherry) is not a background signal, we injected cd44 CRISPR/Cas9 into TgBAC(cd44:cd44-mCherry) fish (Figure 20).

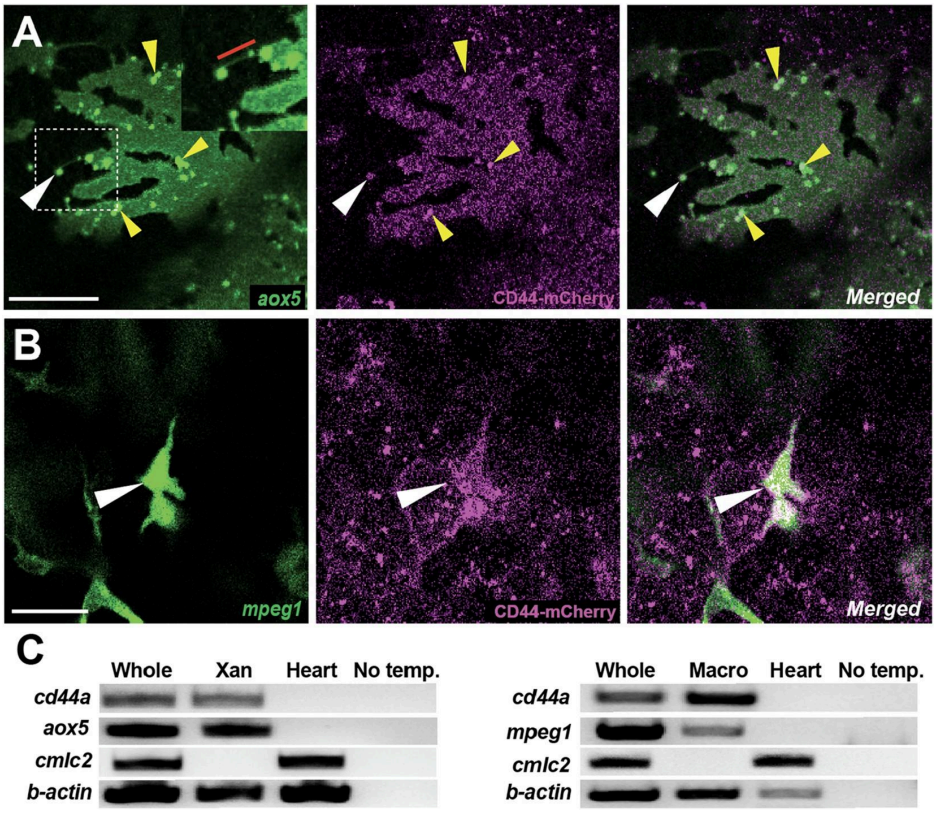

Figure 19. Localization of CD44a protein in xanthoblasts and macrophages.

(A) CD44-mCherry expression across the xanthoblast cell membrane. CD44 is also notably present in the airineme vesicle (white arrowhead) and in the airineme blebs (yellow arrowheads). The airineme filament is indicated with a red bar in the inset. (B) CD44-mCherry expression in macrophages (white arrowheads). (C) RT-PCR for cd44a in isolated xanthophores (xan) and macrophages, and no template control. Whole cDNA was used as a positive control

and a heart sample as a negative control. Scale bars represent 20 µm (A,B).

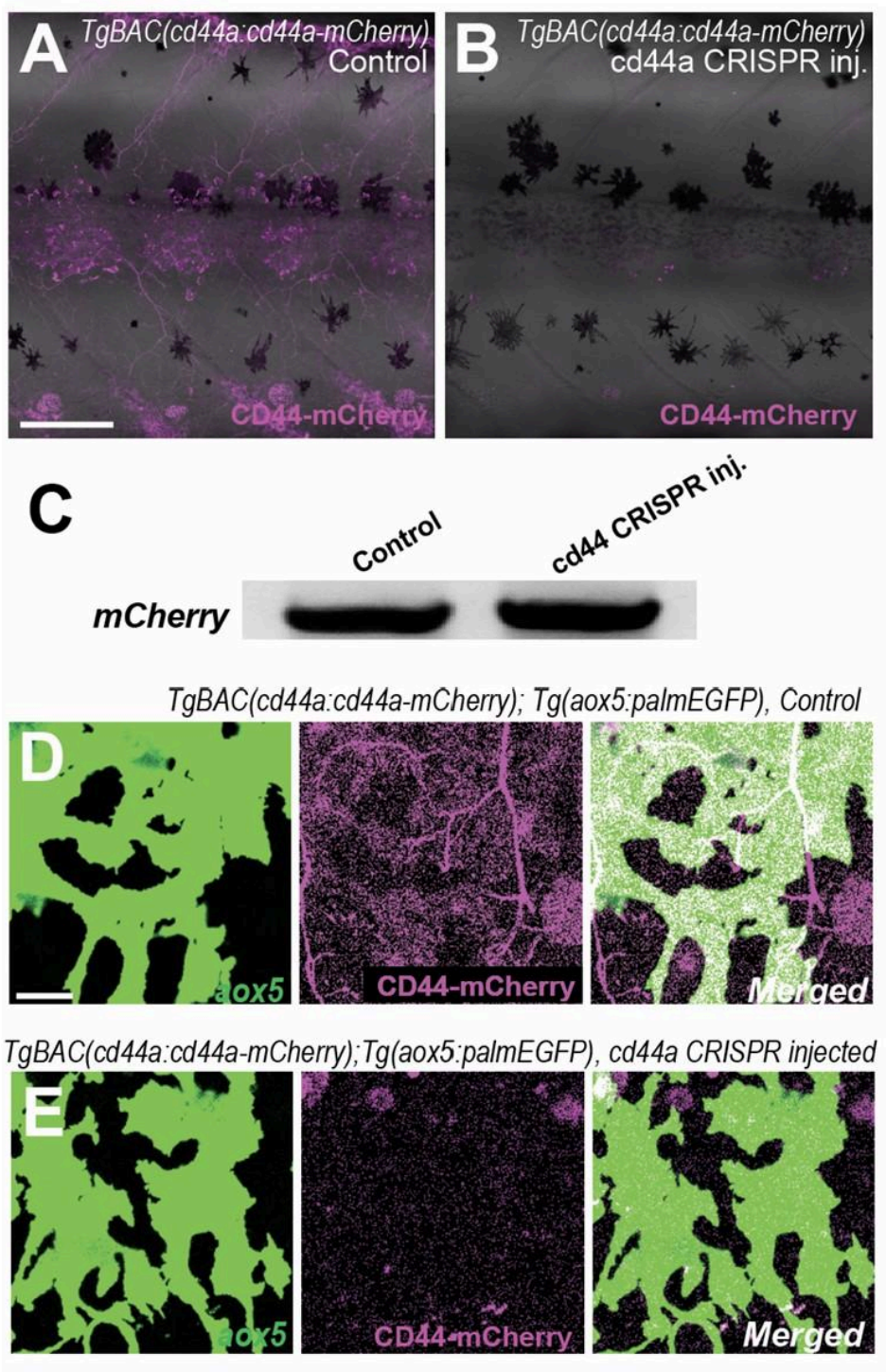

Figure 20. Verification of CD44-mCherry signal.

(A) Expression of CD44-mCherry was not altered in Cas9-only control fish. (B) A dramatic reduction or undetectable CD44-mCherry signal was observed in cd44 CRISPR/Cas9 injected fish. Note that some autofluorescent signals are present. (C) Both control and injected fish were verified as TgBAC(cd44:cd44-mCherry) by detecting mCherry expression. (D) High magnification images with xanthophore marker (aox5) showed CD44-mCherry expression in xanthophores in control. (E) CD44 mCherry signal was not visible in the cd44a CRISPR/Cas9-injected fish. Scale bar represents 200μm (A, B) and 20μm (D, E).

Extracellular domain of CD44 is essential for airineme extension

CD44 serves multiple functions and helps cells adhere to each other and to the extracellular matrix (ECM) through interactions with different ligands. One well-studied ligand for CD44 is hyaluronic acid (HA) (Senbanjo and Chellaiah, 2017). Given that airinemes are actin- and tubulin-based structures, and that the CD44-HA interaction can activate the cytoskeleton in certain contexts, we aimed to investigate whether CD44 controls airineme extension through its interaction with HA (Eom, 2020; Eom et al., 2015; Ponta et al., 2003). We expected to observe hyaluronic acid binding protein (HABP) expression in CD44-expressing xanthoblasts if CD44 acts through HA. However, we did not detect obvious overlapping expression of HABP in xanthoblasts, suggesting that the CD44-HA interaction does not appear to be involved in airineme signaling; however, further studies are required (Figure 21).

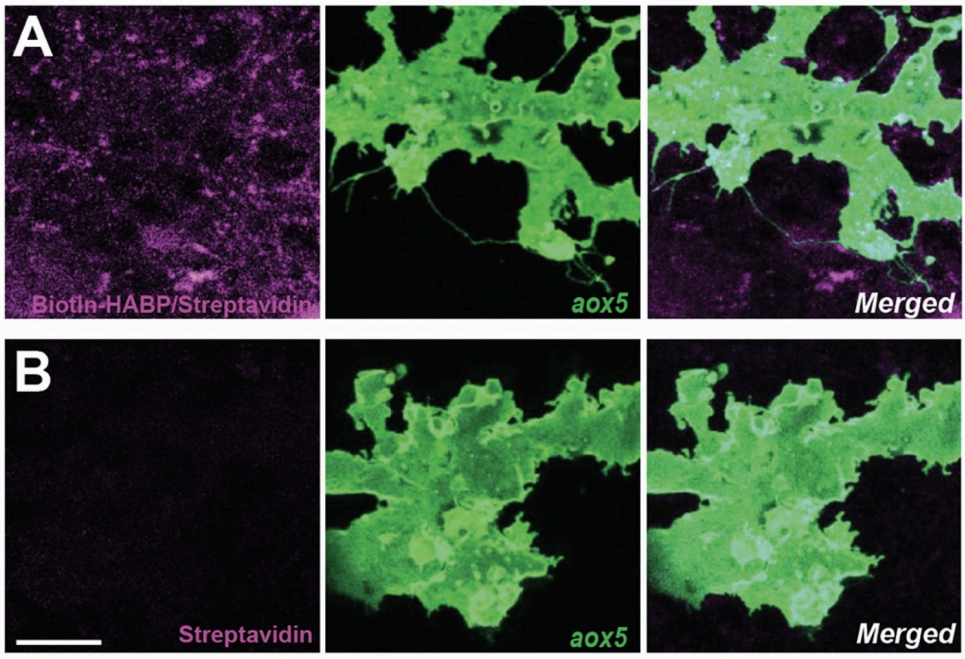

Figure 21. Lack of apparent Hyaluronic acid binding protein (HABP) expression in xanthoblasts. (A) Xanthoblasts appear to show no overlapping expression when traced using Biotin-conjugated HABP and Alexa-546-labelled streptavidin. (B) A control experiment with Alexa-546 streptavidin alone did not result in any detectable signal. Scale bar represents 20μm. Images were overexposed to visualize thin airineme filaments.

Domain studies of CD44 have suggested that its intracellular domain (ICD) functions as a transcription factor, influencing cell migration, angiogenesis, invasion, and other behaviors (Chen et al., 2018; Skandalis, 2023). To investigate whether CD44-ICD plays a role in airineme extension, we generated transgenic lines overexpressing cd44a-ICD in either xanthophore-lineages or macrophages, *Tg(aox5:cd44aICD)* and *Tg(mpeg1:cd44aICD)*. In both transgenic lines, we did not observe any significant changes in airineme extension frequency, suggesting that CD44-ICD does not seem to be involved in airineme extension (Figures 22A,B,B–B”,E).

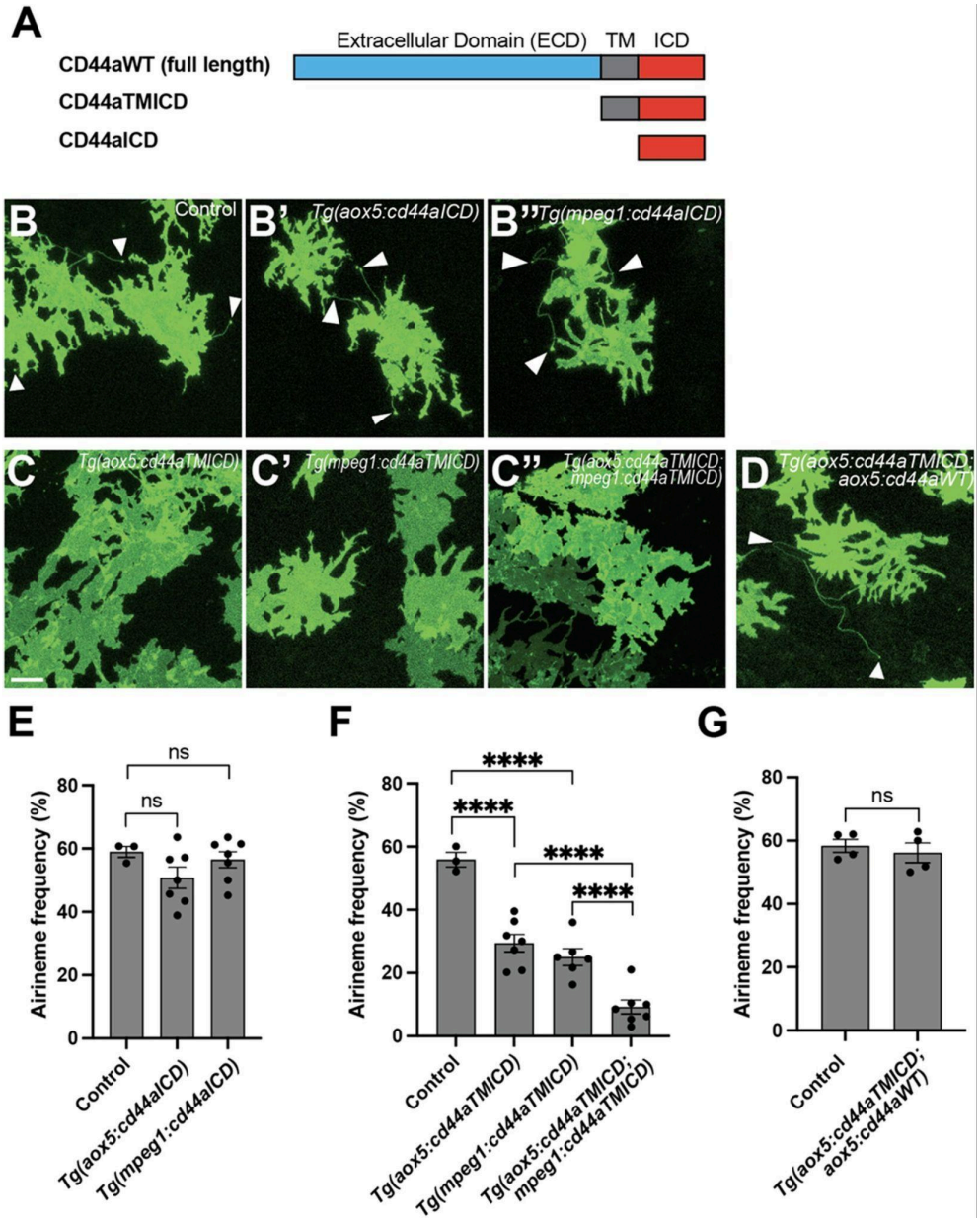

Figure 22. The crucial role of the extracellular domain of CD44 in airineme extension.

(A) The schematics indicate the structure of CD44aWT, CD44aTMICD, and CD44aICD. (B–B") Representative images of xanthophores extending airinemes in control, Tg(aox5:cd44aICD), or Tg(mpeg1:cd44aICD). (C–C") Representative images of xanthophores in Tg(aox5:cd44aTMICD), Tg(mpeg1:cd44aTMICD), or Tg(aox5:cd44aTMICD; mpeg1:cd44aTMICD). (D) Representative image of xanthophores in Tg(aox5:cd44aTMICD; aox5:cd44aWT). White arrowheads mark airinemes (E) Airineme extension frequency was not

significantly altered in transgenic embryos that overexpressed the intracellular domain of cd44 (cd44aICD) specifically in the xanthophore-lineages or macrophages, ($F_{(2, 14)} = 1.736$, $P = 0.2121$, 17 embryos in total). (F) Overexpression of CD44a with a truncated extracellular domain (cd44aTMICD) exhibited a significant reduction in airineme extension frequency in both the xanthophore-lineages and macrophages, ($F_{(2, 13)} = 23.62$, $P < 0.0001$, 16 embryos in total). Airineme extension frequency was further significantly reduced when cd44aTMICD was overexpressed in both cell type simultaneously, ($F_{(2, 17)} = 18.04$, $P < 0.0001$). (G) Airineme extension frequency was restored when WT CD44 was overexpressed in embryos already expressing cd44aTMICD in the xanthophore-lineages, ($P = 0.5767$, 4 embryos each). Statistically significant results were evaluated using a one-way ANOVA, followed by Tukey's HSD post hoc test or Student's t-test. Error bars indicate mean ± SEM.

Subsequently, we explored the potential role of the extracellular domain (ECD) of CD44 in airineme extension. CD44-ECD is known to interact with the extracellular matrix (ECM) or with CD44-ECD from other cells (Senbanjo and Chellaiah, 2017). To test this, we generated transgenic lines overexpressing an ECD-truncated form of cd44a (cd44aTMICD), specifically in xanthophore-lineages, *Tg(aox5:cd44aTMICD)* or macrophages, *Tg(mpeg1:cd44aTMICD)*. These transgenic lines did not impact cell viability or other noticeable cellular behaviors in either xanthophore-lineages or macrophages (Figure 23). Interestingly, we observed a significant decrease in airineme extension frequency in the transgenic lines overexpressing cd44aTMICD (Figures 22A,C,C–C",F). We investigated whether an additional supply of WT CD44 could rescue the phenotype in *Tg(aox5:cd44aTMICD)* by generating a double transgenic line, *Tg(aox5:cd44aTMICD; aox5:cd44aWT)*. These rescue fish exhibited almost full recovery of airineme extension frequency. Together, these results suggest that CD44-ECD is critical for airineme extension (Figures 22A,D,G).

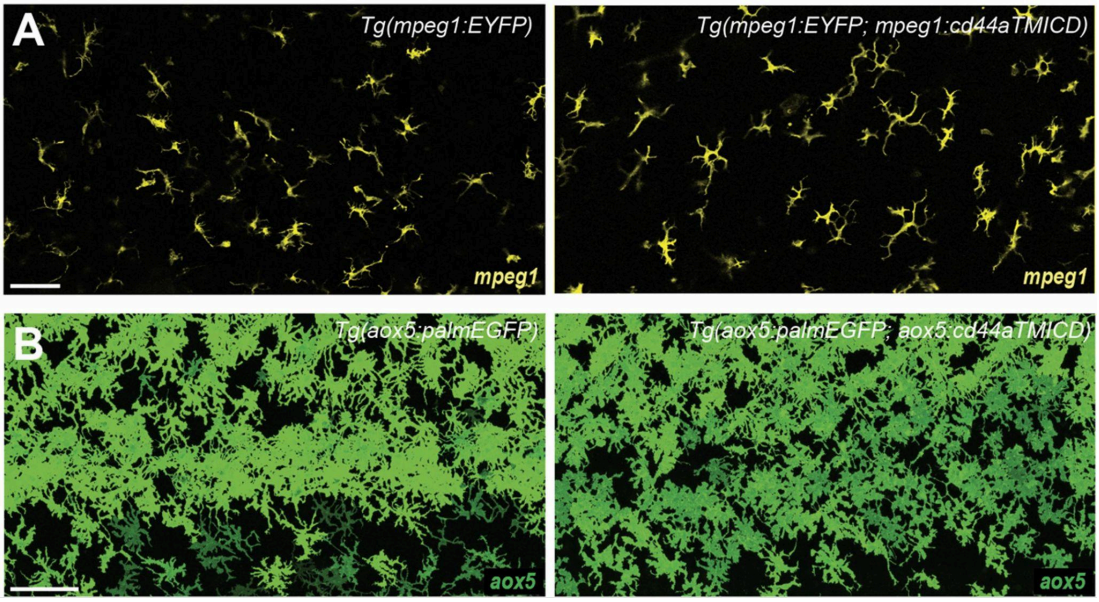

Figure 23. Overexpression of cd44aTMICD does not alter cell survival or behavior.

(A) Macrophages, labelled with an mpeg1 promoter driving membrane YFP, display no difference in cell count or morphology when compared to cells with overexpressed cd44aTMICD under the mpeg1 promoter. (B) Similarly, there is no noticeable change in appearance of xanthophore lineages overexpressing cd44aTMICD when compared to control fish. Scale bars represent 100μm (A, B).

Trans-adhesive interaction via CD44aECD between xanthoblasts and macrophages is critical for airineme extension

We investigated whether the extracellular domain of zebrafish CD44 can mediate adhesion between cells. To test this, we expressed constructs that encode wild-type zebrafish cd44a or ECD-truncated cd44a (cd44aTMICD), both C-terminally fused with mCherry, in *Drosophila* S2 cells (Schneider, 1972). An actin-mCherry fusion construct was used as a control. Transfected S2 cells expressing mCherry were monitored, and after several hours of culture in a rotary incubator, we assessed whether CD44-expressing S2 cells adhere to each other. The

results showed that, unlike the actin control and cd44aTMICD-expressing S2 cells, wild-type cd44a-expressing S2 cells began forming aggregates 30 min after incubation. The degree of aggregation increased over time, reaching a significant level at 3 h. This indicates that zebrafish CD44 mediates trans-adhesion via its ECD between cells (Figures 24A,B).

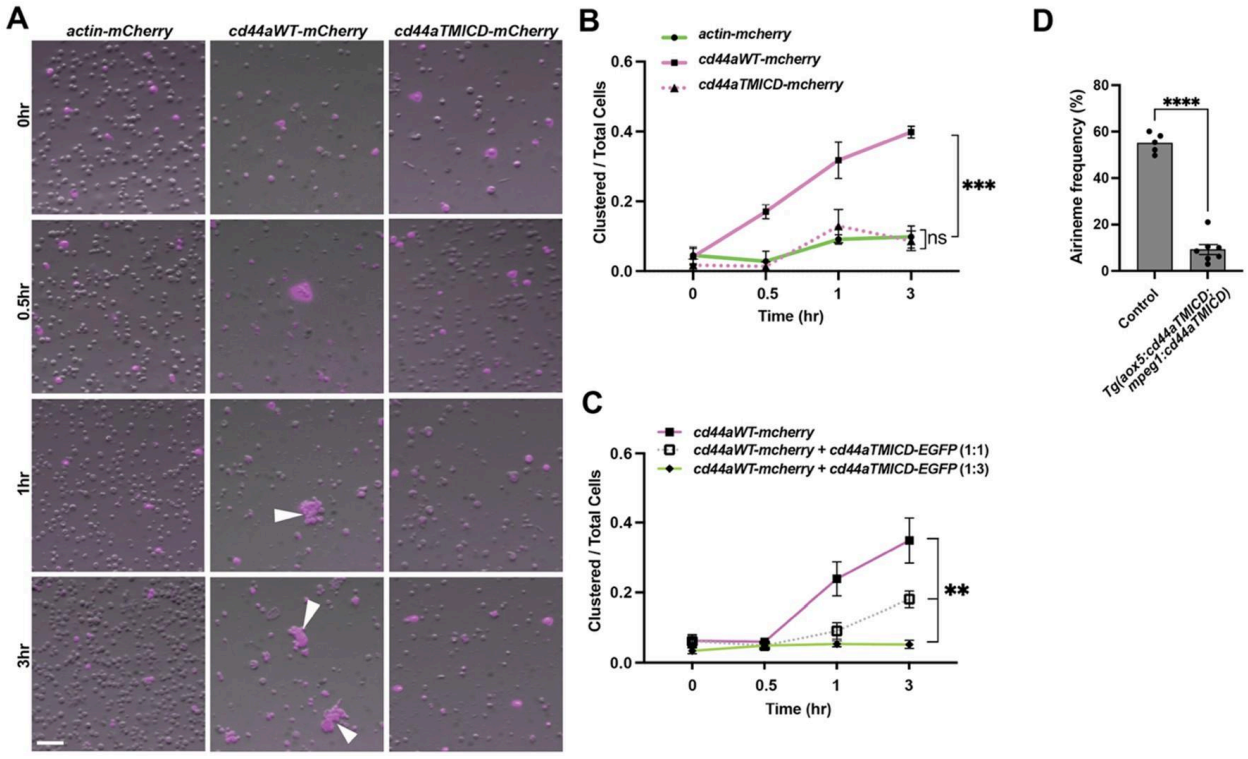

Figure 24. Trans-adhesive interaction via extracellular domain of CD44.

(A) S2 cells were transfected with constructs to express actin-mCherry (control), wild-type cd44a-mCherry, or cd44aTMICD-mCherry. Within 1 h of rotary culture, cell aggregates were formed by those expressing the wild-type cd44a (white arrowheads). (B) Quantification of the transfected cells found within clusters relative to the total number of transfected cells in 3 replicate cultures, ($F_{(2, 6)} = 45.50$, $P = 0.0002$). (C) S2 cells were co-transfected with constructs expressing wild-type cd44a-mCherry and cd44aTMICD-EGFP at ratios of 1:0 (control), 1:1, and 1:3, ($F_{(2, 6)} = 13.7$, $P = 0.0058$). Corresponding images can be found in Supplementary Figure S3. (D) Overexpressing cd44aTMICD in both xanthophore-lineages and macrophages resulted in a significant reduction in airineme extension frequency. Statistically significant results were

evaluated using one-way ANOVA, followed by Tukey's HSD post hoc test or Student's t-test. Scale bars: 100 μm. Error bars indicate mean ± SEM.

Previously, we demonstrated that overexpressed cd44aTMICD inhibits airineme extension frequency. This effect was rescued by the supply of WT cd44a *in vivo* (Figures 22C,D). To further investigate whether the overexpression of CD44aTMICD in the presence of WT CD44a could negatively affect cell adhesion, we co-expressed *cd44aWT-mCherry* and *cd44aTMICD-EGFP* in S2 cells. We observed that the degree of S2 cell aggregation significantly decreased as the ratio of CD44aTMICD-EGFP to CD44aWT-mCherry transfection increased (Figure 24C; Figure 25). Taken together with the *in vivo* data in Figure 22, these results suggest that overexpressed CD44aTMICD exhibits a dominant negative effect by interfering with the ability of wild-type CD44a to mediate cell adhesion. CD44aTMICD might disrupt the organization of membrane microdomains, protein complexes, or dimers/oligomers necessary for CD44 function (Kawaguchi et al., 2020; Ma et al., 2022). However, the underlying mechanism of this interference requires further investigation.

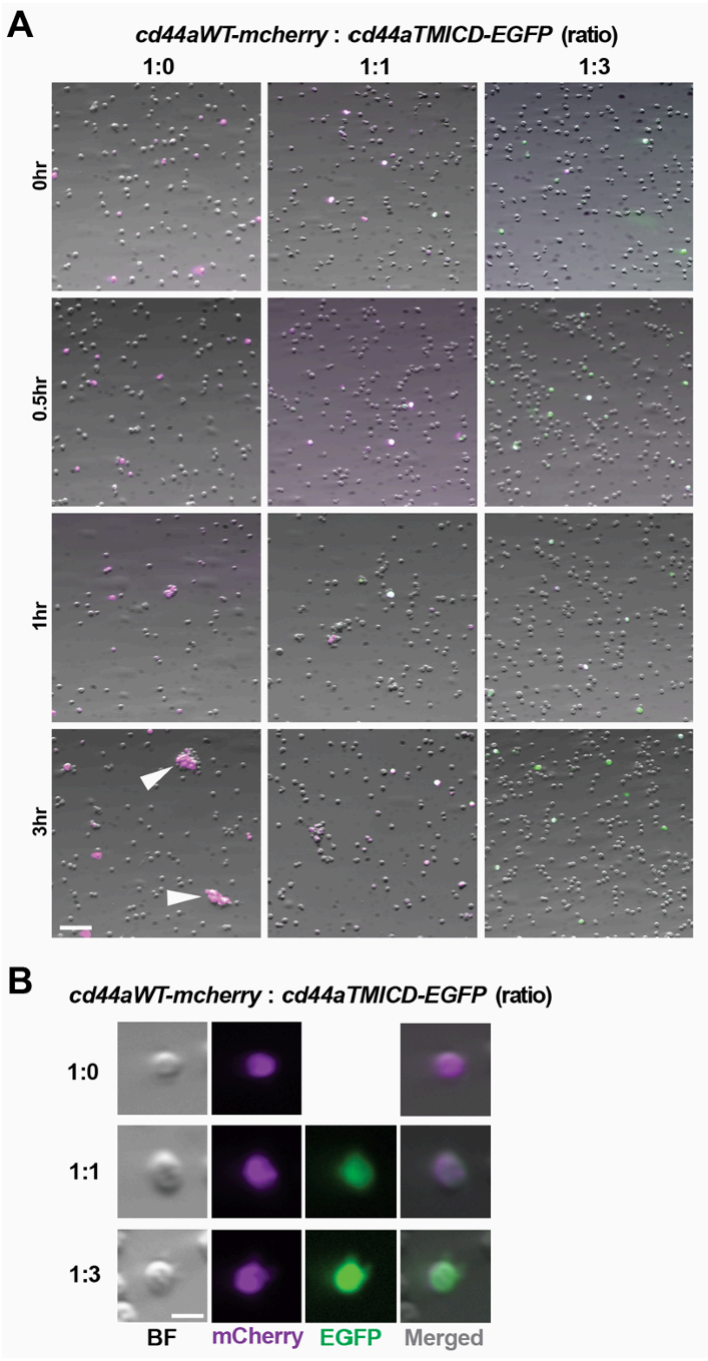

Figure 25. Overexpressed CD44aTMICD interferes with adhesive interaction mediated by wild type CD44a.

(A) S2 cells were transfected with constructs of cd44aWT-mCherry and cd44aTMICD-EGFP at various indicated ratios. Unlike the S2 cells transfected solely with cd44aWT-mCherry, those co-transfected with cd44aTMICD-EGFP exhibited a reduced capacity to form aggregates. Large

cell aggregates were observed in cells expressing the wild type cd44a (white arrowheads). Co-transfected cells appeared white due to the co-expression of EGFP and mCherry (pseudo-colored in magenta), which are fused to either cd44aTMICD or cd44aWT. Cells expressing higher levels of EGFP in the 1:3 group displayed a greenish hue in white. (B) Single-cell resolution of transfected S2 cells at various indicated ratios. Note that CD44aWT-mCherry fusion protein expression was unaffected by co-expression with CD44aTMICD-EGFP. Quantifications can be found in Fig. 4C. Scale bar: 100μm (A), 20μm (B).

These findings prompted us to ask whether trans-adhesive interactions between xanthoblasts and macrophages could play a role in airineme extension in zebrafish. We hypothesized that a greater reduction in airineme extension frequency would be observed if CD44a function were compromised simultaneously in both cell types, compared to its disruption in only one cell type. To test this, we generated a double transgenic line that overexpresses cd44aTMICD in both xanthophore-lineages and macrophages, *Tg(aox5:cd44aTMICD; mpeg1:cd44aTMICD)*. Indeed, we observed a more significant decrease in airineme extension in this double transgenic zebrafish compared to single manipulations (Figures 22F, 22C''), suggesting, at least in part, a requirement for CD44aECD by both xanthoblasts and macrophages for proper airineme signaling as CD44 is expressed in airineme vesicles and macrophages (Figures 19A,B). However, we cannot rule out the possibility that there are other adhesion molecules that may trans-interact with CD44 in both xanthophore-lineages and macrophages.

Next, we asked whether CD44-mediated adhesion is critical when macrophages contact airineme blebs (equivalent to airineme vesicles) and/or when they drag the airineme vesicles. We hypothesized that if such adhesive interaction is important for maintaining the attachment of airineme vesicles to macrophages while dragging, a reduction in airineme length would be observed. This is because the detachment of macrophages from the airineme vesicles would

stop the extension of airineme filaments (Bowman et al., 2023; Eom and Parichy, 2017). However, we did not detect any statistically significant change in airineme length in embryos overexpressing CD44aTMICD in either cell type or both simultaneously (Figure 26). This finding suggests that the trans-adhesive interaction mediated by CD44 plays a more significant role when macrophages are contacting airineme blebs as opposed to pulling the airineme vesicles.

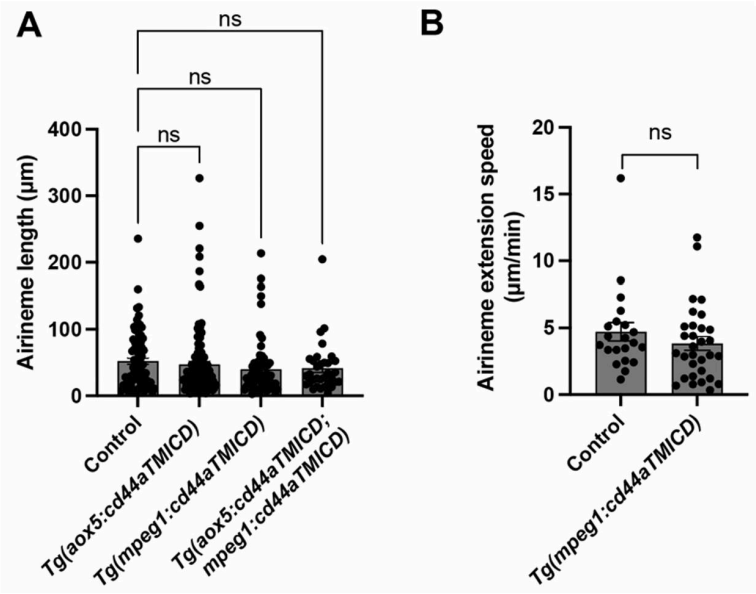

Figure 26. Airineme length and speed remained consistent despite CD44a manipulations.

(A) There was no significant difference in airineme length in embryos where cd44aTMICD was overexpressed either in xanthophore-lineages, macrophages, or in both simultaneously, (F(3, 288)=1.020, P=0.3843). (B) There was no statistically significant difference in airineme extension speed in embryos overexpressing cd44aTMICD in macrophages, P=0.2968, 3 embryos each. Statistical significance was assessed using a One-way ANOVA, followed by a Tukey's HSD post hoc test or a Student's t test. Error bars indicate mean ± SEM.

CD44-mediated airineme signaling is crucial for pigment pattern formation

Airineme-mediated intercellular signaling is indispensable for pigment pattern formation in zebrafish. Our results indicating the importance of CD44a in airineme extension led us to anticipate pigment pattern defects in embryos overexpressing cd44aTMICD. However, noticeable pigment pattern defects were not detected in either transgenic line overexpressing cd44aTMICD in xanthophore-lineages or macrophages. This suggests that residual airineme extensions may still be sufficient to deliver the necessary signals for generating a stripe pattern, or that subtle differences could be challenging to detect (Figure 27B). Nevertheless, when CD44a function was compromised by overexpressing cd44aTMICD in both cell types, a significant number of melanophores were observed to be retained in the interstripe compared to the control, although the total number of melanophores remained unchanged (Figures 27A–C). We also observed consistent pigment pattern defects in cd44 mutants induced by the CRISPR/Cas9 system (Figure 28).

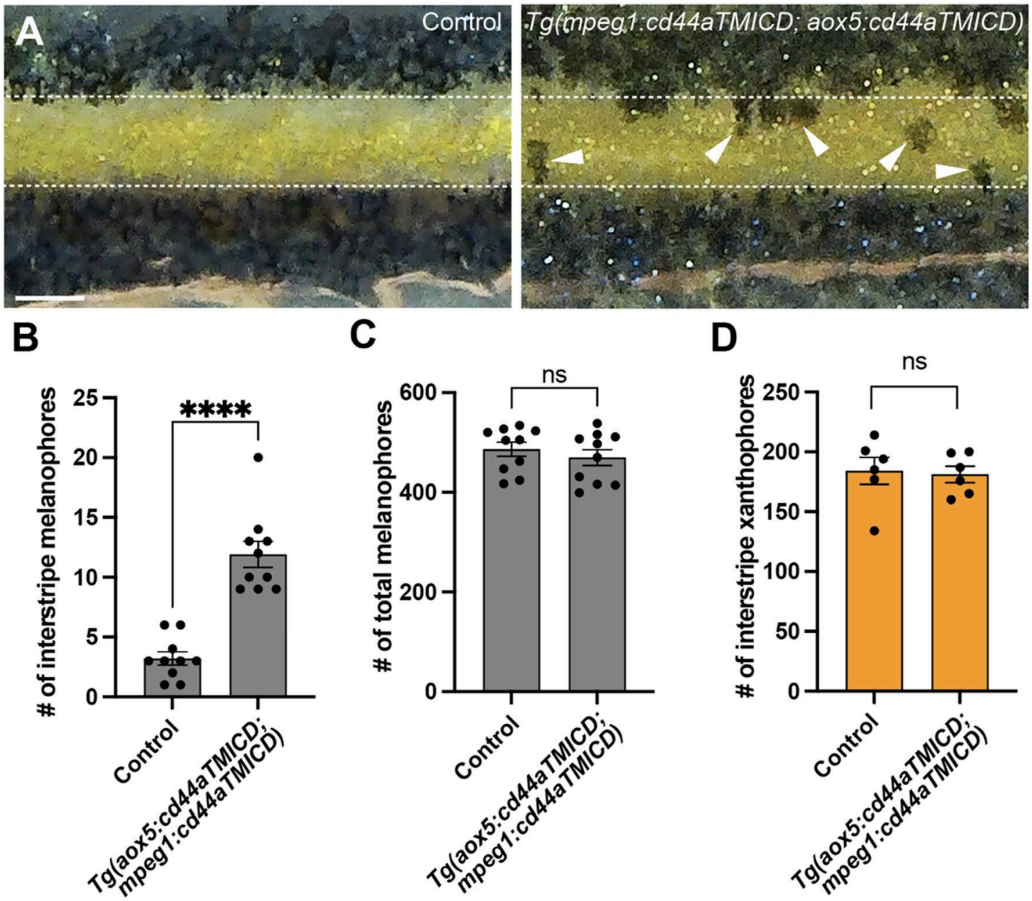

Figure 27. CD44-mediated airineme extension contributes to zebrafish pigment pattern formation.

(A) Unlike the control, melanophores failed to coalesce into stripes and remained in the interstripe zone (white arrowheads) at SSL11 (Parichy et al., 2009). The white dotted lines demarcate stripes and interstripe. (B) In embryos overexpressing cd44aTMICD simultaneously in both xanthophore-lineages and macrophages, the count of interstripe melanophores was significantly higher, (P < 0.0001, 20 embryos in total). (C) However, the total number of melanophores did not differ significantly between the experimental group and controls, (P = 0.4525, 20 embryos in total). (D) The number of xanthophores in the interstripe did not differ significantly between the experimental group and controls (P = 0.8266, 12 embryos total). Statistical significance was assessed using a Student's t-test. Scale bars represent 200 µm. Error bars indicate mean ± SEM.

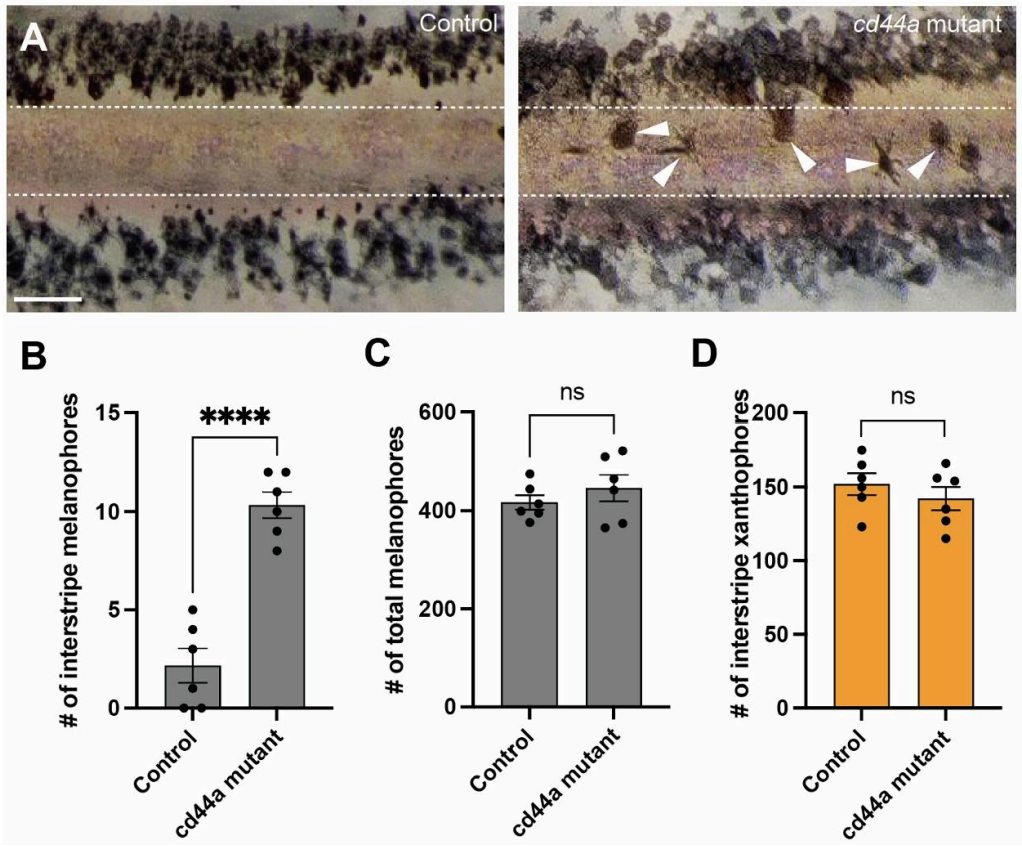

Figure 28. Mutants of cd44 induced by CRISPR/Cas9 exhibit defective zebrafish pigment patterns.

(A) Melanophores failed to coalesce into stripe and remained in the interstripe zone (white arrowheads) in cd44 mutants. White dotted lines demarcate stripes and interstripe. (B) In cd44 mutant embryos, the count of interstripe melanophores was significantly higher, (P<0.0001, 12 embryos in total). (C) However, the total number of melanophores did not differ significantly between the experimental group and controls, (P=0.3732, 12 embryos in total). (D) The number of xanthophores in the interstripe did not differ significantly between the experimental group and controls (P=0.388, 12 embryos in total). Statistical significance was assessed using a Student's t test. Scale bars represent 200μm. Error bars indicate mean ± SEM.

Together, these findings collectively suggest that CD44-mediated trans-adhesive interactions between airineme blebs on xanthoblasts and macrophages play an essential role in airineme-mediated signaling during pigment pattern formation in zebrafish.

DISCUSSION

In this study, we demonstrated that CD44 protein appears to be expressed in xanthoblasts, particularly in the airineme vesicles, as observed using the BAC recombineered C-terminal mCherry fusion transgenic line we generated, *TgBAC(cd44a:cd44a-mCherry)* (Figure 19A, yellow arrowheads). Intriguingly, though, not every airineme bleb expresses CD44 but only some of them do. This observation leads to a few possible explanations. One explanation could be that CD44 expression determines which blebs are used for airineme signaling. It is possible that some blebs do not express CD44 and serve a different function beyond airineme signaling.

In addition, our observation may suggest that there is a mechanism by which CD44 protein in the cell membrane becomes further enriched in the airineme blebs. Similar to CD44, we observed that DeltaC, one of the signaling molecules found in the airineme vesicles, is not expressed in some of the blebs before their extraction by macrophages/metaphocytes (Eom et al., 2015). It is conceivable that there are mechanisms that sort proteins required for airineme signaling into the blebs and ultimately into the airineme vesicles. These might be used to adhere to the macrophage membrane and activate Notch signaling on the target cell surface. It would be interesting to study the underlying molecular mechanisms involved in sorting out the proteins essential for airineme-mediated intercellular signaling into the airineme blebs.

Furthermore, CD44 has previously been reported as a signal for phagocytosis in macrophages (Vachon et al., 2007; Vachon et al., 2006). Therefore, alongside phosphatidylserine (PtdSer), CD44 may serve as an additional recognition signal for macrophages to identify airineme blebs, as well as serve as an adhesive signal between airineme blebs and macrophages (Eom and Parichy, 2017).

This raises an interesting question as to why we did not observe any differences in airineme filament length when the adhesive interaction mediated by CD44 was reduced (Figure 26A). Our interpretation is that this adhesive interaction would be crucial during the initial interaction between macrophages and the airineme blebs, rather than during the process of dragging them. Thus, it seems plausible that CD44 functions as both a recognition and adhesion element at the time when macrophages interact with airineme blebs. On a related note, our previous research, using high-resolution 3D confocal image reconstruction, has shown that airineme vesicles are found inside the dragging macrophages (Eom and Parichy, 2017). This implies that airineme vesicles are physically entrapped within the macrophages during the pulling process, suggesting that adhesive interactions between the membranes of these two signaling components might not be strictly necessary while pulling. Thus, it is conceivable that CD44 might play a dual role. First, it may assist PtdSer in recognizing airineme blebs and

simultaneously provide necessary adhesion during the recognition and subsequent engulfment by the macrophage, but it is not necessary while airineme vesicles are being dragged by macrophages. CD44 could function as a member of a functional membrane microdomain facilitating this interaction. However, future experiments would be required to verify this hypothesis.

We observed residual airineme extension even when we overexpressed cd44aTMICD in both xanthophore-lineages and macrophages (Figure 22F). This residual airineme extension may indicate that either remaining wild-type CD44 continues to mediate adhesion or other adhesion proteins and components are involved in the process. To explore this further, we considered the studied interaction of Matrix Metalloproteinase-9 (MMP9) with CD44 (Senbanjo and Chellaiah, 2017). Cell surface expression of MMP9, along with CD44, is known to facilitate cell migration and invasion in tumors and PC3 cells (Desai et al., 2008; Gupta et al., 2013; Yu and Stamenkovic, 1999). Given our previous findings that airineme-pulling macrophages express high levels of mmp9, which is crucial for macrophage migration and penetration into the hypodermis in zebrafish skin (Bowman et al., 2023), we explored whether CD44 also plays a role in macrophage migration speed (=airineme extension speed) through its interaction with MMP9. However, our analysis did not reveal a significant difference in airineme extension speed in macrophages overexpressing cd44aTMICD (Figure 26B). Although further investigations are necessary, this suggests the possibility that CD44 may function independently of MMP9 in macrophage migration during airineme extension. Alternatively, the overexpression level of cd44aTMICD may not have been sufficient to completely disrupt CD44-MMP9 interactions, or other compensatory mechanisms may be involved.

Taken together, our study discovered that the extracellular domain of CD44 in both airineme-extending xanthoblasts and airineme-pulling macrophages facilitates a trans-adhesive interaction, which appears to be critical for initiating airineme extension. This study provides evidence for the requirement of cellular adhesion between signaling-sending cells and relay

cells in airineme-mediated intercellular signaling. It is also conceivable that similar mechanisms could be conserved in other cellular contexts.

MATERIALS AND METHODS

Transgenesis and transgenic line production

To examine how the loss of extracellular domain (ECD) of the CD44 adhesion molecule may impact interactions between macrophages and xanthoblasts, we generated *mpeg1:cd44aTMICD-v2a-mCherry* and *aox5:cd44aTMICD-v2a-mCherry* constructs using Gateway assembly into a Tol2 backbone and injected them into WT (ABb). The truncated version of CD44a (CD44TMICD) was obtained by extracting CD44aTMICD cDNA from WT (ABb) cDNA. To examine whether interactions between macrophages and xanthoblasts were gene expression dependent via CD44a-ICD, we generated *Tg(aox5:cd44aICD-v2a-mCherry)*$^{ir.rt8}$ and Tg (*mpeg1:cd44aICD-v2a-mCherry)*$^{ir.rt10}$ transgenic lines, which were likewise generated using Gateway assembly into Tol2 backbone and injected into WT (ABb). Similarly, CD44aICD cDNA was isolated from WT (ABb) cDNA. To further examine how ECD of CD44a may impact interactions between macrophages and xanthoblasts, we generated *Tg(aox5:cd44aFL-v2a-mCherry)*$^{ir.rt22}$ to see if we could rescue the phenotypes seen *in Tg(aox5:cd44aTMICD-v2a-mCherry)*$^{ir.rt9}$.

To visualize CD44 localization under native regulatory elements, we inserted mCherry C-terminally using BAC CH211-102L7 with 82 kb 5′ and 92 kb 3′ to the open reading frame.

Hyaluronic acid binding protein (HABP) assay

Zebrafish larvae (SSL7.5) were incubated in fish water containing diluted biotin-HABP (1:150, Amsbio) along with streptavidin-Alexa546 for 1 h. Controls were incubated solely with streptavidin-Alexa546. Fish were then washed twice with fish water and imaged under a confocal microscope.

Time-lapse imaging and still imaging

Ex-vivo imaging of pigment cells and macrophages was performed using a Leica TCS SP8 confocal microscope equipped with a resonant scanner and two HyD detectors. Time-lapse images were taken at 5-min intervals over a span of 10 h. Overnight time-lapse imaging was performed when larvae reached SSL (Standardized Standard Length) 7.5 (Parichy et al., 2009).

S2 cell adhesion assay

S2 cells were obtained from the *Drosophila* Genomics Resource Center (DGRC, S2-DGRC (DGRC Stock 6; https://dgrc.bio.indiana.edu//stock/6; RRID:CVCL_TZ72)) and cultured in Schneider's *Drosophila* Medium (Catalog No. 21720024, Gibco, United States) supplemented with 10% Fetal Bovine Serum (FBS) (Catalog No. 25-514H, Genclone, United States) and 1% Penicillin-Streptomycin (Catalog No. 15140148, Gibco, United States). For transfection, S2 cells were transfected with three different plasmids: *pAW-actin-mCherry, pAW-cd44a-FL(wild type full length)-mCherry,* and *pAW-cd44a-TMICD-mCherry*. Lipofectamine™ LTX Reagent (Catalog No. 15338030, Invitrogen, United States) was used for transfection following the manufacturer's instructions. After 72 h of transfection, the cells were counted, and each type of cell was seeded into 35 mm glass-bottom dishes at a density of 5,000 cells per dish (Catalog No. 706011, Nest Scientific, United States). The dishes were then subjected to rotational incubation for different time intervals, including 30 min, 1 h, and 3 h.

Cellular imaging was performed using a Zeiss microscope equipped with a 599 nm filter to capture the cellular mCherry signal and bright-field images.

To evaluate the out-competing ability of cd44a-TMICD against the wild type cd44a, S2 cells were co-transfected with *pAW-cd44a-FL-mCherry* and *pAW-cd44a-TMICD-EGFP* at ratios of 1:1 and 1:3, using the same transfection protocol described above. After 72 h of transfection, 5,000 cells were transferred into 35 mm glass-bottom dishes and subjected to rotational incubation at intervals of 30 min, 1 h, and 3 h. Cellular imaging was then conducted using a Zeiss microscope under 488 nm and 599 nm filters to capture the EGFP and mCherry signals, along with bright-field images.

Reverse transcription polymerase chain reaction (RT-PCR) analysis of gene expression in zebrafish skin

Metamorphic stage fish were skinned (n = 20 per group) and subsequently washed in 1 x PBS solution. After washing, the samples were briefly centrifuged, and the supernatant was discarded by pipetting. The tissues were resuspended in 1 mL of Stem® Pro® Accutase Cell Dissociation Reagent (Gibco) and incubated for 10 min at 37 °C, or until the cells were dissociated. Following incubation, the cells were passed through a 40 μm cell strainer to remove non-dissociated tissue before being processed through FACS (Fluorescence-Activated Cell Sorting). Using FACS, cells of interest were separated and collected based on their respective membrane markers. Cells expressing membrane markers for EGFP were collected for downstream non-quantitative RT-PCR.

Following collection, cDNA was synthesized using the SuperScript III CellsDirect™ cDNA synthesis kit (Invitrogen). Non-quantitative RT-PCR amplifications were performed for 40 cycles (*actb1, aox5, mpeg1, cd44a, cmlc2*), utilizing PrimeStar GXL DNA Polymerase (Takara).

actb1:5′-CATCCGTAAGGACCTGTATGCCAAC-3′,5′-AGGTTGGTCGTTCGTTTGAATCTC-3';aox5:5′-AGGGCATTGGAGAACCCCCAGT-3′,5′-ACACGTTGATGGCCCACGGT-3';
mpeg1:5′-CCCAGTGTCAGACCACAGAAGATGGAGTC-3′,5′-CATCAACACTTGTGATGACATGGGTGCCG-3';
cd44a:5′-GCTGTACTTCAGGCAGCCCC-3′,5′-GTTTGGACCATTAATGTGTGGGAGG-3';
cmlc2:5′-CAAGAGGGGGAAAACTGCTCAAAG-3′,5′-GCAGCAAGGATGGTTTCCTCTG-3';
mCherry: 5′-ATGGTGAGCAAGGGCGA-3′, 5′-TTACTTGTACAGCTCGTCCATG-3'.

Generation of *cd44a* mutants by the CRISPR/Cas9 system

Mutations in *cd44a* (accession number XM_001922456) were induced by CRISPR/Cas9. Using SMART, a target site was generated in exon 2, with the following sequence 5′-GGTGAACTGTGTCAGAGTTT-3’. Single guide RNA (sgRNA) was then synthesized using the MEGAshortscriptTM T7 High Yield Transcription Kit (Invitrogen) and co-injected into one-cell stage embryos with 1 μg/μL TrueCutTM Cas9 Protein v2 (InvitrogenTM) at a concentration of 300 ng/uL.

Pigment pattern and melanophore counts

Fish were imaged upon reaching SSL11.0 using a Koolertron LCD digital microscope. Images were taken of the entire trunk and were later cropped to include only the area underneath the dorsal fin. The ImageJ cell counter plugin was used to count interstripe and total numbers of melanophores. Numbers for each group were averaged.

Quantification and statistical analysis

Statistical analyses were performed using GraphPad Prism.

CHAPTER 3: CHARACTERIZATION OF AIRINEME BLEBS

Raquel Bowman and Dae Seok Eom conceptualized experiments. Raquel Bowman conducted all experiments.

ABSTRACT

Airinemes are specialized filopodia that mediate intercellular communication during zebrafish pigment pattern development. Previous studies have shown that airinemes originate from membrane blebs on xanthoblasts, which are recognized and extracted by macrophages; however, the mechanisms regulating airineme bleb formation, maturation, and distribution remain poorly understood. In this chapter, I established criteria for identifying putative airineme blebs based on their size and morphology. Using airineme vesicle diameter as a proxy for airineme bleb size, I identified a population of surface blebs between 0.75 and 1.75 μm that exhibited the characteristic outward-protruding morphology of airineme blebs. I then characterized the developmental and spatial distribution of these putative airineme blebs and found that their abundance increased prior to peak airineme production and decreased thereafter. Putative airineme bleb-containing xanthoblasts were distributed throughout the dorsal, ventral, anterior, and posterior regions of the developing trunk, suggesting that their formation is not spatially restricted. I further investigated the relationship between airineme bleb localization and macrophage interactions and found that macrophages preferentially interacted with blebs located near the periphery of xanthoblasts. Finally, I examined phosphatidylserine (PS), a previously established recognition signal for macrophage-mediated airineme bleb extraction, and CD44a, which is important for mediating interactions between airineme blebs and metaphocytes. I found that only a subset of putative airineme blebs were positive for either

marker, suggesting that PS and CD44a may serve as potential markers of airineme bleb maturation. Together, these findings establish practical criteria for identifying airineme blebs and provide a framework for investigating their formation, maturation, and incorporation into the airineme signaling pathway.

INTRODUCTION

Airineme-mediated CCC is a type of specialized filopodial signaling which coordinates pigment pattern formation during zebrafish development. This signaling pathway is initiated by undifferentiated xanthoblasts in the developing stripe regions, which extend long, filamentous protrusions called airinemes to communicate with interstripe target melanophores (Eom et al., 2015). Mature airinemes arise from membranous structures on the surface of xanthoblasts termed airineme blebs which protrude outward from the membrane (Eom et al., 2015). Exposure of phosphatidylserine (PS) on airineme blebs, an established “eat-me” signal, allows roaming metaphocytes to recognize and partially engulf these structures (Bowman et al., 2023; Eom and Parichy, 2017). This interaction is further strengthened through trans-adhesive interactions mediated by the extracellular domain of the cell surface glycoprotein CD44 (Bowman et al., 2025). Metaphocytes subsequently migrate while carrying mature airineme vesicles before depositing them onto nearby target melanophores located in the interstripe (Bowman et al., 2023; Eom and Parichy, 2017). These vesicles contain DeltaC ligand (dlc), which activates Delta-Notch signaling in responsive target melanophores, triggering their eventual migration out of the interstripe and into the prospective stripe region, contributing to proper pigment pattern formation (Eom et al., 2015).

Although the mechanisms underlying airineme transport and signal delivery have become increasingly well characterized, considerably less is known about the membranous structures from which airinemes originate. Airineme blebs represent the earliest identifiable stage of airineme development and are important to study to better understand their maturation, may provide insight into cargo loading, and the mechanisms underlying their eventual pinching off from the membrane. A significant challenge to studying airineme blebs, however, is the lack of a specific marker to study them.

Previous studies have identified several molecular markers associated with airineme blebs including exposure of PS, localization of CD44 and enrichment of Dlc (Eom et al., 2015; Eom and Parichy, 2017; Bowman et al., 2025). Importantly, however, not every membrane bleb on the surface of xanthoblasts is positive for these markers (Bowman et al., 2025). This suggests that airineme blebs represent a subset of membrane blebs on the surface of xanthoblasts or that these markers label distinct stages of bleb maturation, further complicating efforts to reliably identify and characterize airineme blebs.

Another factor contributing to the challenge of studying these structures is that previous studies have primarily focused on mature airinemes and their filaments, rather than the airineme blebs from which they originate. Imaging conditions were optimized to better visualize airinemes and their filaments, which often required longer exposure times. As a result, however, airineme blebs were overly saturated making them difficult to resolve (Eom et al., 2015; Eom and Parichy, 2017; Bowman et al., 2023; Bowman et al., 2025). Although reducing exposure time improves resolution of airineme blebs, their identification remains difficult because no molecular marker has been identified that reliably and specifically labels airineme blebs. The current strategy for labeling airineme blebs is through F_0 injection of the DNA plasmid aox5:palmEGFP, which labels xanthophore-lineage cells with membrane-bound EGFP. A caveat of this approach is that palmEGFP broadly labels cell membranes rather than airineme blebs specifically. Consequently,

this increases the likelihood that other membrane-bound structures within xanthoblasts can be labeled, including organelles and recycled membrane components, making identification of airineme blebs a significant challenge.

Based on previous observations, I hypothesize that airineme blebs can be identified by their distinct morphology and that their maturation status can be inferred from changes in molecular marker expression. In this chapter, I test these hypotheses by investigating whether (1) size and morphology are suitable criteria for identifying airineme blebs, (2) airineme bleb abundance changes throughout developmental stages leading up to peak airineme production, (3) PS exposure is associated with airineme bleb maturation, and (4) macrophages preferentially interact with airineme blebs located at the cell periphery.

Establishing reliable criteria for identifying airineme blebs is important in understanding the underlying mechanisms of airineme bleb biogenesis and maturation. Beyond advancing our understanding of airineme-mediated signaling, this work also provides a framework for studying other vesicular membrane structures which may have conserved mechanisms of biogenesis.

RESULTS

Identification of airineme blebs

Previous work has shown that airinemes originate from airineme blebs on the surface of xanthoblasts (Eom et al., 2015) (Figure 29A-A"'). As noted above, there are several molecular markers associated with airineme blebs, but whether these markers are airineme bleb specific has yet to be determined, necessitating an alternative identification strategy. To address this limitation, we sought to identify airineme blebs based on two criteria, (1) diameter and (2) morphology.

Given that airineme vesicles are derived directly from airineme blebs, we measured the diameters of mature airineme vesicles and used them as an approximation for airineme bleb size (Figure 29B). Initial observations revealed that as airineme vesicles propagated through extracellular space, they appeared to undergo morphological changes, transitioning from spherical to oblong (data not shown). The changes in airineme vesicle morphology, however, were found to be an artifact of time-lapse imaging. Over the course of a time-lapse, airineme vesicle morphology may appear to be oblong if image capture occurs at the same time as active airineme extension. With this in mind, we measured the diameters of airineme vesicles at the first time point in which the vesicle appeared spherical. Based on these observations, we found that airineme vesicle diameter ranges from 0.5 to 2.25 μm with a mean diameter of 1.38 ± 0.50 μm (Figure 29B). One potential limitation of this approach is that airineme vesicles may be a source of actin and tubulin for growing airineme filaments, in which case we would expect airineme vesicle diameter to decrease over time. To address this possibility, we measured the diameters of airineme vesicles at both the first and last time point they were observed to be spherical (Figure 29C, 29C'). We found that airineme vesicle diameter does not significantly change during airineme extension, further validating our method of using airineme vesicle diameter as an approximation for airineme bleb size (Figure 29C').

Using the upper and lower standard deviation values for airineme vesicle diameter, we next sought to determine which surface blebs on xanthoblasts are likely to be airineme blebs and what their distribution is. Blebs were categorized into three size groups: large (>1.75 μm), medium (0.75-1.75 μm), and small (<0.75 μm). Binning surface blebs by size revealed that 5.74% were greater than 1.75 μm, 27.44% were between 0.75-1.75 μm, and 66.82% were less than 0.75 μm (Figure 29D). Still, the identification of airineme blebs cannot be determined by size alone.

To further confirm which subpopulation of surface blebs is likely to be airineme blebs, we next looked at the morphology of these structures. Previous research has shown that airineme

blebs protrude outward from the xanthoblast membrane (Eom et al., 2015). Cross-sectional analysis revealed that surface blebs greater than 1.75 μm (purple arrowheads) and smaller than 0.75 μm (pink arrowheads) were generally level with the xanthoblast membrane, whereas surface blebs between 0.75 and 1.75 μm (green arrowheads) protruded outward from the membrane (Figure 29F-F'''). Three-dimensional rendering of xanthoblasts further confirmed this distinction with surface blebs in the 0.75 to 1.75 μm range exhibiting a pronounced outward bulge compared with smaller and larger surface blebs (Figure 29E, E') (green arrowheads).

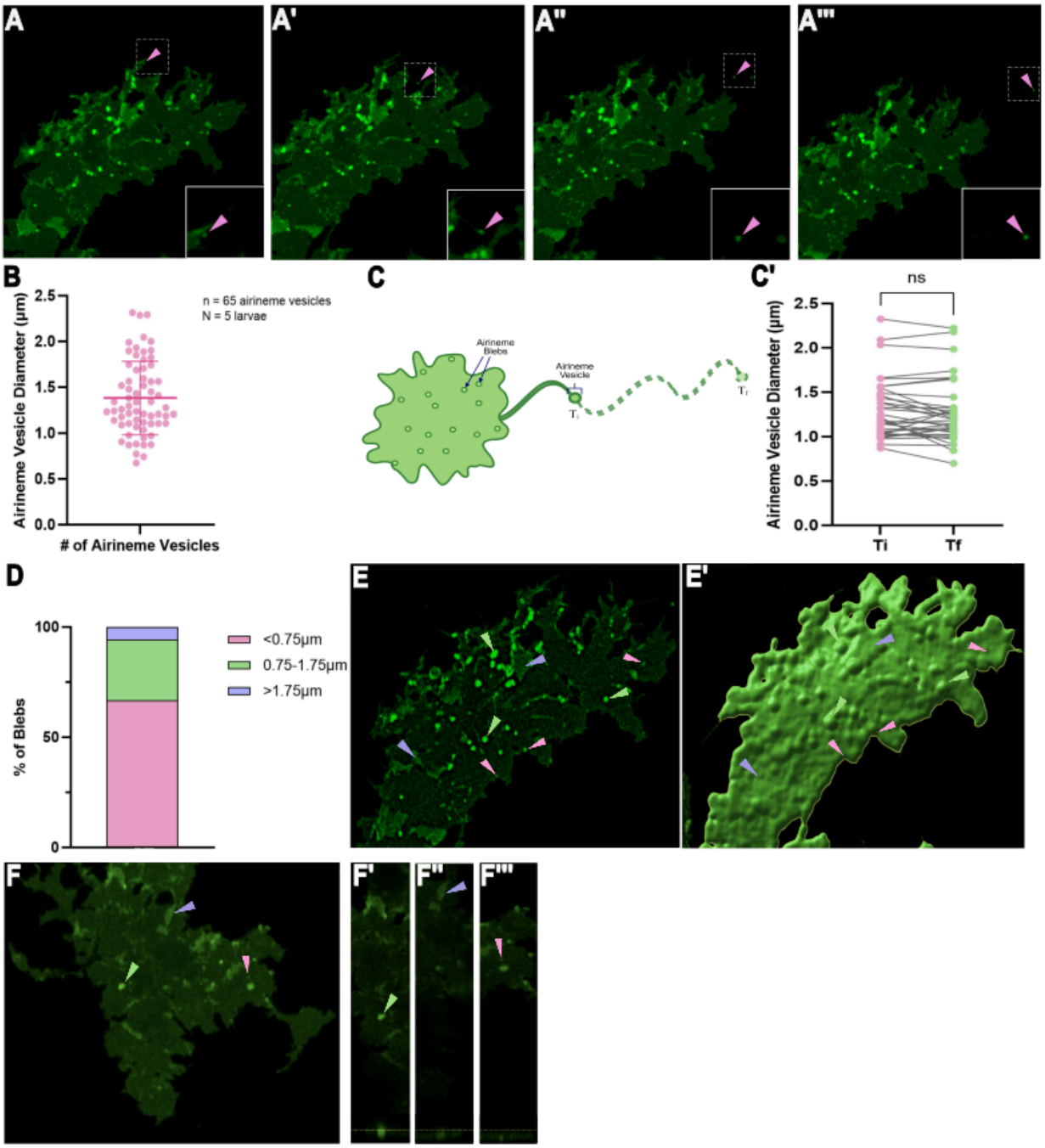

Figure 29. Characterization of airineme blebs.

(A-A'") Airinemes derive from airineme blebs on the surface of xanthoblasts. Pink arrowheads indicate airineme blebs (A) and airineme vesicles (A'-A'") (B) Measurements of airineme vesicle diameter which was used as a proxy for airineme bleb diameter (N = 5 larvae, n = 65 airineme

vesicles). (C) Schematic depicting at which time points vesicle diameter was measured to determine if airineme vesicles change in size over time. (C') Quantification of airineme vesicle size from Ti (T initial) and Tf (T final) (N = 5 larvae, n = 34 airineme vesicles). (D) Quantification of the percentage of surface blebs in the categories <0.75 μm, 0.75-1.75 μm, and >1.75 μm (N = 3 larvae, n = 64 cells). (E-E') Three-dimensional rendering depicting that surface blebs in the category of 0.75-1.75 μm protrude outward from the xanthoblast membrane (green arrowheads). Blebs <0.75 μm and >1.75 μm are non-distinguishable from the xanthoblast membrane *(pink arrowheads, purple arrowheads). (F-F'") Cross-sectional view of each surface bleb subtype. Blebs between 0.75-1.75 μm protrude outward from the xanthoblast membrane (green arrowheads, dotted line), while blebs <0.75 μm and >1.75 μm do not (pink arrowheads, purple arrowheads, dotted line).*

Airineme bleb distribution

Previous research has shown that airinemes are preferentially extended by xanthoblasts during the metamorphic stages (SSL 6.5-8.0), with a distinct peak at SSL 7.5 (Eom et al., 2015) (Figure 30A). Given this developmental pattern, we wondered whether the number of airineme blebs per cell correlates with the number of airinemes produced by those cells. To address this question, we counted the number of airineme blebs per cell and measured the number of airinemes produced by these cells per hour. Our analysis revealed a moderate positive correlation between the number of airineme blebs per cell and the number of airinemes produced per cell per hour (Figure 30B). Based on these findings, we hypothesized that the number of putative airineme blebs would increase in the stages leading up to peak airineme production. Moreover, we hypothesized that beyond SSL 7.5, there might be a decrease in airineme blebs, which correlates with a decrease in airineme production. To investigate this, we

counted the number of putative airineme blebs per cell on the entire fish trunk for each developmental stage spanning SSL 5.0 to 8.0 (Figure 30C). Consistent with our hypothesis, we found that there was an increase in the number of putative airineme blebs per cell at SSL 7.0, just prior to peak airineme extension, which decreases at SSL 8.0 (Figure 30C).

In our initial approach, we counted every cell on the fish trunk for each developmental stage. While our approach provided insight into which developmental stage airineme blebs were most abundant, it remained unclear if airineme bleb-containing xanthoblasts were preferentially located in any quadrant of the fish trunk. To address this limitation, we divided the fish trunk into dorsal and ventral, as well as anterior and posterior compartments using the horizontal myoseptum and dorsal fin as anatomical landmarks (Figure 30E, 30F). This analysis revealed that there were no significant differences in the number of putative airineme blebs per cell in the dorsal, ventral, anterior or posterior compartments, suggesting that airineme bleb-bearing xanthoblasts are not preferentially localized to any one compartment (Figure 30E', 30F').

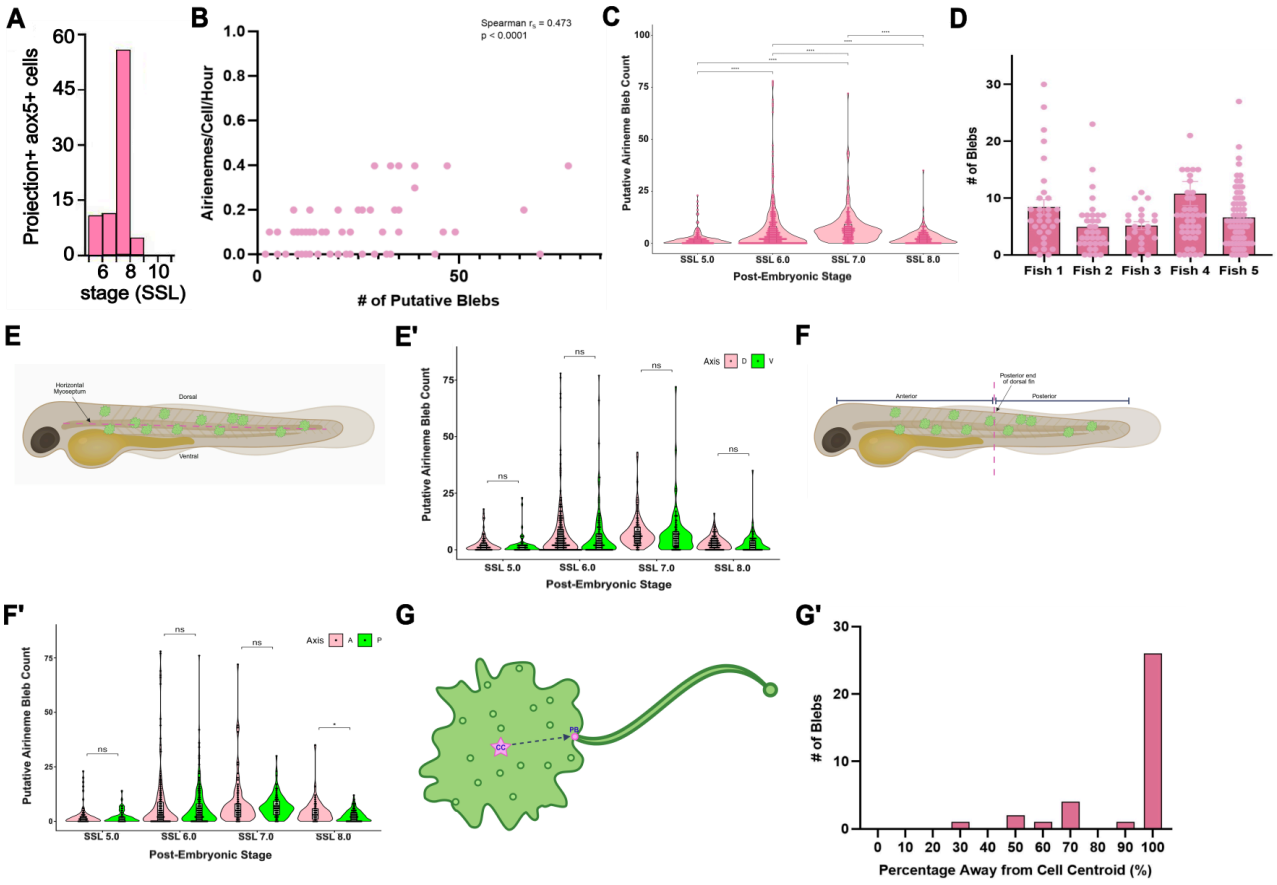

Figure 30. Spatial and temporal distribution of airineme blebs.

(A) Peak airineme extension occurs in zebrafish at SSL 7.5. (B) The number of airinemes per cell per hour versus the number of putative airineme blebs (Spearman Correlation: 0.473). (C) The number of putative airineme blebs per cell at developmental stages 5.0 (N = 5 larvae, n = 154 cells), 6.0 (N = 8 larvae, n = 393 cells), 7.0 (N = 5 larvae, n = 193 cells) and 8.0 (N = 3 larvae, n = 207 cells). (D) Individual fish variation for the number of putative airineme blebs per cell at SSL 7.0 (N = 5 larvae, n = 193 cells). (E) Schematic depicting the partitioning of larvae into dorsal and ventral compartments using the horizontal myoseptum as an anatomical landmark. (E') Violin plot depicting the number of putative airineme blebs per cell in dorsal and ventral compartments for each developmental stage. Wilcoxon test with Benjamini-Hochberg adjustment (NS). (F) Schematic depicting the partitioning of larvae into anterior and posterior

compartments using the most posterior part of the dorsal fin as an anatomical landmark. (F') Violin plot depicting the number of putative airineme blebs per cell in anterior and posterior compartments for each developmental stage. Wilcoxon test with Benjamini-Hochberg adjustment (NS). (G) Schematic depicting the distance from projecting blebs (PB) to the cell centroid (CC). (G') Quantification of the percent distance of PBs from the CC. N = 5 larvae, n = 35 projecting blebs.

Airineme bleb maturation and macrophage engagement

Having identified the airineme bleb subpopulation and characterized its developmental distribution, we wanted to investigate the maturation of these structures. A previous study on airinemes has shown that migrating macrophages recognize PS signals on airineme blebs, causing macrophages to pick them up and pull them through extracellular space (Eom and Parichy, 2017). Given this information, we hypothesized that a portion of airineme blebs are likely PS-positive while the rest are negative, potentially reflecting differences in bleb maturity. To investigate this idea, we co-injected fish with two DNA plasmids: aox5:palmEGFP and pnp4a:secA5-mCherry. The latter drives expression of secreted Annexin5 from iridophores, which diffuses and binds to PS signals on nearby cells. Indeed, we found that not all putative airineme blebs exhibited PS signals, raising the possibility that PS may serve as a marker of airineme bleb maturation (Figure 31A-A'). Additionally, given the importance of CD44a in mediating airineme bleb-metaphocyte interactions, we wondered whether CD44a could be a marker for airineme bleb maturation. To investigate this possibility, we injected DNA plasmid aox5:palmEGFP into TgBAC(cd44a:cd44a-mCherry) fish. Similar to our findings for PS, we found that a subset of putative airineme blebs are CD44a-positive (green arrowheads) while

another subset were CD44a-negative (yellow asterisks), raising the possibility that CD44a may also serve as a marker of airineme bleb maturation (Figure 31B-B').

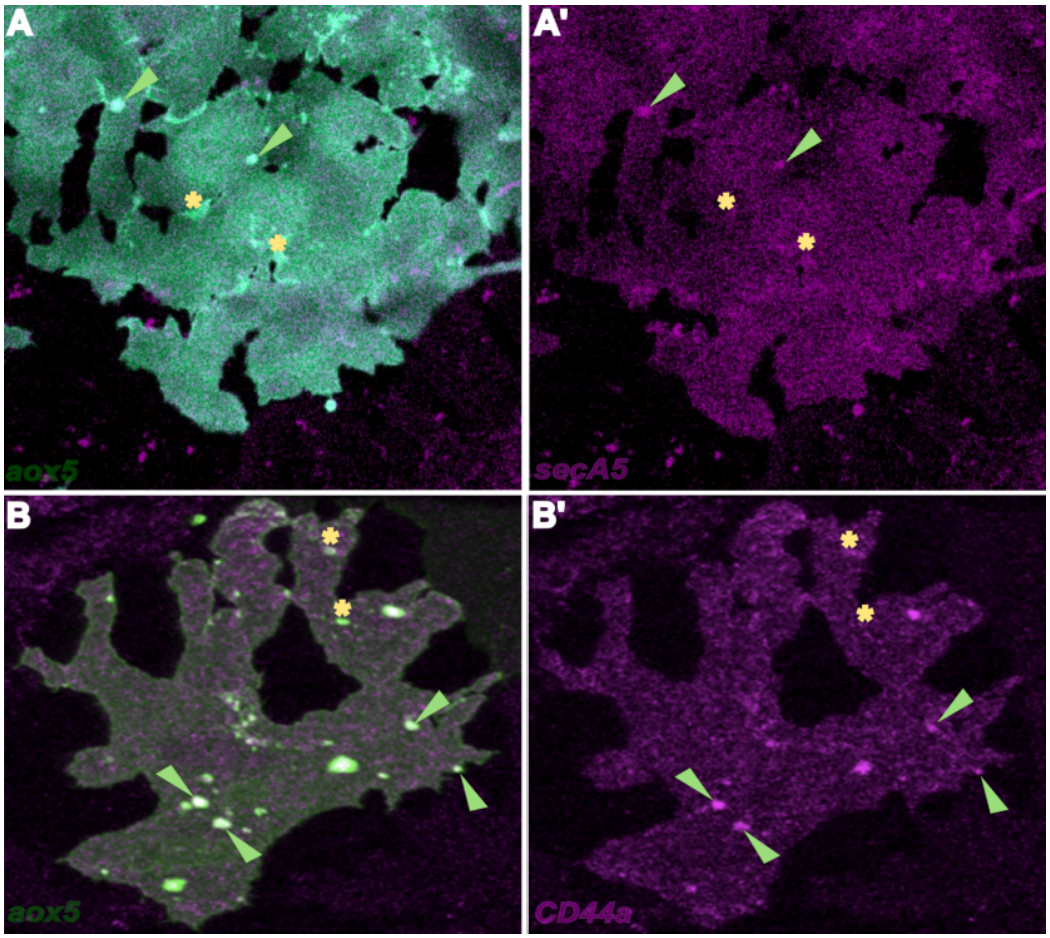

Figure 31. PS status of putative airineme blebs.

(A) Co-injection of aox5:palmEGFP and pnp4a:secA5mCherry into WT(ABb). Green arrow heads reflect putative airineme blebs (defined by size criteria) which co-localize with mCherry. Yellow asterisks indicate putative airineme blebs that do not co-localize with mCherry. (B) Injection of aox5:palmEGFP into TgBAC(cd44a:cd44a-mCherry) fish. Green arrow heads reflect putative airineme blebs (defined by size criteria) which co-localize with mCherry. Yellow asterisks indicate putative airineme blebs that do not co-localize with mCherry.

Examination of PS-positive airineme blebs revealed that these structures were distributed across the xanthoblast membrane, with some located centrally and others at the cell periphery. We therefore sought to determine whether the positioning of airineme blebs impacted macrophage preference. To investigate this idea, we measured the distance between airineme blebs and the center of xanthoblasts (Figure 30G). This analysis revealed that macrophages preferentially interact with airineme blebs located at the cell periphery rather than the cell center (Figure 30G'). This finding raises the possibility that changes in membrane properties at the cell periphery may facilitate macrophage extraction of airineme blebs.

DISCUSSION

We showed that size and morphology can be used as practical criteria for identifying a population of surface blebs that likely represent airineme blebs. Using airineme vesicle diameter as an approximation for airineme bleb size, we identified three subgroups of surface blebs (<0.75 μm, 0.75-1.75 μm, and >1.75 μm), with size thresholds defined as ±1 standard deviation from the mean vesicle diameter. Among these subgroups, we determined, based on their size and protruding morphology, that surface blebs between 0.75 and 1.75 μm were likely to represent airineme blebs (Table 2).

Table 2. Comparing the subgroups of surface blebs on the membranes of xanthoblasts.

Feature	<0.75 μm	0.75-1.75 μm	>1.75 μm
Proportion of all surface blebs	66.82%	27.44%	5.74%
Morphology	Internal Structure	External Structure	Internal Structure
PS Status	Negative	Some Positive	Negative
CD44a Status	Negative	Some Positive	Negative

Moreover, we found that spatial positioning of these putative airineme blebs is associated with macrophage preference, with macrophages preferentially interacting with blebs located at the cell periphery. Surprisingly, although PS is required for airineme bleb recognition by metaphocytes, and CD44a is required for mediating airineme bleb-metaphocyte interactions, only a portion of blebs within this subgroup were PS-positive or CD44a-positive, indicating that PS and CD44a status are not captured by our original identification criteria. Additionally, we demonstrated that airineme blebs are present throughout metamorphosis, increasing at the stage just before SSL 7.5 and decreasing beyond SSL 7.5. Moreover, we found no differences in the percentage of xanthophore lineage cells bearing airineme blebs in the dorsal, ventral, anterior, or posterior compartments. These findings could indicate that airineme bleb-bearing xanthoblasts do not exhibit obvious compartmental enrichment, but additional analyses should be performed at the half stages including SSL 7.5 when airineme production is most abundant to confirm this possibility.

The increase in airineme bleb-bearing xanthoblasts preceding peak airineme production raises the possibility that xanthoblasts enter a preparatory state. One possibility is that this preparatory process is regulated by a hormonal or developmental cue, as yet unidentified, that precedes peak airineme production. Testing this hypothesis will require identification of candidate signaling pathways that are upregulated prior to peak airineme production, which remains an open area for future research.

A previous study has shown that PS is necessary for macrophage recognition of airineme blebs (Eom and Parichy, 2017). Our work showed that a subset of our identified airineme bleb population were PS-positive while others were PS-negative. This raises two possibilities: PS-negative blebs represent immature airineme blebs that have not yet acquired PS, or they may instead represent another type of extracellular structure such as extracellular vesicles (EVs). Investigating these two possibilities will require tracking PS-negative blebs over

time to see whether these structures acquire PS or if they remain negative. If PS-negative airineme blebs become positive, this would suggest that PS is a marker for airineme bleb maturation status; if they remain PS-negative throughout tracking, this would suggest that this subgroup does not represent airineme blebs. Similarly, the presence of both CD44a-positive and CD44a-negative putative airineme blebs raises the possibility that CD44a may also be associated with airineme bleb maturation. Determining the temporal order of cargo acquisition may also help establish whether molecular marker acquisition corresponds to discrete stages of airineme bleb maturation. While studies have shown that Dlc is present within airineme blebs and vesicles, it remains unknown when airineme blebs acquire this cargo, in what order, and by what mechanism this occurs. Addressing these questions will require future studies directly tracking cargo dynamics within individual airineme blebs over time.

Several limitations of this study should be noted. First, the lack of a specific marker for airineme blebs required us to rely on F_0 injection of DNA plasmid aox5:palmEGFP as a labeling strategy. Although our size and morphology based criteria allowed us to exclude a majority of non-airineme blebs, it remains possible that our airineme bleb counts also included non-airineme surface blebs. Conversely, it is also possible that smaller surface blebs that we determined to be non-airineme blebs represent immature airineme blebs that may grow upon acquisition of cargo. Similarly, some of the larger surface blebs classified as non-airineme blebs may represent membrane-bound organelles or recycled membrane components, as originally hypothesized. Alternatively, these structures may represent two or more airineme blebs in close proximity, which would be indistinguishable from a single larger bleb using our current classification approach. Addressing both of these possibilities will require tracking airineme blebs at higher resolution to determine whether these structures change in volume over time and whether they fuse together. Moreover, the use of F_0 injection for our experiments raises the possibility that individual fish vary in the number of cells labeled and the strength of fluorescent

protein expression, potentially leading to differences in the number of detectable putative blebs. To address this possibility, we plotted the number of putative blebs for five individual fish at SSL 7.0, which revealed some variation between fish but no apparent large differences in the number of putative blebs (Figure 30D). Additionally our approach for identifying airineme bleb size assumes that airineme bleb size is preserved once blebs become mature airineme vesicles; whether this is the case remains unknown, and represents a limitation of our current classification strategy. Although we did not detect any significant changes in airineme vesicle diameter, consistent with the use of vesicle diameter as an approximation for bleb size, it is worth noting that appreciable changes in airineme vesicle size may fall below our current imaging resolution. Further confirmation that our subgroup of interest accurately represents airineme blebs could be achieved by co-labeling surface blebs with DeltaC (Dlc) ligand, both of which has been functionally implicated in airineme-mediated signaling: Dlc localizes to airineme vesicles and is required to activate Notch signaling in target melanophores (Eom et al., 2015; Bowman et al., 2025). In addition to size and morphology, co-labeling with this marker would further validate that our proposed subgroup represents airineme blebs.

In this chapter, we established criteria for identifying airineme blebs based on size and morphology, characterized their development and spatial distribution, and identified PS as a potential marker of airineme bleb maturation. Beyond airineme biology specifically, our findings carry broader significance for the field of specialized filopodia-mediated signaling. To date, airinemes are the only subclass of specialized filopodia that require additional cell types for signal transduction. By establishing reliable criteria for identifying airineme blebs, we have provided a foundation for studying how airineme-mediated signaling is regulated at its earliest stages. More broadly, the process by which airineme blebs form and mature may be conserved amongst other extracellular structures such as extracellular vesicles (EVs). EVs are membrane-bound structures which contain diverse cargo, including DNA, RNA, proteins, lipids, and metabolites, and have been isolated in a variety of biological fluids and organisms (Kalra et

al., 2016). EVs can mediate both short- and long-range CCC and are broadly classified into several subtypes, including exosomes, ectosomes (also referred to as microvesicles), and apoptotic bodies (Pollet et al., 2018; Kalra et al., 2016). Of particular interest are ectosomes, which form through direct budding from the plasma membrane which is similar to the protruding morphology observed in airineme blebs (Kalra et al., 2016; Tricarico et al., 2017; Pollet et al., 2018). These similarities are particularly relevant because both structures arise through outward budding of the plasma membrane and are influenced by changes in membrane composition and cell-surface interactions. For example, it has been shown that ectosome formation is reliant upon PS exposure which induces membrane curvature and favors ectosome formation (Kalra et al., 2016; van Niel et al., 2018; Record et al., 2018). Similarly, airineme blebs require exposure of PS for recognition by macrophages, raising the possibility that PS may play additional roles in airineme bleb formation or maturation beyond macrophage recognition (Eom and Parichy, 2017). Furthermore, CD44 has been implicated in the docking of ectosomes onto target cells, while our previous work demonstrated that CD44 is required for establishment of trans-adhesive interactions between airineme blebs and metaphocytes (van Niel et al., 2018; Bowman et al., 2025). Although airineme blebs and ectosomes are distinct extracellular structures, these similarities raise the possibility that some of the factors which control ectosome biogenesis may also play an important role in airineme bleb biogenesis, providing broader insight into how outward-budding vesicular structures form and mature.

Together with the findings presented in Chapters 1 and 2, this work establishes a framework for understanding how airineme bleb formation and maturation occurs, as well as macrophage involvement in airineme-mediated CCC. These findings provide a foundation for determining how airineme blebs are formed, matured, and ultimately incorporated into the airineme signaling pathway.

EXPERIMENTAL MODEL AND SUBJECT DETAILS

Zebrafish

Fish were maintained at 28.5 C, 16:8 L:D. Zebrafish were wild-type AB^wp or its derivative WT(ABb), as well as, Tg(mpeg1:palmEGFP), Tg(mpeg1:mCherry). Experiments were performed prior to the development of secondary sexual characteristics, so the number of females and males used in the study could not be determined, however, all stocks used generated approximately balanced sex ratios, so the experiments likely sampled similar numbers of females and males. All animal work in this study was conducted with the approval of the University of California Irvine Institutional Animal Care and Use Committee (Protocol #AUP-22-023) in accordance with institutional and federal guidelines for the ethical use of animals.

METHOD DETAILS

Time-lapse and still imaging

Ex vivo imaging of pigment cells was done using a Leica TCS SP8 confocal microscope equipped with a resonant scanner and two HyD detectors. Time-lapse images were taken at 5-min intervals over a span of 10 hr. Overnight time-lapse imaging was performed when larvae reached SSL 7.5. For both time-lapse and still imaging, images were taken at lower exposures to ensure maximum visibility of airineme blebs on the surface of xanthoblasts.

Vesicle diameter measurements

Measurements of each airineme vesicle diameter were taken at the first time point in which the vesicle appears perfectly spherical. Diameter was measured using the line tool in FIJI. For vesicle diameter initial and final, vesicle diameter was measured at the first instance of sphericity and again at the last time point where sphericity was observed.

Bleb counting

In LasX, scale bars were drawn at 400% magnification for the following sizes 0.75, 1.0 and 1.75 um. These scale bars were traced and superimposed on transparent film onto the same images open at 400% magnification in FIJI. Using the cell counter plugin in FIJI, blebs were categorized as <1.75 if their diameters exceeded 1.75 um, 0.75-1.75 um if their diameters fell into the size range, or >0.75 um if their diameters were equal to or less than 0.75 um.

Developmental stage bleb counts

Fish were imaged each stage beginning from SSL 5.0 to SSL 8.0. Images were taken beginning from the most anterior portion underneath the dorsal fin until the beginning of the caudal tail. Each image was divided into anterior/posterior and dorsal/ventral sections. The most posterior end of the dorsal fin was used to separate the fish into anterior and posterior compartments, while the horizontal midline served as a landmark to separate the fish into dorsal and ventral compartments. Bleb counts for each cell in each axis were performed as described above in the bleb counting section.

Cell area size measurements

The perimeter of each cell was manually traced in FIJI and area was calculated using the measurement tool within FIJI.

Center versus periphery bleb analysis

Each cell was manually traced in FIJI and duplicated into a second window where the background was cleared, threshold was applied, and remaining holes were filled using the binary function. On the same duplicated image cell centroid was calculated. The x,y coordinates of the cell centroid were then duplicated onto the original, unprocessed image. Distance was measured using the line tool, between each projecting bleb and the cell centroid in um. Percentage from cell centroid was calculated as follows: (distance from center to projecting bleb/distance from center to nearest cell edge)*100.

QUANTIFICATION AND STATISTICAL ANALYSIS

Statistical analyses were performed using GraphPad Prism software version 10.4.1 for PC (GraphPad Software, San Diego, CA, USA).

CHAPTER 4: SUMMARY AND CONCLUSIONS

CCC is essential for coordinating developmental processes including differentiation and tissue patterning. Although endocrine, synaptic, juxtacrine, and paracrine signaling represent well-characterized mechanisms of CCC, they are not the only signaling modalities that exist in nature. CCC can also be mediated by specialized filopodia such as intercellular bridges, cytonemes, tunneling nanotubes, and airinemes. Of these structures, airinemes represent a unique system which requires the coordinated activities of pigment cells, immune cells, and specialized signaling structures to achieve precise signal delivery during zebrafish pigment pattern formation (Eom et al., 2015; Eom and Parichy, 2017; Bowman et al., 2023).

Previous airineme-related studies have revealed some of the molecular players involved in mediating airineme signaling. They have shown, for example, that airinemes arise from membranous surface blebs on xanthoblasts that expose PS, and that PS-exposure is a signal recognized by migrating macrophages, allowing them to extract the blebs (Eom and Parichy, 2017). Moreover, they have shown that following airineme extrusion, macrophages continue to migrate with airineme vesicles and their filaments, and deposit them onto target melanophores (Eom et al., 2015; Eom, 2020). These studies have furthermore shown that airineme vesicles contain Dlc ligand, which activates Delta-Notch signaling in target melanophores once docking has occurred (Eom et al., 2015; Eom, 2020). The activation of Delta-Notch in target melanophores by airinemes triggers melanophore migration out of the developing interstripe and into the prospective stripe region. When airineme-mediated signaling is inhibited, ectopic melanophores persist in the interstripe, signifying the importance of airineme-mediated CCC in melanophore clearance during pigment pattern formation (Eom et al., 2015; Eom, 2020).

These studies have largely expanded our understanding of airineme-mediated CCC, yet several gaps in knowledge remain. The work presented in this dissertation explores a few of these unknowns including the subpopulation of macrophages that is responsible for airineme-signal transport, the molecular players involved in macrophage-airineme bleb

interactions, and a framework for studying airineme biogenesis and maturation. Each of these is described below.

In chapter 1, I demonstrated that there are at least two macrophage subpopulations that exist in zebrafish skin – dendritic cells and amoeboid cells. Furthermore, these cell populations could be distinguished based on their morphologies and migratory behaviors. I showed that dendritic cells were larger and had a more branched appearance, while amoeboid cells were smaller, rounded, and had fewer branches (Bowman et al., 2023). Additionally, I demonstrated that dendritic cells migrated significantly slower compared to amoeboid cells, and are located more apically in the skin, while amoeboid cells migrated faster and localized more often to the hypodermis where airineme-projecting xanthoblasts are located (Bowman et al., 2023). I identified that the amoeboid macrophage subpopulation overlaps in expression with a subpopulation of macrophages derived from zebrafish ectoderm, termed 'metaphocytes' (Lin et al., 2019; Lin et al., 2020). Lastly, using a combination of inhibitor treatments and cell-specific manipulations, I demonstrated that metaphocytes are dependent on MMP9 to dive through skin tissue to the hypodermis and interact with airineme-projecting xanthoblasts (Bowman et al., 2023).

Originally macrophages had been characterized as near-homogenous populations of cells whose primary function was phagocytosis (Mass et al., 2023). More recently, however, researchers have found that macrophages are heterogeneous, and can establish tissue-specific niches (Mass et al., 2023). Moreover, studies have shown that in addition to their phagocytic roles, macrophages also play important roles in tissue homeostasis, tissue patterning, and development. For example, in macrophage depleted mice (*PU.1 -/-*), researchers have shown that the loss of macrophages results in abnormal hindbrain vasculature and retinal vessel remodeling, highlighting their role in vascular patterning (Stefater III et al., 2011). Additionally, studies have also shown that macrophages play an important role in regulating systemic blood pressure. In response to salt-induced hypertension, macrophages secrete VEGF-C, which

expands lymphatic capacity and aids in fluid drainage, leading to decreases in systemic blood pressure, exemplifying their importance in homeostatic maintenance (Stefater III et al., 2011). The work of Eom and Parichy has further added to the list of roles played by macrophages by showing that these immune cells also act as signaling vehicles for airinemes filaments (Eom and Parichy, 2017). My work has now expanded on these findings by demonstrating that macrophage heterogeneity may extend to specialization in CCC, with distinct macrophage subpopulations exhibiting different cellular behaviors and potentially specialized roles in developmental signaling.

In chapter 2, I showed that the surface glycoprotein CD44 is required for establishing trans-adhesive interactions between airineme bleb-bearing xanthoblasts and metaphocytes (Bowman et al., 2025). Furthermore, I showed that CD44 protein co-localizes with metaphocytes, airineme vesicles, and airineme blebs. Using cell-specific manipulations, I demonstrated that CD44-ECD is necessary for airineme-mediated signaling. When CD44-ECD function is disrupted in either metaphocytes or xanthophore-lineage cells, airineme frequency is significantly decreased, an effect that is compounded when CD44-ECD is disrupted in both cell types simultaneously (Bowman et al., 2025). Although my work did not demonstrate a role for CD44 in reinforcing metaphocyte-airineme interactions during pulling, it did suggest a dependence of CD44-ECD in mediating airineme bleb-metaphocyte interactions in the initial stages of airineme signaling. Together, these findings suggest that airineme signaling is dependent not only on the presence of a specialized macrophage population, but also on molecular mechanisms that selectively establish interactions between signaling and transport cells.

Lastly, in chapter 3, I established a method for studying airineme blebs, which were previously understudied structures in airineme-mediated signaling. I demonstrated that airineme blebs can be identified amongst other membrane blebs on the surface of xanthoblasts, using size and morphology as criteria. Previous airineme-mediated CCC studies had shown that

airineme signaling peaks at distinct developmental time points, however the relationship between the developmental timing of these events and airineme bleb formation had remained unknown. My work has addressed this gap in knowledge by tracking the number of putative airineme blebs per cell through development. I demonstrated that in the stages leading up to peak airineme production, there is an increase in the number of putative airineme blebs per cell. Additionally, I have shown that phosphatidylserine (PS), which was previously shown to act as a recognition marker for macrophages, and CD44a, which plays an important role in mediating airineme bleb-metaphocyte interactions, may serve as molecular markers of airineme bleb maturation (Eom and Parichy, 2017).

In combination, the work presented in chapters 1, 2 and 3 serves as a foundation for future airineme-related studies. With regard to airineme blebs, it remains unknown how they form or how cargo is acquired, but the methods described in this dissertation can be used to further investigate these questions. For example, given the dynamic size range of airineme blebs, it is possible that the different sizes of airineme blebs represent different states of maturity. Smaller blebs may represent airineme blebs which have yet to acquire cargo, whereas larger blebs may represent cargo-filled airineme blebs. Similarly, the temporal order of cargo acquisition, and whether cargo-filled airineme blebs migrate to the cell periphery for metaphocyte pickup, should be investigated. These questions may be addressed through live imaging and labeling using cargo-specific markers PS, CD44, and Dlc which may reveal when cargo is acquired, whether cargo is associated with airineme bleb maturation, and whether cargo presence initiates bleb migration. Beyond these characterizations, future directions for the study of airineme blebs should also look to disseminate the underlying mechanisms governing airineme bleb formation and scission.

One potential avenue for identifying these mechanisms is to investigate molecular candidates known to regulate the formation of other vesicular structures. Of particular interest are extracellular vesicles (EVs), which contain numerous cargoes including DNA, RNA, proteins

and lipids, and have been shown to play a role in mediating both short- and long-range CCC (Kalra et al., 2016). Interestingly, a subset of EVs called ectosomes share a number of morphological and molecular features with airineme blebs. For example, ectosomes and airineme blebs are both of a similar size range and directly bud outwards from the plasma membrane (Pollet et al., 2018; Kalra et al., 2016; Tricarico et al., 2017). Moreover, PS exposure is required by both ectosomes and airineme blebs (Kalra et al., 2016; van Niel et al., 2018; Record et al., 2018; Eom and Parichy, 2017). Additionally, researchers have shown a dependence of CD44 in mediating ectosome docking onto target cells (van Niel et al., 2018). In chapter 2, I revealed that CD44 is necessary for mediating trans-adhesive interactions between airineme blebs and metaphocytes. Interestingly, in addition to airineme bleb-bearing xanthoblasts and metaphocytes, target melanophores also express high levels of CD44 protein (Figure 32). The expression of CD44 by target melanophores raises the possibility that CD44 may also participate in airineme interactions at the receiving cell, although this remains to be tested. Given the similarities between ectosomes and airineme blebs, it is possible that the factors regulating vesicle formation and release are conserved between these two structures. This possibility does not imply that airineme blebs are ectosomes; rather, the structural and molecular similarities raise the possibility that some conserved mechanisms of plasma membrane budding may contribute to their formation.

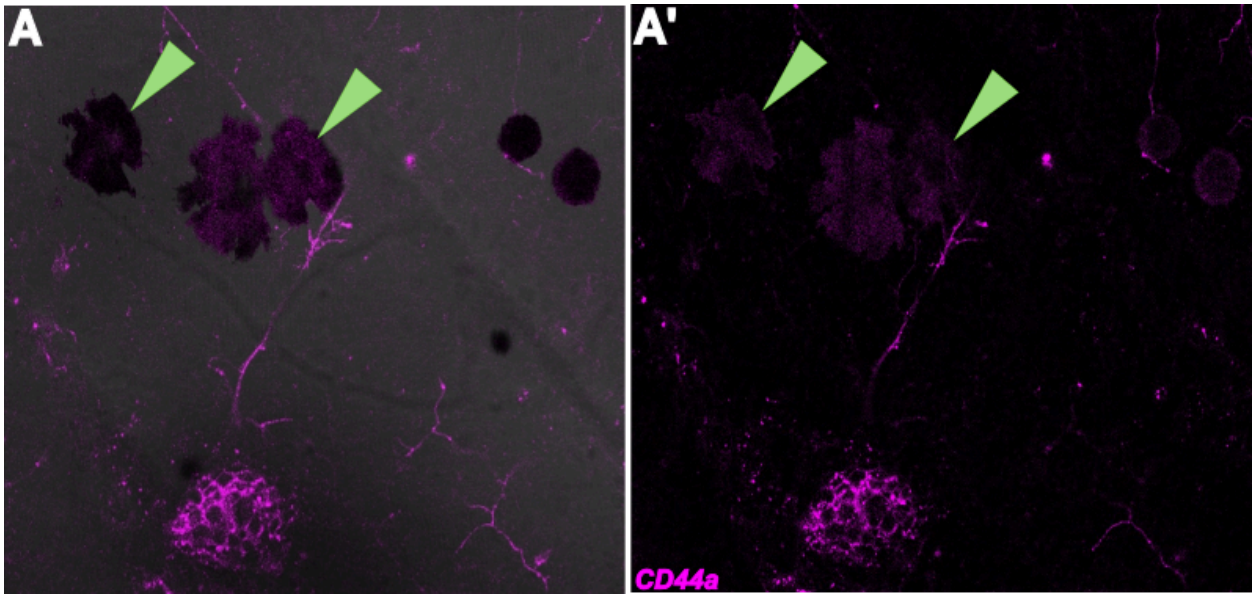

Figure 32. CD44a expression in melanophores.

(A-A') Confocal images of zebrafish skin depicting melanophores (green arrowheads) co-expressing CD44a-mCherry signals (magenta).

Studies on ectosomes suggest that there are multiple mechanisms of formation and release which could also apply to airineme bleb biogenesis. I will discuss two of these mechanisms in brief. The first of these mechanisms suggests that ectosomes are formed through changes in lipid composition at the level of the plasma membrane. For example, when levels of Ca^{2+} increase, lipid translocases such as flippases and floppases are activated which can generate lipid rearrangement at the plasma membrane (van Niel et al., 2018). This includes the exposure of PS, which can induce local membrane curvature and has been shown to promote ectosome formation (Kalra et al., 2016; van Niel et al., 2018). The importance of this rearrangement is highlighted by manipulations in P4 ATPase TAT-5, which is involved in translocating phospholipids to the inner leaflet of the plasma membrane in C. Elegans (Juan and Furthauer, 2018). The loss of TAT-5 results in increased exposure of phosphatidylEthanolamine on the outer cell surface, generating local membrane curvatures,

leading to increased ectosome release (Juan and Furthauer, 2018). Given the ability of PS to induce local membrane curvatures which induce ectosome shedding, it is possible that in addition to being a recognition signal, PS exposure may also promote the outward budding of airineme blebs (Eom and Parichy, 2017).

A secondary mechanism which has been proposed to regulate the formation of ectosomes is the Endosomal Sorting Complex Required for Transport (ESCRT) (van Niel et al., 2018). The ESCRT pathway is composed of multiple complexes including ESCRT 0, I, II, III and the vacuolar protein sorting 4 (Vps4) complex. Among these, studies suggest that complexes ESCRT-I, ESCRT-III and Vps4 are involved in ectosome formation and scission. Specifically, it has been shown that Arrestin Domain-Containing Protein 1 (ARRDC1) recruits ESCRT-I to the plasma membrane, which subsequently recruits ESCRT-III to the budding neck of forming ectosomes and facilitates constriction (Juan and Furthauer, 2018; Christ et al., 2017). ESCRT-III then recruits Vps4 which depolymerizes ESCRT-III filaments through ATP hydrolysis, resulting in membrane scission (Christ et al., 2017). In zebrafish, it has been shown that mutants lacking functional Vps4a inefficiently disassemble ESCRT-III filaments and have larger vesicle compartments, suggesting that vesicles can still form in these mutants but are not shed (Shipman et al., 2024). While a mechanism for airineme bleb scission has yet to be identified, the role of vps4a in membrane scission in EVs, which has also been validated in zebrafish, represents a good candidate for future studies.

Rather than functioning as a single signaling event, the findings presented throughout this dissertation support a model in which airineme-mediated communication is assembled through a series of coordinated cellular interactions. Signaling begins with the formation and maturation of airineme blebs on xanthoblasts, continues through selective recognition and transport by metaphocytes, leading to the delivery of signaling cargo to target melanophores (Figure 33). At each step, specific cellular behaviors and molecular interactions regulate whether signaling proceeds successfully, suggesting that airineme-mediated CCC is governed

through multiple regulatory checkpoints rather than a single transport event. Additionally, the work presented in this dissertation may serve as a platform for better understanding of general mechanisms governing filopodia-mediated CCC, including newly described protrusions. For example, a recent study has shown that live mast cells can extend long, filamentous protrusions which make contact with nearby large peritoneal macrophages and induce repair (Salm et al., 2026). Interestingly, these protrusions have a curved morphology and vesicles at their tips which is reminiscent of airineme morphology (Salm et al., 2026; Eom et al., 2015). These similarities raise the possibility that related mechanisms of protrusion-mediated communication may operate across different tissues and species.

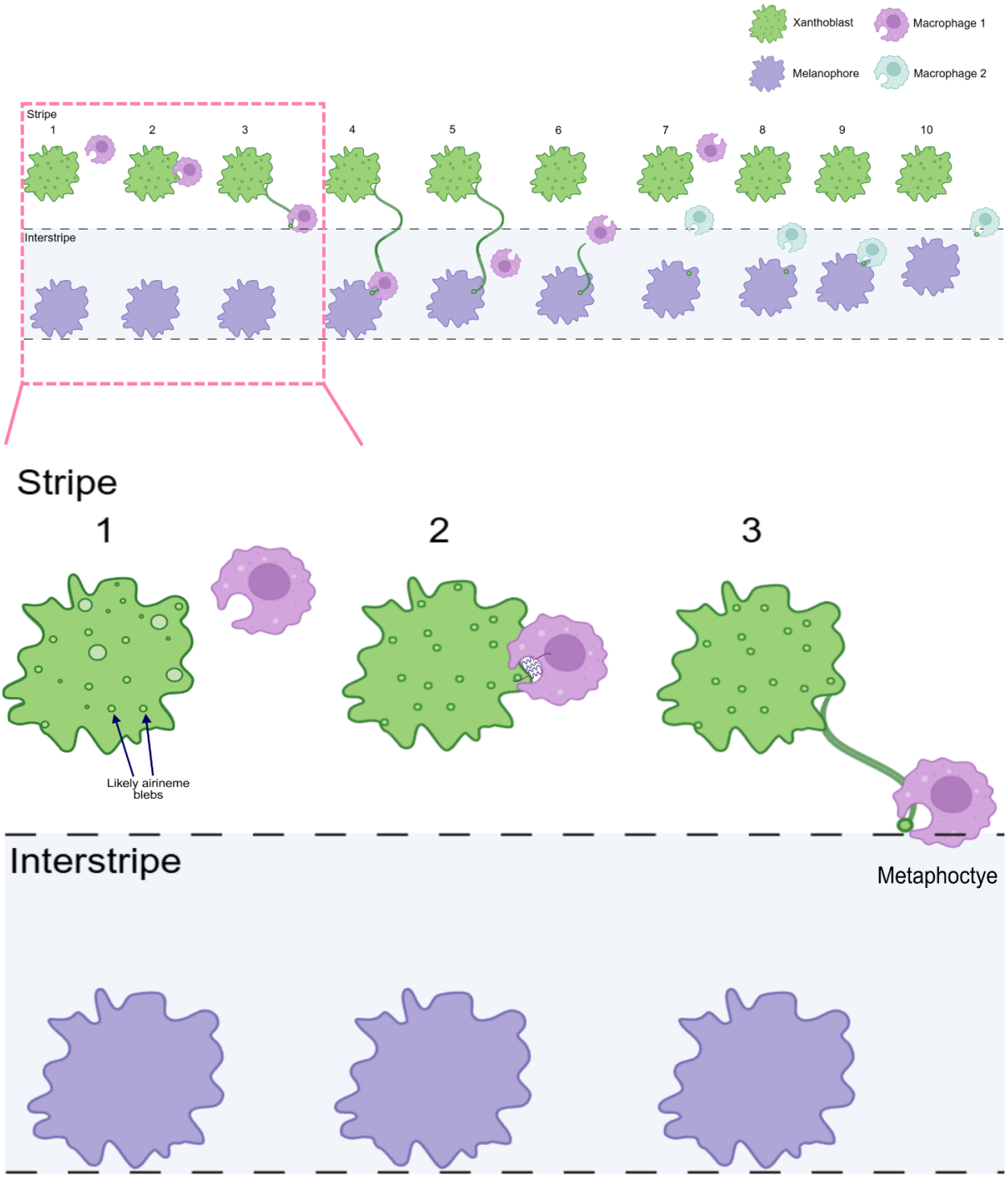

Figure 33. Summary of chapter findings.

Migrating metaphocytes interact with airineme blebs located at the cell periphery. These blebs lie in the range of 0.75 to 1.0 um in diameter and outwardly protrude from the cell membrane.

Blebs outside of this range also exist on the xanthoblast membrane but are unlikely to represent airineme blebs. Metaphocytes recognize PS exposure on airineme blebs and participate in trans-adhesive interactions with these bulbous structures through the action of CD44-ECD.

Altogether this dissertation demonstrates that airineme-mediated CCC is a multistep process involving precursor blebs that form into mature airinemes, a macrophage subpopulation with a specialized role in airineme-mediated CCC, and the molecular players involved in mediating adhesive interactions between them. My work has furthered our understanding of airineme-mediated signaling which may also extend to our understanding of filopodial-mediated CCC as a whole. Furthermore, these findings demonstrate that CCC can depend on coordinated interactions between signaling cells, immune cells, and extracellular signaling structures, highlighting the diversity and complexity of mechanisms used by cells to communicate across tissue space.

REFERENCES (OR BIBLIOGRAPHY)

Armingol, E., Officer, A., Harismendy, O. & Lewis, N. E. Deciphering cell–cell interactions and communication from gene expression. *Nat Rev Genet* **22**, 71–88 (2021).

Ando, K., Shibata, E., Hans, S., Brand, M. & Kawakami, A. Osteoblast Production by Reserved Progenitor Cells in Zebrafish Bone Regeneration and Maintenance. *Developmental Cell* **43**, 643-650.e3 (2017).

Belian, S. & Zurzolo, C. Breaking cellular boundaries: molecular mechanisms of tunneling nanotube formation and fusion. *Biochemical Society Transactions* **54**, 259–280 (2026).

Blériot, C., Chakarov, S. & Ginhoux, F. Determinants of Resident Tissue Macrophage Identity and Function. *Immunity* **52**, 957–970 (2020).

Bohaud, C. *et al.* The Role of Macrophages During Mammalian Tissue Remodeling and Regeneration Under Infectious and Non-Infectious Conditions. *Front. Immunol.* **12**, 707856 (2021).

Bosenberg, M. W. & Massagué, J. Juxtacrine cell signaling molecules. *Current Opinion in Cell Biology* **5**, 832–838 (1993).

Bouzat, C. & Mukhtasimova, N. The nicotinic acetylcholine receptor as a molecular machine for neuromuscular transmission. *Current Opinion in Physiology* **4**, 40–48 (2018).

Bowman, R. L., Wang, D. & Eom, D. S. A macrophage subpopulation promotes airineme-mediated intercellular communication in a matrix metalloproteinase-9 dependent manner. *Cell Reports* **42**, 112818 (2023).

Bowman, R. L., Kim, J., Parsons, M. J. & Eom, D. S. CD44 facilitates adhesive interactions in airineme-mediated intercellular signaling. *Front. Cell Dev. Biol.* **13**, 1522710 (2025).

Brou, C. & Zurzolo, C. Building the bridges: molecular mechanisms of tunneling nanotube formation. *Cell. Mol. Life Sci.* **83**, 235 (2026).

Caviglia, S. & Ober, E. A. Non-conventional protrusions: the diversity of cell interactions at short and long distance. *Current Opinion in Cell Biology* **54**, 106–113 (2018).

Chen, C., Zhao, S., Karnad, A. & Freeman, J. W. The biology and role of CD44 in cancer progression: therapeutic implications. *J Hematol Oncol* **11**, 64 (2018).

Christ, L., Raiborg, C., Wenzel, E. M., Campsteijn, C. & Stenmark, H. Cellular Functions and Molecular Mechanisms of the ESCRT Membrane-Scission Machinery. *Trends in Biochemical Sciences* **42**, 42–56 (2017).

Cohen, M., Georgiou, M., Stevenson, N. L., Miodownik, M. & Baum, B. Dynamic Filopodia Transmit Intermittent Delta-Notch Signaling to Drive Pattern Refinement during Lateral Inhibition. *Developmental Cell* **19**, 78–89 (2010).

Combarnous, Y. & Nguyen, T. M. D. Cell Communications among Microorganisms, Plants, and Animals: Origin, Evolution, and Interplays. *IJMS* **21**, 8052 (2020).

Curado, S., Stainier, D. Y. R. & Anderson, R. M. Nitroreductase-mediated cell/tissue ablation in zebrafish: a spatially and temporally controlled ablation method with applications in developmental and regeneration studies. *Nat Protoc* **3**, 948–954 (2008).

Daly, C. A., Hall, E. T. & Ogden, S. K. Regulatory mechanisms of cytoneme-based morphogen transport. *Cell. Mol. Life Sci.* **79**, 119 (2022).

Davies, L. C., Jenkins, S. J., Allen, J. E. & Taylor, P. R. Tissue-resident macrophages. *Nat Immunol* **14**, 986–995 (2013).

Dawson, J. E. *et al.* Contact area and tissue growth dynamics shape synthetic juxtacrine signaling patterns. *Biophysical Journal* **124**, 93–106 (2025).

Deguchi, E., Matsuda, M. & Terai, K. Live imaging of paracrine signaling: Advances in visualization and tracking techniques. *Cell Struct. Funct.* **50**, 1–14 (2025).

De Joussineau, C. *et al.* Delta-promoted filopodia mediate long-range lateral inhibition in Drosophila. *Nature* **426**, 555–559 (2003).

Desai, B., Ma, T. & Chellaiah, M. A. Invadopodia and Matrix Degradation, a New Property of Prostate Cancer Cells during Migration and Invasion. *Journal of Biological Chemistry* **283**, 13856–13866 (2008).

Driever, W. & Nüsslein-Volhard, C. The bicoid protein determines position in the Drosophila embryo in a concentration-dependent manner. *Cell* **54**, 95–104 (1988).

Du, L., Sohr, A., Yan, G. & Roy, S. Feedback regulation of cytoneme-mediated transport shapes a tissue-specific FGF morphogen gradient. *eLife* **7**, e38137 (2018).

Ellett, F., Pase, L., Hayman, J. W., Andrianopoulos, A. & Lieschke, G. J. mpeg1 promoter transgenes direct macrophage-lineage expression in zebrafish. *Blood* **117**, e49–e56 (2011).

Eom, D. S., Bain, E. J., Patterson, L. B., Grout, M. E. & Parichy, D. M. Long-distance communication by specialized cellular projections during pigment pattern development and evolution. *eLife* **4**, e12401 (2015).

Eom, D. S. & Parichy, D. M. A macrophage relay for long-distance signaling during postembryonic tissue remodeling. *Science* **355**, 1317–1320 (2017).

Eom, D. S. Airinemes: thin cellular protrusions mediate long-distance signalling guided by macrophages. *Open Biol.* **10**, 200039 (2020).

Fawcett, D. W., Ito, S. & Slautterback, D. The Occurrence of Intercellular Bridges in Groups of Cells Exhibiting Synchronous Differentiation. *The Journal of Cell Biology* **5**, 453–460 (1959).

Frohnhöfer, H. G., Krauss, J., Maischein, H.-M. & Nüsslein-Volhard, C. Iridophores and their interactions with other chromatophores are required for stripe formation in zebrafish. *Development* **140**, 2997–3007 (2013).

Gibson, D. G. *et al.* Enzymatic assembly of DNA molecules up to several hundred kilobases. *Nat Methods* **6**, 343–345 (2009).

Ginhoux, F. & Guilliams, M. Tissue-Resident Macrophage Ontogeny and Homeostasis. *Immunity* **44**, 439–449 (2016).

Gomez Perdiguero, E. *et al.* The Origin of Tissue-Resident Macrophages: When an Erythro-myeloid Progenitor Is an Erythro-myeloid Progenitor. *Immunity* **43**, 1023–1024 (2015).

Gong, Y., Hart, E., Shchurin, A. & Hoover-Plow, J. Inflammatory macrophage migration requires MMP-9 activation by plasminogen in mice. *J. Clin. Invest.* **118**, 3012–3024 (2008).

González-Méndez, L., Gradilla, A.-C. & Guerrero, I. The cytoneme connection: direct long-distance signal transfer during development. *Development* **146**, dev174607 (2019).

Greenbaum, M. P., Iwamori, T., Buchold, G. M. & Matzuk, M. M. Germ Cell Intercellular Bridges. *Cold Spring Harbor Perspectives in Biology* **3**, a005850–a005850 (2011).

Guilliams, M., Thierry, G. R., Bonnardel, J. & Bajenoff, M. Establishment and Maintenance of the Macrophage Niche. *Immunity* **52**, 434–451 (2020).

Günthert, U. *et al.* Are CD44 variant isoforms involved in human tumour progression? *Cancer Surv* **24**, 19–42 (1995).

Gupta, A. *et al.* Promising Noninvasive Cellular Phenotype in Prostate Cancer Cells Knockdown of Matrix Metalloproteinase 9. *The Scientific World Journal* **2013**, 493689 (2013).

Haeusler, R. A., McGraw, T. E. & Accili, D. Biochemical and cellular properties of insulin receptor signalling. *Nat Rev Mol Cell Biol* **19**, 31–44 (2018).

Hall, E. T. *et al.* Cytoneme signaling provides essential contributions to mammalian tissue patterning. *Cell* **187**, 276-293.e23 (2024).

Harfe, B. D. *et al.* Evidence for an Expansion-Based Temporal Shh Gradient in Specifying Vertebrate Digit Identities. *Cell* **118**, 517–528 (2004).

Henderson, J. M. *et al.* Tunnelling nanotube formation is driven by Eps8/IRSp53-dependent linear actin polymerization. *EMBO J* **42**, EMBJ2023113761 (2023).

Herbomel, P., Thisse, B. & Thisse, C. Ontogeny and behaviour of early macrophages in the zebrafish embryo. *Development* **126**, 3735–3745 (1999).

Herbomel, P. & Levraud, J.-P. maging Early Macrophage Differentiation, Migration, and Behaviors in Live Zebrafish Embryos. in *Developmental Hematopoiesis* vol. 105 199–214 (Humana Press, New Jersey, 2004).

Hirata, M., Nakamura, K., Kanemaru, T., Shibata, Y. & Kondo, S. Pigment cell organization in the hypodermis of zebrafish. *Developmental Dynamics* **227**, 497–503 (2003).

Huang, H. & Kornberg, T. B. Myoblast cytonemes mediate Wg signaling from the wing imaginal disc and Delta-Notch signaling to the air sac primordium. *eLife* **4**, e06114 (2015).

Jiang, D. *et al.* Migrasomes provide regional cues for organ morphogenesis during zebrafish gastrulation. *Nat Cell Biol* **21**, 966–977 (2019).

Juan, T. & Fürthauer, M. Biogenesis and function of ESCRT-dependent extracellular vesicles. *Seminars in Cell & Developmental Biology* **74**, 66–77 (2018).

Kalra, H., Drummen, G. & Mathivanan, S. Focus on Extracellular Vesicles: Introducing the Next Small Big Thing. *IJMS* **17**, 170 (2016).

Kawaguchi, M. *et al.* Extracellular Domains I and II of cell-surface glycoprotein CD44 mediate its trans-homophilic dimerization and tumor cluster aggregation. *Journal of Biological Chemistry* **295**, 2640–2649 (2020).

Korenkova, O. *et al.* Tunneling nanotubes enable intercellular transfer in zebrafish embryos. *Developmental Cell* **60**, 524-534.e3 (2025).

Korn, C. & Augustin, H. G. Mechanisms of Vessel Pruning and Regression. *Developmental Cell* **34**, 5–17 (2015).

Kornberg, T. B. & Roy, S. Cytonemes as specialized signaling filopodia. *Development* **141**, 729–736 (2014).

Kornberg, T. B. & Roy, S. Communicating by touch – neurons are not alone. *Trends in Cell Biology* **24**, 370–376 (2014).

Kuil, L. E. *et al.* Zebrafish macrophage developmental arrest underlies depletion of microglia and reveals Csf1r-independent metaphocytes. *eLife* **9**, e53403 (2020).

Lagente, V., Le Quement, C. & Boichot, E. Macrophage metalloelastase (MMP-12) as a target for inflammatory respiratory diseases. *Expert Opinion on Therapeutic Targets* **13**, 287–295 (2009).

Lander, A. D., Nie, Q. & Wan, F. Y. M. Do Morphogen Gradients Arise by Diffusion? *Developmental Cell* **2**, 785–796 (2002).

Lee, R. T. H., Asharani, P. V. & Carney, T. J. Basal Keratinocytes Contribute to All Strata of the Adult Zebrafish Epidermis. *PLoS ONE* **9**, e84858 (2014).

Lin, X. *et al.* An Ectoderm-Derived Myeloid-like Cell Population Functions as Antigen Transporters for Langerhans Cells in Zebrafish Epidermis. *Developmental Cell* **49**, 605-617.e5 (2019).

Lin, X., Zhou, Q., Lin, G., Zhao, C. & Wen, Z. Endoderm-Derived Myeloid-like Metaphocytes in Zebrafish Gill Mediate Soluble Antigen-Induced Immunity. *Cell Reports* **33**, 108227 (2020).

Liu, X. *et al.* Homophilic CD44 Interactions Mediate Tumor Cell Aggregation and Polyclonal Metastasis in Patient-Derived Breast Cancer Models. *Cancer Discovery* **9**, 96–113 (2019).

Liu, S., Daly, C. A., Ogden, S. K. & Zurzolo, C. Regulation and function of specialized membrane protrusions in intercellular communication. *Nat Rev Mol Cell Biol* **27**, 684–701 (2026).

Ljubojevic, N., Henderson, J. M. & Zurzolo, C. The Ways of Actin: Why Tunneling Nanotubes Are Unique Cell Protrusions. *Trends in Cell Biology* **31**, 130–142 (2021).

Lone, J. B., Long, J. Z. & Svensson, K. J. Size matters: the biochemical logic of ligand type in endocrine crosstalk. *Life Metabolism* **3**, load048 (2024).

López-Otín, C., Blasco, M. A., Partridge, L., Serrano, M. & Kroemer, G. The Hallmarks of Aging. *Cell* **153**, 1194–1217 (2013).

Lundberg, J. O. & Weitzberg, E. Nitric oxide signaling in health and disease. *Cell* **185**, 2853–2878 (2022).

Ma, Z. *et al.* Molecular mechanism of CD44 homodimerization modulated by palmitoylation and membrane environments. *Biophysical Journal* **121**, 2671–2683 (2022).

Mark's Maturation, Fecundation and Segmentation of Limax *Bulletin of the Museum of Comparative Zoology at Harvard College, Vol. VI, No. 12 Maturation, Fecundation and Segmentation of Limax Campestris Binney.* E. L. Mark. *The American Naturalist* **16**, 392–392 (1882).

Mass, E., Nimmerjahn, F., Kierdorf, K. & Schlitzer, A. Tissue-specific macrophages: how they develop and choreograph tissue biology. *Nat Rev Immunol* **23**, 563–579 (2023).

Miletti-González, K. E. *et al.* Identification of Function for CD44 Intracytoplasmic Domain (CD44-ICD). *Journal of Biological Chemistry* **287**, 18995–19007 (2012).

Miller, J., Fraser, S. E. & McClay, D. Dynamics of thin filopodia during sea urchin gastrulation. *Development* **121**, 2501–2511 (1995).

Müller, P. & Schier, A. F. Extracellular Movement of Signaling Molecules. *Developmental Cell* **21**, 145–158 (2011).

Nighot, M. *et al.* Matrix Metalloproteinase MMP-12 Promotes Macrophage Transmigration Across Intestinal Epithelial Tight Junctions and Increases Severity of Experimental Colitis. *Journal of Crohn's and Colitis* **15**, 1751–1765 (2021).

Pagán, A. J. *et al.* Myeloid Growth Factors Promote Resistance to Mycobacterial Infection by Curtailing Granuloma Necrosis through Macrophage Replenishment. *Cell Host & Microbe* **18**, 15–26 (2015).

Paolicelli, R. C. *et al.* Synaptic Pruning by Microglia Is Necessary for Normal Brain Development. *Science* **333**, 1456–1458 (2011).

Parichy, D. M., Elizondo, M. R., Mills, M. G., Gordon, T. N. & Engeszer, R. E. Normal table of postembryonic zebrafish development: Staging by externally visible anatomy of the living fish. *Developmental Dynamics* **238**, 2975–3015 (2009).

Parichy, D. M., Rawls, J. F., Pratt, S. J., Whitfield, T. T. & Johnson, S. L. Zebrafish *sparse* corresponds to an orthologue of c- *kit* and is required for the morphogenesis of a subpopulation of melanocytes, but is not essential for hematopoiesis or primordial germ cell development. *Development* **126**, 3425–3436 (1999).

Park, S., Kim, H., Wang, Y., Eom, D. S. & Allard, J. Zebrafish airinemes optimize their shape between ballistic and diffusive search. *eLife* **11**, e75690 (2022).

Patterson, L. B. & Parichy, D. M. Zebrafish Pigment Pattern Formation: Insights into the Development and Evolution of Adult Form. *Annu. Rev. Genet.* **53**, 505–530 (2013).

Pedersen, M. E., Vuong, T. T., Rønning, S. B. & Kolset, S. O. Matrix metalloproteinases in fish biology and matrix turnover. *Matrix Biology* **44–46**, 86–93 (2015).

Peters, C., Wolf, A., Wagner, M., Kuhlmann, J. & Waldmann, H. The cholesterol membrane anchor of the Hedgehog protein confers stable membrane association to lipid-modified proteins. *Proc. Natl. Acad. Sci. U.S.A.* **101**, 8531–8536 (2004).

Petrie, T. A., Strand, N. S., Tsung-Yang, C., Rabinowitz, J. S. & Moon, R. T. Macrophages modulate adult zebrafish tail fin regeneration. *Development* **141**, 2581–2591 (2014).

Petrov, K. A., Nikolsky, E. E. & Masson, P. Autoregulation of Acetylcholine Release and Micro-Pharmacodynamic Mechanisms at Neuromuscular Junction: Selective Acetylcholinesterase Inhibitors for Therapy of Myasthenic Syndromes. *Front. Pharmacol.* **9**, 766 (2018).

Pisharath, H. & Parsons, M. J. Nitroreductase-Mediated Cell Ablation in Transgenic Zebrafish Embryos. in *Zebrafish* (eds Lieschke, G. J., Oates, A. C. & Kawakami, K.) vol. 546 133–143 (Humana Press, Totowa, NJ, 2009).

Pollet, H., Conrard, L., Cloos, A.-S. & Tyteca, D. Plasma Membrane Lipid Domains as Platforms for Vesicle Biogenesis and Shedding? *Biomolecules* **8**, 94 (2018).

Ponta, H., Sherman, L. & Herrlich, P. A. CD44: From adhesion molecules to signalling regulators. *Nat Rev Mol Cell Biol* **4**, 33–45 (2003).

Ramírez-Weber, F.-A. & Kornberg, T. B. Cytonemes. *Cell* **97**, 599–607 (1999).

Record, M., Silvente-Poirot, S., Poirot, M. & Wakelam, MichaelJ. O. Extracellular vesicles: lipids as key components of their biogenesis and functions. *Journal of Lipid Research* **59**, 1316–1324 (2018).

Richardson, M. K. Diffusible gradients are out - an interview with Lewis Wolpert. *Int. J. Dev. Biol.* **53**, 659–662 (2009).

Riddle, R. D., Johnson, R. L., Laufer, E. & Tabin, C. Sonic hedgehog mediates the polarizing activity of the ZPA. *Cell* **75**, 1401–1416 (1993).

Robertson, I. B. & Rifkin, D. B. Regulation of the Bioavailability of TGF-β and TGF-β-Related Proteins. *Cold Spring Harb Perspect Biol* **8**, a021907 (2016).

Roh-Johnson, M. *et al.* Macrophage-Dependent Cytoplasmic Transfer during Melanoma Invasion In Vivo. *Developmental Cell* **43**, 549-562.e6 (2017).

Rostam, H. M., Reynolds, P. M., Alexander, M. R., Gadegaard, N. & Ghaemmaghami, A. M. Image based Machine Learning for identification of macrophage subsets. *Sci Rep* **7**, 3521 (2017).

Roy, S., Hsiung, F. & Kornberg, T. B. Specificity of *Drosophila* Cytonemes for Distinct Signaling Pathways. *Science* **332**, 354–358 (2011).

Roy, S., Huang, H., Liu, S. & Kornberg, T. B. Cytoneme-Mediated Contact-Dependent Transport of the *Drosophila* Decapentaplegic Signaling Protein. *Science* **343**, 1244624 (2014).

Rusakov, D. A., Savtchenko, L. P., Zheng, K. & Henley, J. M. Shaping the synaptic signal: molecular mobility inside and outside the cleft. *Trends in Neurosciences* **34**, 359–369 (2011).

Rustom, A., Saffrich, R., Markovic, I., Walther, P. & Gerdes, H.-H. Nanotubular Highways for Intercellular Organelle Transport. *Science* **303**, 1007–1010 (2004).

Salm, L. *et al.* A nerve and mast cell sentinel system releases extracellular condensates to induce macrophage repair. *Journal of Experimental Medicine* **223**, e20260410 (2026).

Schneider, I. Cell lines derived from late embryonic stages of *Drosophila melanogaster*. *Development* **27**, 353–365 (1972).

Schulz, C. *et al.* A Lineage of Myeloid Cells Independent of Myb and Hematopoietic Stem Cells. *Science* **336**, 86–90 (2012).

Senbanjo, L. T. & Chellaiah, M. A. CD44: A Multifunctional Cell Surface Adhesion Receptor Is a Regulator of Progression and Metastasis of Cancer Cells. *Front. Cell Dev. Biol.* **5**, (2017).

Shipman, A. *et al.* Defects in Exosome Biogenesis Are Associated with Sensorimotor Defects in Zebrafish *vps4a* Mutants. *J. Neurosci.* **44**, e0680242024 (2024).

Siebel, C. & Lendahl, U. Notch Signaling in Development, Tissue Homeostasis, and Disease. *Physiological Reviews* **97**, 1235–1294 (2017).

Singh, A. B. & Harris, R. C. Autocrine, paracrine and juxtacrine signaling by EGFR ligands. *Cellular Signalling* **17**, 1183–1193 (2005).

Skandalis, S. S. CD44 Intracellular Domain: A Long Tale of a Short Tail. *Cancers* **15**, 5041 (2023).

Stanganello, E. & Scholpp, S. Role of cytonemes in Wnt transport. *Journal of Cell Science* jcs.182469 (2016) doi:10.1242/jcs.182469.

Stefater, J. A., Ren, S., Lang, R. A. & Duffield, J. S. Metchnikoff's policemen: macrophages in development, homeostasis and regeneration. *Trends in Molecular Medicine* **17**, 743–752 (2011).

Su, J. *et al.* Cell–cell communication: new insights and clinical implications. *Sig Transduct Target Ther* **9**, 196 (2024).

Tickle, C. Making digit patterns in the vertebrate limb. *Nat Rev Mol Cell Biol* **7**, 45–53 (2006).

Tickle, C. & Towers, M. Sonic Hedgehog Signaling in Limb Development. *Front. Cell Dev. Biol.* **5**, (2017).

Tricarico, C., Clancy, J. & D'Souza-Schorey, C. Biology and biogenesis of shed microvesicles. *Small GTPases* **8**, 220–232 (2017).

Tokarz, V. L., MacDonald, P. E. & Klip, A. The cell biology of systemic insulin function. *Journal of Cell Biology* **217**, 2273–2289 (2018).

Travnickova, J. *et al.* Macrophage morphological plasticity and migration is Rac signalling and MMP9 dependent. *Sci Rep* **11**, 10123 (2021).

Turing, A. M. The chemical basis of morphogenesis. *Philosophical Transactions of the Royal Society of London. Series B, Biological Sciences* **237**, 37–72 (1952).

Vachon, E. *et al.* CD44-mediated phagocytosis induces inside-out activation of complement receptor-3 in murine macrophages. *Blood* **110**, 4492–4502 (2007).

Vachon, E. CD44 is a phagocytic receptor. *Blood* **107**, 4149–4158 (2006).

Van Niel, G., D'Angelo, G. & Raposo, G. Shedding light on the cell biology of extracellular vesicles. *Nat Rev Mol Cell Biol* **19**, 213–228 (2018).

Vanorny, D. A. & Mayo, K. E. The role of Notch signaling in the mammalian ovary. *Reproduction* **153**, R187–R204 (2017).

Varol, C., Mildner, A. & Jung, S. Macrophages: Development and Tissue Specialization. *Annu. Rev. Immunol.* **33**, 643–675 (2015).

Vereyken, E. J. *et al.* Classically and alternatively activated bone marrow derived macrophages differ in cytoskeletal functions and migration towards specific CNS cell types. *J Neuroinflammation* **8**, 58 (2011).

Vérollet, C. *et al.* Extracellular proteolysis in macrophage migration: Losing grip for a breakthrough. *Eur J Immunol* **41**, 2805–2813 (2011).

Watanabe, M. & Kondo, S. Is pigment patterning in fish skin determined by the Turing mechanism? *Trends in Genetics* **31**, 88–96 (2015).

Wolpert, L. Positional information and the spatial pattern of cellular differentiation. *Journal of Theoretical Biology* **25**, 1–47 (1969).

Wolpert, L. Role of diffusible gradients in regeneration. *Dev Biol* **30**, concl4-5 (1973).

Wang, S. J., Wong, G., De Heer, A., Xia, W. & Bourguignon, L. Y. W. CD44 variant isoforms in head and neck squamous cell carcinoma progression. *The Laryngoscope* **119**, 1518–1530 (2009).

Wang, Y. *et al.* Cytoneme-mediated intercellular signaling in keratinocytes is essential for epidermal remodeling in zebrafish. *eLife* **13**, RP97400 (2025).

Weng, X., Maxwell-Warburton, S., Hasib, A., Ma, L. & Kang, L. The membrane receptor CD44: novel insights into metabolism. *Trends in Endocrinology & Metabolism* **33**, 318–332 (2022).

Yamashita, Y. M., Inaba, M. & Buszczak, M. Specialized Intercellular Communications via Cytonemes and Nanotubes. *Annu. Rev. Cell Dev. Biol.* **34**, 59–84 (2018).

Yu, Q. & Stamenkovic, I. Localization of matrix metalloproteinase 9 to the cell surface provides a mechanism for CD44-mediated tumor invasion. *Genes Dev.* **13**, 35–48 (1999).

Zhang, C. & Scholpp, S. Cytonemes in development. *Current Opinion in Genetics & Development* **57**, 25–30 (2019).